Symmetry of Halonium Complexes in Solution

ANNA-CARIN CARLSSON

UNIVERSITY OF GOTHENBURG

Department of Chemistry and Molecular Biology
University of Gothenburg
2012

DOCTORAL THESIS

Submitted for partial fulfilment of the requirements for the degree of
Doctor of Philosophy in Chemistry

Symmetry of Halonium Complexes in Solution

ANNA-CARIN CARLSSON

ISBN 978-91-628-8407-9

Available online at: http://hdl.handle.net/2077/27982

Department of Chemistry and Molecular Biology

University of Gothenburg

SE-412 96 Gothenburg

Sweden

Printed by Ineko AB

Kållered, 2012

To my family

ABSTRACT

In this thesis the symmetry of two interaction types involving electropositive halogens have been studied in solution; the N–X^+–N halogen bond (X = Br or I), and the C–X^+–C interaction of previously characterised, cyclic, 1,2-bridged halonium ions (X = Cl or Br), respectively. The three N–X^+–N model structures included are bispyridine, 1,2-bis(pyridine-2-ylethynyl)benzene and 1,2-bis((4-methylpyridin-2-yl)ethynyl)benzene halonium triflate complexes. Model structures representing the C–X^+–C interaction are the dimethylethylene- and ethylenehalonium ions.

All structures included in this thesis are comprised of symmetrically arranged atoms, but have the possibility to exist as either a static, symmetric structure, or as two asymmetric, fast equilibrating tautomers. For a symmetric structure, the positive halogen is positioned with equal distances to the electron donor nitrogens/carbons. In asymmetric structures, the halogen is always closer to one of the nitrogens/carbons, and is consistently jumping between the two nitrogens/carbons. In this investigation the NMR spectroscopic method Isotopic Perturbation of Equilibrium (IPE) has been applied for distinguishing a single symmetric structure from rapidly, interconverting tautomers. The technique measures ^{13}C NMR isotope shifts, $^{n}\Delta_{obs}$, resulting from unsymmetrical introduction of deuterium isotopes in the molecule for which the symmetry is in doubt. Based on the magnitudes, signs, and temperature-dependency of $^{n}\Delta_{obs}$ obtained from ^{13}C NMR spectra of a mixture of non-labelled and deuterium labelled molecules, the symmetry of the molecule being considered can be determined.

The IPE NMR experiments revealed that all bis(pyridine)based halonium complexes were best represented as static, symmetric structures in dichloromethane. The symmetric N–X^+–N arrangement was also shown to be independent of environmental factors, such as increased solvent polarity and tight binding of the counter ion. Thus, these observations indicated that the formation of a symmetric N–X^+–N halogen bond is energetically favourable. The ^{15}N and ^{13}C chemical shifts of the pyridine rings revealed significantly stronger N–X^+–N interaction for the iodonium complexes than for the corresponding bromonium complexes, suggesting a covalent character of the N–I^+–N interaction and an ionic character of the N–Br^+–N interaction. Strongest interaction was observed for the bispyridine halonium complexes, in which the N–N distances are freely adjustable to provide the most favourable interaction.

Ionisation of 2,3-dihalobutane or 1,2-dihaloethane precursors in SbF_5-SO_2 at -80 °C were attempted for generation of the desired ethylenehalonium ions. Both bromonium ions were characterised as asymmetric, equilibrating structures; the dimethylethylenebromonium ions from their $^{n}\Delta_{obs}$ values, and the ethylenebromonium ion from the dynamic behaviour, typical for asymmetric structures in a slow equilibrium, of the signals shown in its ^{1}H and ^{13}C NMR spectra. The ^{1}H NMR spectral pattern of the ethylenechloronium ion was also consistent with asymmetric structures in a slow equilibrium. The symmetry of the dimethylethylenechloronium ions could not be determined, as they, if formed at all, immediately rearranged. SO_2 was revealed to be sufficiently nucleophilic to add to the cations formed. Hence, the source of the asymmetry observed is ascribed the labile addition of SO_2 to either cyclic halonium ions or open β-halocarbenium ions.

Keywords: bis(pyridine)-based halonium complexes, ethylenehalonium ions, structure symmetry, isotopic perturbation of equilibrium, solution NMR spectroscopy, isotope effects, N–X^+–N halogen bond, C–X^+–C interaction

LIST OF PUBLICATIONS

This thesis is based on the following papers, which are referred to in the text by their Roman numbers I – III. Reprints were made with permission from the publishers.

I **Symmetry of $[N\text{-}X\text{-}N]^+$ halogen bonds in solution**
Anna-Carin C. Carlsson, Jürgen Gräfenstein, Jesse L. Laurila, Jonas Bergquist, and Máté Erdélyi
Chemical Communication **2011**, DOI: 10.1039/C1CC15839B, *in press*

II **Halogen Bond Symmetry Revisited: Steric and Solvent effects**
Anna-Carin C. Carlsson, Jürgen Gräfenstein, Adnan Budnjo, Jesse L. Laurila, Jonas Bergquist, Alavi Karim, Roland Kleinmaier, Ulrika Brath, and Máté Erdélyi
Manuscript

III **Mischaracterization of 1,2-Bridged Bromonium Ions**
Anna-Carin C. Carlsson, Jeffery W. Schubert, Máté Erdélyi, and Brian K. Ohta
Submitted to Angewandte Chemie International Edition

CONTRIBUTION REPORT

I Performed most of the synthetic work, and all NMR experiments. Interpreted the results, and contributed significantly to the writing of the manuscript.

II Performed most of the synthetic work, and all IPE NMR experiments. Interpreted the results, and contributed significantly to the writing of the manuscript.

III Synthesised the precursors of the 1,2-dimethyl- and parent ethylenehalonium ions, and performed the following ionisation experiments under superacidic conditions. Contributed to the IPE NMR studies, and to the interpretation of the results. Provided minor contribution to the writing of the manuscript.

LIST OF ABBREVIATIONS

Ac	acetyl
Ad	adamantyl
Ar	aryl
Bu	butyl
coll	2,4,6-trimethylpyridine, *sym*-collidine
COSY	correlation spectroscopy
DCE	1,2-dichloroethane
DEPT	distortionless enhancement by polarization transfer
DFT	density functional theory
DMAE	2-(dimethylamino)ethanol
DMF	*N*,*N*-dimethylformamide
DMSO	dimethyl sulfoxide
DNA	deoxyribonucleic acid
E	electrophile
Et	ethyl
Et_2O	diethyl ether
EtOAc	ethyl acetate
equiv.	equivalent(s)
GC	gas chromatography
HB	hydrogen bonding
HETCOR	heteronuclear correlation spectroscopy
HMBC	heteronuclear multiple bond correlation
HPLC	high performance liquid chromatography
HRMS	high resolution mass spectrometry
HSQC	heteronuclear single quantum correlation
IDCP	iodine dicollidine perchlorate
IPE	isotopic perturbation of equilibrium
i-Pr	isopropyl
IR	infrared
IUPAC	International Union of Pure and Applied Chemistry
LC	liquid chromatography

Me	methyl
MS	mass spectrometry
MW	microwave(s)
n-BuLi	*n*-butyllithium
NMR	nuclear magnetic resonance
NQR	nuclear quadrupole resonance
Nu	nucleophile
Ph	phenyl
Pr	propyl
Py	pyridine
rt	room temperature
Tf	trifluoromethanesulfonyl
TfOH	trifluoromethanesulfonic acid
TFA	trifluoroacetic acid
THF	tetrahydrofuran
TLC	thin layer chromatography
TMS	trimethylsilyl
TOF	time-of-flight
UV	ultraviolet
UV-Vis	ultraviolet-visible
VT	variable temperature
X	any halogen atom; fluorine, chlorine, bromine, or iodine
XB	halogen bonding
ZPE	zero point energy

TABLE OF CONTENTS

1 GENERAL INTRODUCTION

Among the over 4,000 halogenated compounds isolated from natural sources, such as marine organisms, bacteria, and terrestrial plants, there are many that show biological activities, including anticancer and antibacterial properties.[1-3] Approximately one medicinal drug out of three in therapeutic use today is a halogen-containing compound.[4] Furthermore, over 50% of the molecules selected for high throughput screening are halogenated.[5] This implies that halogens comprise important properties useful for the mechanisms of action of drug molecules, and that, in addition, they play key roles in molecular recognition events crucial for certain disease outcomes. In Figure 1 some examples of halogenated pharmaceutical drugs, both synthetic and natural compounds, are shown.[1, 6] The halogens in these molecules are considered to, *via* secondary interactions with certain biomolecules within our bodies, be involved in the regulation of specific biological activities.[4, 6]

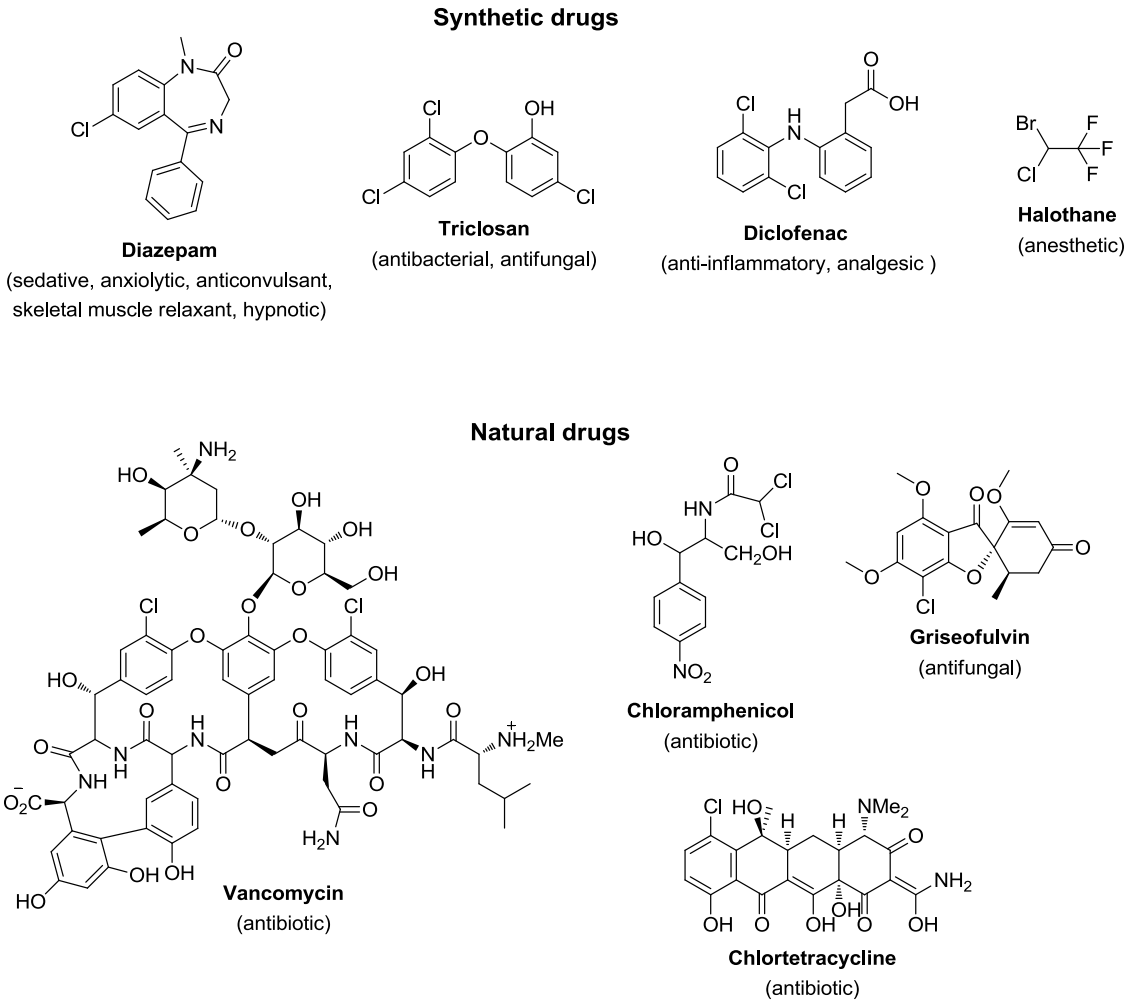

Figure 1. Some examples of synthetic and natural halogenated drug molecules.

The beneficial effects of halogen substitution on the structure-activity relationship of a drug molecule and its interactions with specific target protein or enzyme may be caused by an increased lipophilicity which favours the passage of the drug through biomembranes, the inductive, electron attracting effect of the electronegative halogen, or by the advantageous anisotropic characteristics of the halogens.[4] The polarisability of the halogens allows them to, depending on their electrostatic potentials, be involved in both hydrogen bonding and halogen bonding interactions.[6-8] In the former interaction, the halogen represents a donor of electron density, whereas in the latter it represents an acceptor of electron density. A better understanding and knowledge of how halogenated molecules interact in biological systems would provide valuable tools for development of new drugs in the future.[9]

Due to the fact that most biological processes, as well as chemical reactions, take place in solution environment, it is preferable to gain knowledge of halogen interactions from experimental studies in the solution phase. In this thesis, two different categories of halogen interactions in solution are explored; the N–X^+–N interaction (X = Br or I) of $[N–X–N]^+$ halonium complexes and the C–X^+–C interaction (X = Br or Cl) of three-membered ring ethylenehalonium ions, respectively (Figure 2). Common to both interaction types is the presence of an electropositive halogen. The $[N–X–N]^+$ halonium complexes are sources of electrophilic halogens and represent reactive halogenating agents,[10-13] whereas the cyclic halonium ions are mainly described as active intermediates in organic reaction formed upon electrophilic halogen addition to olefins.[14-17]

The focus of the studies described in this thesis has been to determine the symmetries in solution of the two interaction types, the N–X^+–N interaction and C–X^+–C interaction, respectively, distinguishing between a symmetric binding with the halogen centred and an asymmetric binding with the halogen being closer to one of the nitrogens or carbons (Figure 2). The N–X^+–N interaction may be related to N–H–N or O–H–O hydrogen bonds.[18] As symmetric hydrogen bonds, comprised of a centred hydrogen and two equal bond N–H or O–H lengths, are considered to be very strong,[19] and provide extra stabilisation in enzyme catalysis reactions,[20-24] symmetric N–X^+–N bonds are also expected to be strongly stabilised. The same is expected for the corresponding C–X^+–C interaction; the symmetric ion with the halogen covalently centred in between the two carbons are expected to be more stable than an asymmetric ion with two unequal C-X bond lengths.

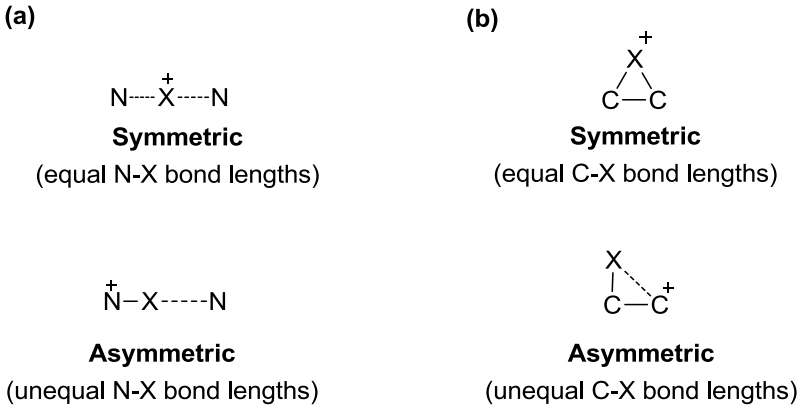

Figure 2. Symmetric and asymmetric binding interactions; **(a)** in $[N–X–N]^+$ halonium complexes (X = Br or I) and **(b)** in three-membered ring halonium ions (X = Cl or Br).

2 ELECTROPOSITIVE HALOGENS

The four elements fluorine (F), chlorine (Cl), bromine (Br) and iodine (I) are referred to as halogens, and represent a series of non-metal elements from Group 17 of the periodic table (Figure 3). Due to their electron configuration with seven electrons in the outermost shell, the halogens are electronegative and highly reactive elements, with fluorine being the most electronegative and most reactive of them all.

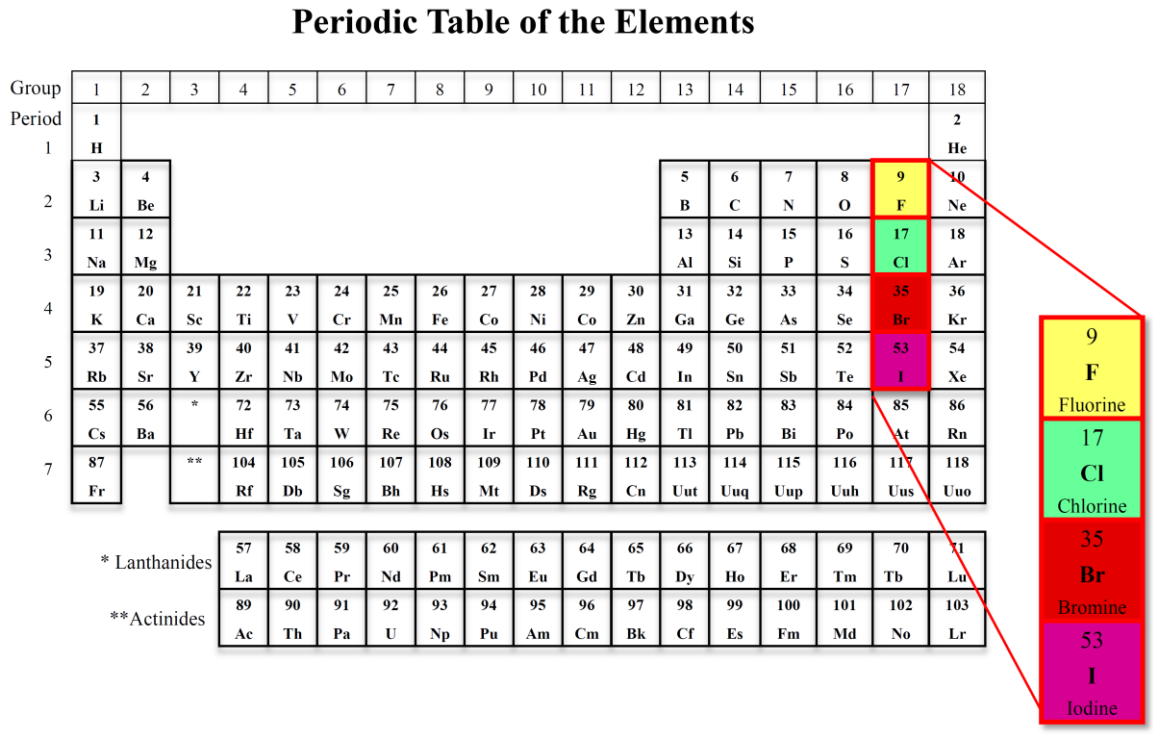

Figure 3. The periodic table of elements, with the halogens of Group 17 being high-lighted in their common colour codes; yellow for fluorine, pale-green for chlorine, red-brown for bromine, and violet for iodine.

The general trends when going downwards within the group in the periodic table are decreasing electronegativity and reactivity, and increasing melting and boiling point as well as increasing polarisability with increasing atom number. Because of their polarisable nature, the halogens can also be anisotropic, thus being capable of separating or accumulating both positive and negative charges in two distinct regions of the atom surface. The polarisation of the halogens is dependent on the atom size; the larger the atom, the larger the surface area to disperse electrons over, and the better charge separation ability. Thus, the large iodine atom is very polarisable, whereas the polarisability of the much smaller fluorine is very poor, almost non-existing.[25] An increased

polarisability is also associated with stronger intermolecular attractive forces, which is the reason for that molecular, diatomic halogens represent all three states of matter at room temperature; the smallest F_2 and Cl_2 molecules being gases, the larger Br_2 a liquid, and the largest I_2 a solid.

Although halogens are anisotropic and can act both as electron donors and acceptors, their properties have so far mostly been investigated in interactions and reactions in which they act as electronegative atoms, and anions. However, this thesis work focuses on interactions where the halogens are electropositive. This chapter describes halogens that carries either a full or a partial positive charge.

2.1 Halonium Ions

A halonium ion is a cation comprised of a halogen atom (X; where X = F, Cl, Br or I) that is bound to two organic residues, commonly two carbon atoms. The halogen carries the positive charge, and possesses an octet of electrons but bears a formal charge of +1. The halonium ions formed from F, Cl, Br and I are called fluoronium (F^+), chloronium (Cl^+), bromonium (Br^+), and iodonium (I^+), respectively. There are two main classes of halonium ions relating to their molecular structures: (1) open-chain halonium ions and (2) cyclic halonium ions. Diarylhalonium ($Ar–X^+–Ar$), alkylarylhalonium ($R–X^+–Ar$), and dialkylhalonium ($R–X^+–R$) ions belong to the first class of open-chain or acyclic structures. In Figure 4, some general examples of halonium ions from the second class with cyclic structures are depicted. In this class, aromatic heterocyclic and bicyclic halonium ions are included.

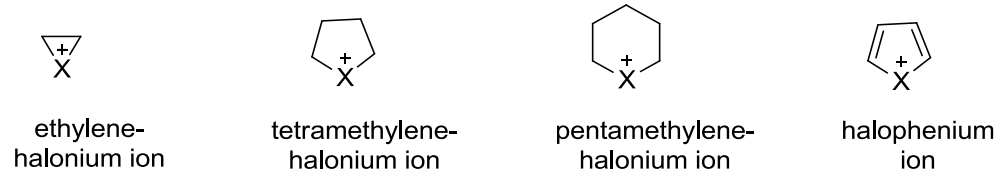

Figure 4. Cyclic halonium ions; three-membered ring ethylenehalonium, five-membered ring tetramethylenehalonium, six-membered ring pentamethylenehalonium, and heteroaromatic halophenium ions.

Due to their positive charge, halonium ions are highly reactive, electrophilic species, which react readily with nucleophiles. In organic reactions in solution, they are often formed as short-lived, high-energy intermediates along the reaction pathways. Reaction mechanisms involving three-membered-ring, also referred to as 1,2-bridged, halonium ions have been extensively studied.[14, 17, 26-30] In perhaps all introductory organic chemistry textbooks of today, the three-membered-ring

bromonium ion is described as the sole intermediate responsible for the *anti*-stereospecificity observed for the addition of molecular bromine to alkenes.[31-33] Halonium ions are also important intermediates in electrophilic halocyclisation reactions; *i.e.*, reactions that include both an electrophilic halogen addition to a carbon-carbon double bond and cyclisation by subsequent addition of an intramolecular nucleophile (*e.g.*, alcohol, carboxylic acid, amine, amide, and carbon nucleophile) to the halonium ion formed. Very recently, a review that highlights such halonium-induced cyclisation reactions, describing the latest developments in the field and the various electrophilic halogen sources available for halonium ion formation was published.[34] Some halonium ions are stable, and exist as solid, crystalline salts.[35-36] Being sources of electrophilic halogen, such solid halonium ions are of great importance as preparative reagents in organic synthesis.[35]

In 1975, Olah summarised the properties, syntheses and chemistry of all classes of halonium ions discovered so far in the book "*Halonium Ions"*.[37] Nearly a decade later, Koser published a detailed review on the same theme.[38]

2.1.1 Brief Historical Aspects of Halonium Ions

In 1894, the very first example of a halonium ion, a stable open-chain diaryliodonium (Ar–I^+–Ar) ion, was reported by Hartmann and Meyer.[39] They described phenyl(*p*-iodophenyl)iodonium bisulphate (**2**) as the product generated from the autocondensation reaction of iodosylbenzene (**1**), a hypervalent organoiodine(III) species, in the presence of sulphuric acid (Scheme 1).

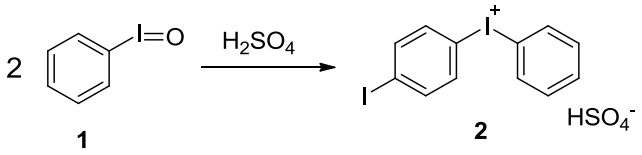

Scheme 1. Formation of the first described diaryliodonium salt **2** *via* autocondensation of iodosylbenzene (**1**).[39]

Over the years, the interest for the synthesis of various stable diaryliodonium ions, with a variety of substituent patterns in the aromatic rings, has increased tremendously.[40-41] The diaryliodonium salts are mainly of use as preparative reagents in organic synthesis. Recently, a review was published, giving an update of the developed syntheses of diaryliodonium salts, and their important applications as synthetic reagents in *e.g.*, α-arylations of carbonyl compounds, arylation of heteroatom nucleophiles, and metal-catalyzed cross-coupling reactions.[35] Due to their biological activities[40, 42] and photochemical properties,[43-46] diaryliodonium ions have also proved to be useful as antimicrobial agents and as cationic photoinitiators in polymerization reactions.

The corresponding diarylchloronium (Ar–Cl^+–Ar), and diarylbromonium (Ar–Br^+–Ar), salts are uncommon.[38] These ions are considerably less stable than the diaryliodonium ion, and thus their applications as synthetic reagents are limited. The first syntheses of acyclic diarylchloronium and diarylbromonium salts from thermal decomposition of phenyldiazonium salts in halobenzene were reported in the 1950s by Nesmeyanov and co-workers.[47]

In 1937, Roberts and Kimball were the first to propose the today widely accepted organic reaction mechanism for electrophilic halogen addition to olefins, in which cyclic ethylenehalonium ions are the key intermediates.[48] They suggested that either carbenium ion stabilised by bridging by its neighbouring β-bromine atom or cyclic, three-membered-ring ethylenebromonium ion intermediates were accounted for the observed *trans* stereoselectivity in molecular bromine addition to ethylene (Figure 5). They based their argument on the fact that the initial intermediate in the bromination could not have an open-chain structure, since rapid rotation around the C–C single bond would result in a product mixture of equal amounts of both *cis* and *trans* isomers.

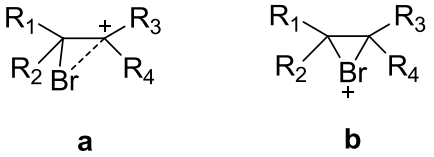

Figure 5. Intermediate structures in Br_2 addition to alkenes proposed by Roberts and Kimball;[48] **(a)** carbenium ion stabilised by partial bridging by the neighbouring β-bromine; **(b)** three-membered ring bromonium ion.

Olah and Bollinger reported in 1967 the first preparation and direct spectroscopic observation by ^{1}H NMR spectroscopy of cyclic tetramethylethylenehalonium ions **4**. The ions were generated from the corresponding 2,3-dihalides **3**, under stable ion conditions in SbF_5-SO_2 solution at -60 °C (Scheme 2).[49] Their observation gave evidence for the cyclic halonium ion structure, thus providing the breakthrough for the generation and characterisation of a wide variety of three-membered-ring ethylenehalonium ions, where X = Cl, Br, or I, under similar experimental conditions.

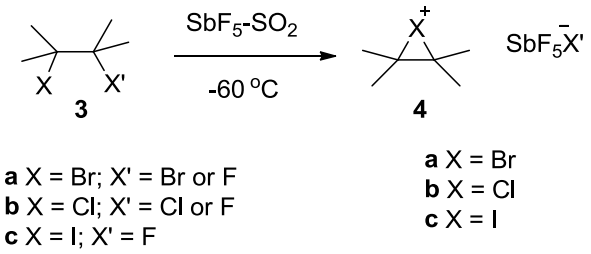

Scheme 2. Formation of three-membered-ring tetramethylethylenehalonium ions **4a-c**.[49]

Shortly thereafter, Olah and Peterson showed that five-membered-ring tetramethylenehalonium ions (**6**) (Cl^+, Br^+, and I^+ ions) also could be prepared and observed by ^1H NMR spectroscopy by using similar stable ion conditions (Scheme 3).[50] Peterson and co-workers later described the preparation and spectroscopic observation of several tetramethylenehalonium ions and, in addition, of six-membered-ring pentamethylenehalonium ions (Br^+ and I^+ ions) in stable ion conditions.[51]

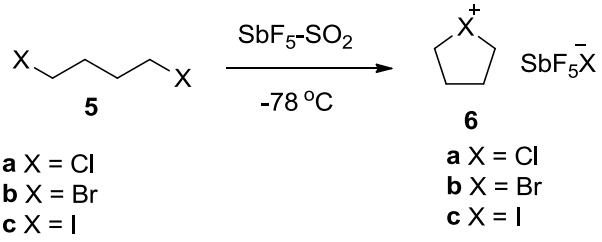

Scheme 3. Formation of five-membered-ring tetramethylenehalonium ions **6a-c**.[50]

Olah and DeMember reported the first preparation and direct observation of open-chain dialkylhalonium (R–X^+–R) ions in 1969.[52] The ions were generated by treatment of excess haloalkane with antimony pentafluoride or with methyl hexafluoroantimonate in liquid SO_2 solution at low temperature; the former synthesis being limited to the generation of symmetric dialkylhalonium ions (Scheme 4).[52-53]

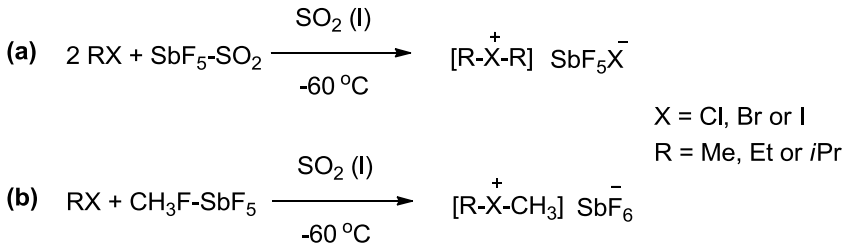

Scheme 4. Formation of dialkylhalonium ions; **(a)** symmetric halonium ions with identical R-groups; **(b)** methylalkylhalonium ions.[52]

The very first successful isolation of dimethylhalonium fluoroantimonate salts **7** as fluffy white crystals, stable at room temperature only under dry conditions, was reported in 1970.[54] These halonium salts were prepared by treatment of a slight excess of the corresponding halomethane with methyl hexafluoroantimonate in liquid SO_2 at -40 °C (Scheme 5).[54-55] In addition to the dimethylhalonium fluoroantimonate salts, successful isolation of tetramethyleneiodonium and pentamethyleneiodonium fluoroantimonates has been reported.[51, 56]

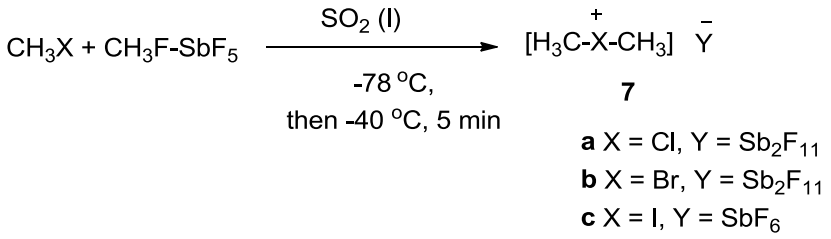

Scheme 5. Formation of solid dimethylhalonium salts.[54]

The preparation and direct observation of open-chain alkylarylhalonium ($R–X^+–Ar$) ions by NMR spectroscopy was first reported by Olah and Melby in 1972.[57] A variety of alkylarylhalonium ions (**9**) were generated by reacting aryl bromides or iodides (**8**) with methyl or ethyl fluoroantimonate in SO_2 at low temperature (Scheme 6).

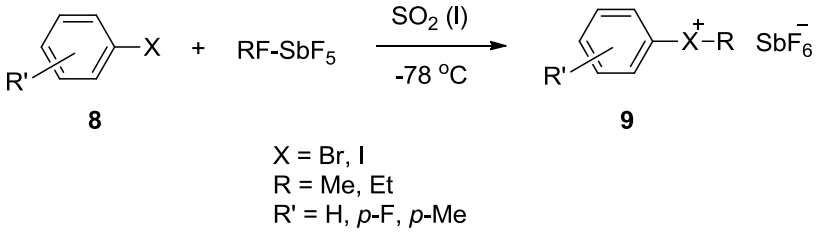

Scheme 6. Formation of alkylarylhalonium ions.[57]

In general, all alkylhalonium ions prepared under stable ion conditions at low temperatures are highly electrophilic and very potent alkylating agents for nucleophiles, even the very weak ones.[55, 58] In addition, these classes of ions are usually stable at low temperatures only, typically at -60 °C or below. At higher temperatures, secondary reactions are common. Dialkylhalonium ions can be used to alkylate aromatic hydrocarbons in a Friedel-Craft fashion under stable ion conditions.[55] They also act as cationic polymerisation initiators when alkylating alkenes.[55]

The first stable salts of three-membered-ring halonium ions were reported in 1969 and 1970 by Strating, Wieringa, and Wynberg.[59-60] By reacting Br_2 or Cl_2 with the sterically hindered olefin adamantylideneadamantane (Ad=Ad), yellow and white solids were isolated, which they described as the bromonium and chloronium adamantylideneadamantane tribromide (Br_3^-,**10a**) and trichloride (Cl_3^-, **10b**) salts, respectively. This was, however, not fully confirmed until 1994 when Brown and co-workers succeeded in characterising the corresponding bromonium and iodonium triflate salts (**10c,d**) by X-ray crystallography (Figure 6).[36] Later, Kochi and co-workers published the X-ray structure of the corresponding chloronium hexachloroantimonate salt **10e** (Figure 6).[61]

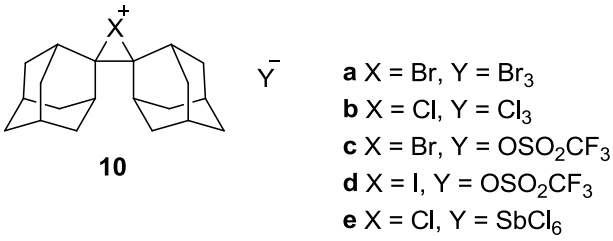

Figure 6. Crystalline halonium ions of adamantylideneadamantane.[36, 59-61]

2.2 HALOGEN BONDING

Halogen bonding, commonly referred to as X-bonding, is a general term describing short-range, noncovalent molecular interactions between electropositive halogens and neutral or anionic electron donating species with, for instance, N, O, S or P functionalities and π electrons representing the electron donors. Halogen bonds (X-bonds) are analogous to the classical hydrogen bonds (H-bonds), as both involve donor-acceptor interaction between a Lewis acid/Lewis base pair. In an X-bond, a polarised, electropositive halogen replaces the hydrogen of an equivalent H-bond as the Lewis acid in the Lewis acid/Lewis base pair.

Since its discovery, the halogen bond interaction has been characterised by many ways, *e.g.*, electron donation-acceptance charge-transfer interaction,[62-63] dipolar dispersion interaction,[64] and electrostatic interaction *via* a positive σ-hole.[65] During the last two decades, the need to gain an understanding about what the interaction type that describes a halogen bond best is has grown. In January 2010, an IUPAC project entitled "*Categorizing Halogen bonding and Other Noncovalent Interactions Involving Halogen Atoms*" was initiated, the objective being to give a modern

definition of halogen bonding, and to include the definition in the *IUPAC Gold Book*.[66] This project is about to come to an end within a short time.

Intense research has resulted in applications of halogen bonding in a variety of research fields,[67] *e.g.*, crystal engineering,[68-77] supramolecular chemistry,[78-80] polymer sciences,[81-82] liquid crystals,[83-87] conductive materials,[88-90] and medicinal chemistry.[6-9, 91] Hitherto, halogen bonds have been investigated mostly in the solid and gaseous[92-93] phases, or with computational methods.[64-65, 94-96] Lately, the halogen bond interactions have also been recognised in biological macromolecules, such as DNA.[97-100] Only a handful of studies of halogen bonds have, so far, been carried out in the solution phase.[63, 101-111] Recent investigations have indicated that NMR spectroscopy is applicable for the detection of halogen bonds in solution.[63, 102-103, 105-106, 108-111]

2.2.1 Halogen Bonding – A Historic Perspective

Already in 1863, Guthrie observed the ability of I_2 to form bonding adducts with ammonia.[112] Upon addition of molecular I_2 to a saturated solution of ammonium nitrate a solid compound was formed, which rapidly decomposed into ammonia and I_2 when exposed to air. From his observation, Guthrie concluded that the compound formed was $NH_3 \cdot I_2$. This was the first evidence reported that halogen atoms are able to form binding interactions with electron donating species. In the very beginning of the 20th century, Lachman observed that solutions of free I_2 have different colours depending on the nature of the solvent; brown solutions for electron donating solvents (*e.g.*, alcohols, ethers, ketones, carboxylic acids, nitriles, and nitrogen bases), and violet for non-basic, less polar solvents (*e.g.*, hydrocarbons, chloro- and bromohydrocarbons, and carbon disulfide).[113] The brown colour was interpreted as the formation of "molecule-solvent+I_2" complexes. The complexation ability of I_2 with electron donating solvents was further studied; spectrophotometric studies showed evident dissimilarities in absorption between brown and violet solutions, and different reactivities were observed, the brown solutions with complexed I_2 being more reactive than violet solutions with free I_2.[114] Later, it was also observed that the position of absorption bands in the visible region for I_2 in different solvents moved gradually from violet to brown coloured solutions.[115] A large shift in absorption frequency maximum indicated a strong complexation, whereas a smaller shift indicated the formation of a weaker I_2-solvent complex. For the red-violet coloured I_2-benzene solution this absorption shift was only small, yet apparent, indicating a small degree of complexation. In 1949, the 1:1 complexation of I_2 with aromatic π electron donating compounds was further revealed by Benesi and Hildebrand, who concluded

from evident UV-Vis spectra changes (shifted absorption band in the visible region and intense new band in the ultraviolet region) and colour changes, that I_2 forms complexes spontaneously with aromatic hydrocarbons in non-polar solvents (CCl_4 and *n*-heptane).[116] They suggested the 1:1 complexation was similar to an acid-base interaction. Keefer and Andrews showed from similar UV-Vis studies that Br_2, Cl_2 and ICl also are prone to form complexes with aromatic electron donors.[117-118]

The above mentioned spectrophotometric observations together strongly contributed to Mulliken's detailed theory of charge-transfer complexes, which describes the intermolecular interaction between electron donors and acceptors, the electrons of the donor (Lewis base; neutral π and *n* bases, and ionic base, *e.g.*, unsaturated or aromatic hydrocarbons, NR_3, OR_2, X^-, CN^-, and OH^-) being partially transferred to the acceptor (Lewis acid; X_2, hydrogen halide).[119-121] The charge-transfer complexes were classified as being either outer or inner complexes; in the outer, associative complexes the intermolecular interaction between the electron donor and acceptor was weak and had very little charge transfer, whereas in the inner, dissociative complexes the interaction was strong with an extensive degree of charge transfer, giving the complexes ionic character.[121]

Under the same period Mulliken postulated his theory, in the 1950's, Hassel and co-workers performed X-ray crystallographic studies of Br_2 complexes with 1,4-dioxane (Figure 7).[122] Their obtained structure revealed a linear arrangement of the O–Br and Br–Br bonds, and close contacts between the oxygen atoms of dioxane and bromine atoms. The O-Br distance (2.71 Å) in the crystal was significantly shorter than the sum of the van der Waals radii of oxygen and bromine (3.35 Å),[123] but longer than the sum of their covalent radii (1.9 Å),[124] thus indicating a strong secondary interaction in an electron donor-acceptor complex with the oxygen donating its electron lone pair to the bromine acceptor atom. Hassel and co-workers continued their crystallographic studies with additional halogen and electron-donating species.[125-126]

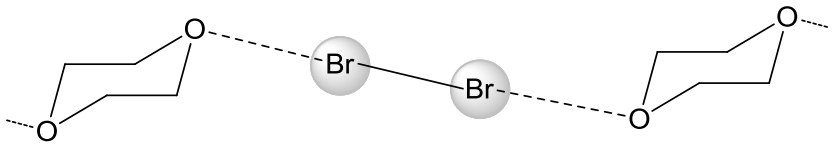

Figure 7. Chains in the 1:1 adduct of 1,4-dioxane and bromine, the oxygen donating its lone pair to the bromine acceptor atom. Hassel's first X-ray crystallographic evidence of a halogen bond.[122]

In 1969, Hassel was awarded the Nobel Prize in Chemistry for his outstanding discovery that halogens can act as electrophilic, electron acceptors, and self-assemble into highly, directionally organised crystalline charge-transfer complexes in presence of electron donors.[62, 127] An early review about electron donor-acceptor complexes involving halogens as acceptors was provided by Bent in 1968.[128] However, there were some disagreement regarding the actual charge transfer in these complexes, but the general consensus was that the complexes involved weak electrostatic interactions, including both dispersion and dipole forces.[129] The use of the term "halogen bond" was not implemented until 1978 by Dumas and co-workers, who investigated complexes of $SiCl_4$ or $SiBr_4$ with several electron donating organic solvents.[130] Since then, Dumas's term has largely replaced the earlier charge-transfer definition.

In the next two decades, computational quantum mechanical and database studies of organohalogens and dihalogens with oxygen and nitrogen electron donors indicated that the major attraction forces of the halogen bond interaction is due to the electrostatic interaction between the polarisable halogen and the electron donor.[131-132] Especially, advances in understanding the interaction nature of halogens were made through the analysis of a large number of crystal structures involving halogens with short intermolecular distances, less than the sum of the van der Waals radii of the atoms involved, available from the Cambridge Structural Database.[132] It was interpreted that short intermolecular distances provided proof of a strong interaction between the atoms involved. For halogens covalently bound to carbons, an obvious trend was found. Close contacts with electron donors, such as nitrogens and oxygens, were highly directional with angles of 160°-180° with the C–X bond, whereas with electrophiles, such as metal cations, the angles were much smaller, between 90° and 120° (Figure 8). The studies revealed that the high directionality of the halogen bond is the result of an anisotropic distribution of electron density around the halogen nucleus.[131-132] Along the covalent C-X bond, the outermost portion, the "head", of the halogen interacts favourably with the negative electrostatic potential of the electron donor. Notable was also that amongst the different halogens, the tendency to form short halogen bond interactions is in the order I > Br > Cl >> F, which parallels the order of the polarisabilities of the atoms. The highly directional interactions observed were later confirmed by computational calculations by Politzer and co-workers.[65, 96] The linearity of the halogen-electron donor interaction was explained to originate from the existence of a positive σ–hole, representing the tip of the halogen along the C-X bond. The σ–hole is described in more detail in Section 2.2.3.

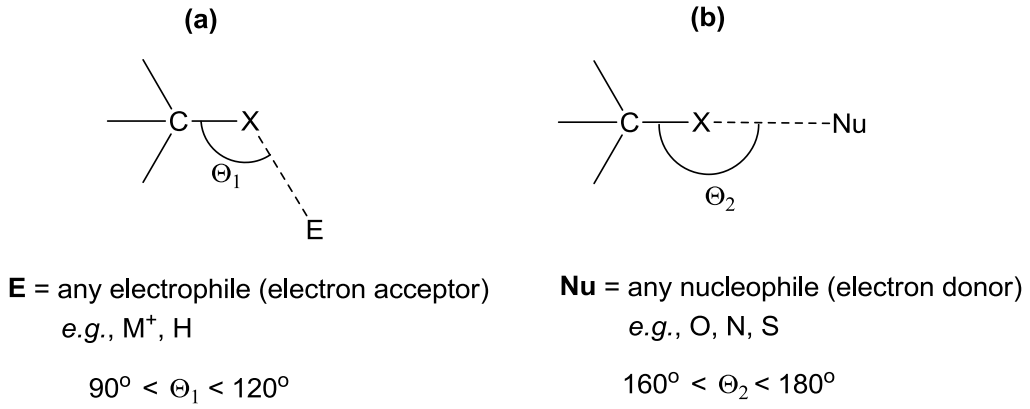

Figure 8. Directional interaction tendencies of a covalent C-X bond; **(a)** interaction angles with electrophilic species, **(b)** interaction angles with nucleophilic species.[96, 131-132]

Ever since the very beginning of the 21th century, the term halogen bonding has been used to describe any noncovalent interaction that involves electropositive halogens as acceptors of electron density.[92, 133]

2.2.2 General Definition of Halogen Bonding

Metrangolo and Resnati and co-workers introduced the general scheme Y–X···D, illustrated in Figure 9, for defining a halogen bond (X-bond).[18] In this scheme, X represents the halogen (Lewis acid) that is covalently bound to Y and interacts non-covalently with D, the electron donor (Lewis base). The halogen X is most likely polarisable I, Br or Cl atoms, and only rarely an F atom. Y can be any atom (*e.g.*, C, N or halogen), and D can be any electron donor of either neutral or anionic character. The attractive nature of the X-bond makes the X···D distances shorter than the sum of the van der Waals radii of the participating atoms. The stronger the X-bond is, the shorter the X···D distance is. The Y–X distances are usually slightly elongated, and the Y–X–D angle is close to 180° meaning the three atoms involved in the X-bond are organised in a linear fashion. The electropositive halogen (X) is sometimes referred to as an X-bond donor, whereas the electron donor (D) is called an X-bond acceptor. This nomenclature is opposite to the conventional classification of an electron donor-acceptor interaction.

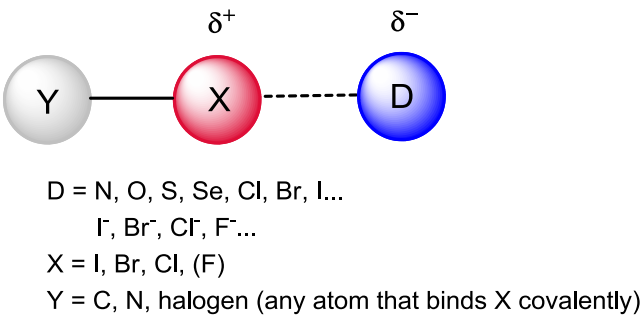

Figure 9. General scheme describing the noncovalent halogen bond interaction, the halogen X representing an electrophilic Lewis acid and the electron donor D a nucleophilic Lewis base.[18]

2.2.3 The σ-Hole

The "σ-hole" interaction as the description of halogen bonding was first introduced by Clark *et al.*.[65] Computational calculations of electrostatic potentials of CF_3X organohalogens, with X = F, Cl, Br and I, showed that there is a positive electrostatic potential on the outermost portion of the halogen's surface, centered along the C-X axis and surrounded by negative electrostatic potential (Figure 10). This centered electropositive tip of the halogen is called the σ-hole. In Figure 10, a positive electrostatic potential is illustrated in red, and a negative in blue. The positive σ-hole can favourably interact non-covalently, with electronegative sites, such as the electron lone pairs of Lewis bases and π electrons of aromatic or other unsaturated system, in a linear (or close to linear) direction. Electronegative potentials (blue) are found along the lateral sides of the halogen, indicating that the interaction with electrophiles is preferred in a perpendicular direction against the C-X axis. The size of the positive σ-hole, *i.e.*, the extent of the electron density depletion, depends on the polarisability and electronegativity of the halogen. Consequently, the more polarisable (I > Br > Cl >> F) and the less electronegative (I < Br < Cl < F) the halogen is, the stronger is the halogen bond. In Figure 10 is also illustrated that, in this particular case, the highly electronegative fluorine does not form a positive σ-hole, and that the less electronegative chlorine forms a very small σ-hole.

Figure 10. Calculated electrostatic potentials for CF_3X organohalogens. The electropositive σ-hole (red) centred on the tip along the C-X bond. The size of the σ-hole is largest for the most polarisable halogens (I > Br > Cl >> F). Here no σ-hole is generated for F. Along the lateral sides of the C-X bond, the electrostatic potential is negative (blue).[65] The picture is reproduced with permission from the publisher (ref. 65).

For a general R–X molecule, where R represents any group covalently attached to the halogen, the size of the σ-hole can be tuned.[96, 134] By increasing the electron-withdrawing power of the R-group, the magnitude of the positive electrostatic potential of the tip of the halogen also increases. In general, chlorine is rarely involved in halogen bonding unless the R-group is sufficiently electron-withdrawing. It has been argued that fluorine is unable to form halogen bonds due to its high electronegativity and low polarisability. Recent reports, however, give evidence that, when covalently linked with a particularly electron-withdrawing R-group, fluorine can be involved in halogen bonding.[25, 135-136]

An explanation of the origin of the positive electrostatic potential representing the σ-hole on an orbital level has been given by Murray, Politzer and co-workers.[96, 137] The valence shell of a halogen atom contains seven electrons, and in its spherical ground state the halogen has an electropositive potential in all directions, *i.e.*, the charge of the positive nucleus dominates over the dispersed negative electrons. Each of the three valence p orbitals contains, on average, 5/3 electrons. When the halogen forms a covalent bond, for instance along its *z*-axis, it gets a valence state with the electronic configuration $s^2p_x^2p_y^2p_z^1$. In the ±*z* directions, along the R–X axis, the electrostatic potential remains positive in all radial directions due to the half-filled p_z orbital. However, along the ±*x* and ±*y* directions, the electrostatic potentials are negative on the halogen surface, due to the two doubly-occupied p_x and p_y orbitals. The unpaired electron of the p_z orbital is the one participating in the R–X covalent bond. The bond formation results in a charge redistribution, and a depletion of electron density in the outer lobe of the p_z orbital. If this electron depletion is sufficient, a positive σ-hole is generated (Figure 11).

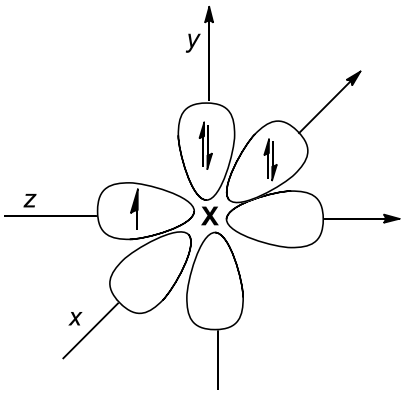

Figure 11. Distribution of five electrons over the three valence p orbitals of the halogen, p_x, p_y and p_z. The C-X bond is formed along the *z*-axis. The electrostatic potential is positive along the ±z- axis due to the unpaired electron in the p_z orbital. Along the ±*x*- and ±*y*-axes the electrostatic potentials are negative as both the p_x and p_y orbitals have paired electrons.[96, 137]

2.2.4 Halogen Bonding versus Hydrogen Bonding

The terms halogen bonding, halogen donor and acceptor arose to emphasise the similarities between halogen bonding and hydrogen bonding, which are since long time recognised.[5, 18, 62, 92, 130] Both halogen and hydrogen bonds are short-range, electrostatically-driven, noncovalent interactions between a covalently bound, electropositive halogen or hydrogen (Lewis acid) and an electron donor (Lewis base). The Lewis acid represents the X-bond or H-bond donor, and the Lewis base the X-bond or H-bond acceptor. Both halogen and hydrogen bonding are highly directional interactions. Their directions, however, differ slightly; halogen bonds are nearly linear with the R–X···D angle close to 180°, whereas the hydrogen bonds are more likely to be non-linear, sometimes the R'–H···D angles are considerably less than 180°.[137] Here R represents any atom covalently bound to X, R' any atom (*e.g.*, O, N, S) covalently bound to H, and D the electron donor. Moreover, halogen and hydrogen bonds are usually of comparable strengths, normally in the range 5-30 kJ/mol.[18] However, the strength of halogen and hydrogen bonds can sometimes be much stronger, in extreme cases up to 180 kJ/mol (180 kJ/mol in I^-···I–I and 160 kJ/mol in F^-···H–F).[18-19, 138-139] Due to the similarities in bond strength, halogen bonding often competes and interferes with hydrogen bonding. Competition between halogen and hydrogen bonds has been extensively studied by computational calculations,[140-142] and experimentally in the gaseous phase[92] and in supramolecular crystals.[133, 143-145] Recently, competitive studies have also been explored in biomolecular recognition processes,[99, 146] and in molecular conformational studies in solution.[147] Competition between halogen and hydrogen bonding in solution was first

studied by Di Paolo and Sandorfy, and was suggested to play a role in the mechanism of action of volatile anaesthetics.[148] The cooperation between halogen and hydrogen bonding interactions in molecular recognition studies of urea-based anion receptors in solution has been investigated by Tayler and co-workers.[102]

As halogens also are of electronegative nature, they can themselves act as H-bond acceptors (Lewis bases), donating their electrons to the electropositive hydrogen of the H-bond donor. As described in Section 2.2.3 above, negative electrostatic potentials, originating from the electrons of the non-bonding orbitals, are found on the lateral sides of the halogen. The positive H-bond donor, therefore, interacts with the halogen in a nearly perpendicular direction to the R–X axis, with typical R–X···H angles of 90°-120°. For halogens participating as electron donors in hydrogen bonding, the strength of the interaction increases with the electronegativity of the halogen (F > Cl > Br > I).

2.3 $[N–X–N]^+$ Halonium Complexes

Positive halogen(I) cations, X^+, are not sufficiently stable to exist in the condensed phase. However, they can be stabilised by complexation with a coordinating base, commonly an aromatic nitrogen-containing heterocycle. In the 1930's, Carlsohn made extensive studies of such stabilised iodine(I) salts, in which pyridine or its analogues were used as coordinating ligands.[149] He was first to suggest the existence of the Py_2I^+ cation, where iodine(I) is coordinated to two pyridines. From the early 1950s, the preparations of a wide range of iodine(I) and bromine(I) salts with pyridine, picoline or quinoline as the mono- or dicoordinating base (Figure 12), and with a variety of counter ions (*e.g.*, benzoates, NO_3^-, ClO_4^-, and SbF_6^-) were described in the literature.[150-153] In general, the preparation of these salts involved the reaction of the corresponding silver(I) salt with I_2 or Br_2 in a dry, mildly polar solvent (*e.g.*, chloroform, dichloromethane), in the presence of the coordinating base. Common was also to start from the silver(I) salts already complexed with the coordinating base.[153] During the reaction, solid silver halide was precipitated, and usually separated by filtration. The halogen(I) salt was often crystallised by addition of a non-polar solvent (*e.g.*, diethyl ether, petroleum ether, and hexane). Anhydrous reaction conditions were very important as the halogen(I) salts were found to be water sensitive, and were generally hydrolysed rapidly on exposure to light and moist air.[153]

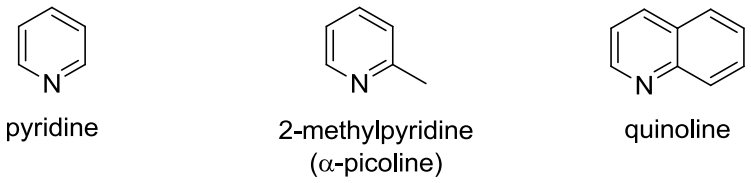

Figure 12. Examples of coordinating nitrogen bases in $[N–X–N]^+$halonium complexes.

In 1961, Hassel and Hope provided the first structural evidence for the existence of the Py_2I^+ cation. From X-ray studies of the crystals formed between pyridine and I_2, it was concluded that the crystals were comprised of the Py_2I^+ cation with I_3^- as counter ion.[154] It was also revealed that the two pyridine rings of Py_2I^+ were nearly coplanar, and that the linear N–I–N arrangement was centrosymmetric, with equal N–I distances (2.16 Å). Vibrational spectroscopic studies (IR and Raman) of pyridine or picoline dicoordinated iodine(I) and bromine(I) salts with a variety of counterions (*e.g.*, ClO_4^- PF_6^-, BF_4^-, NO_3^-), both in crystal and in solution, also supported the linearity of the N–X–N bond, and the coplanar arrangement of the coordinating bases.[155-157] Moreover, based on the vibrational shift frequencies it was suggested that the N–X–N interaction of dicoordinated halogen(I) cations involved a large degree of charge transfer.[157] Charge distribution studies of Py_2I^+ and Py_2Br^+ salts with ^{14}N NQR have been reported.[158-159] The characteristics of Py_2I^+ and Py_2Br^+ complexes and some of their analogues have also been investigated in solution by UV spectroscopy,[160] vibrational spectroscopy (IR and Raman),[157, 161-163] and ^1H and ^{13}C NMR spectroscopy.[164-165]

The crystal structures of several dicoordinated halogen(I) salts have been determined. Some of these $[N–X–N]^+$ halonium complexes whose crystal structure has been solved are depicted in Figure 13.[166-171] Bis(quinuclidine)bromonium tetrafluoroborate is the only known bromine(I) complex that is coordinated between two aliphatic amines.[170] All N–X–N bonds are in linear, or close to linear, arrangement, and the N–X distances are generally longer than the sum of the covalent radii of the participating atoms (N–I ~2.1 Å; N–Br ~1.9 Å),[124] but shorter than the sum of their van der Waals radii (N–I 3.53 Å; N–Br 3.40 Å).[123] Interestingly, among the complexes shown in Figure 13, in the iodine(I) complexes the N–I–N bond is centrosymmetric with equal N–I distances,[167-169] whereas in the bromine(I) complexes the N–Br–N bond is unsymmetrical with one N–Br distance being slightly longer than the other one.[166, 170-171]

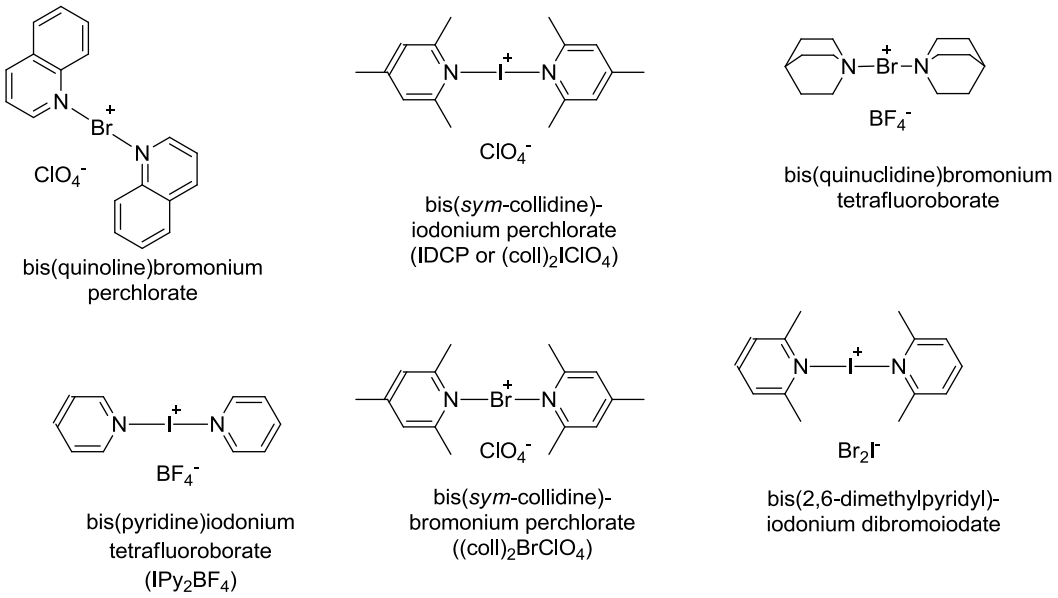

Figure 13. $[N–X–N]^+$ halonium complexes with known crystal structures.[166-171]

The electronic structure of the N–X–N bond of the cations has long been discussed, and various suggestions have been made. In Figure 14, five alternatives (**a-e**) of the N–X–N bonding are illustrated.[170]

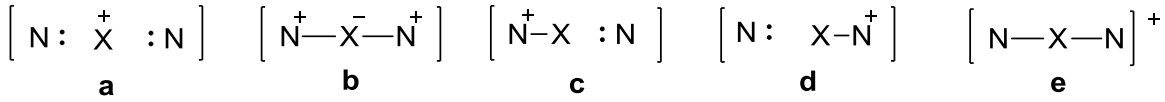

Figure 14. Five possible electronic structures of the N–X–N bond (**a-e**).[170]

In alternative **a,** the central X^+ ion is electrostatically coordinated by the nitrogen lone pairs. Alternative **b** represents a hypervalent, three-centre-four-electron covalent bond with an expanded octet of 10 electrons surrounding the X atom, each nitrogen contributing with one single electron each to the X atom.[172] Alternative **c** and **d** both represent unsymmetrical N–X–N bonds, where the X atom has a filled octet of electrons and is covalently bound to one of the nitrogens, and electrostatically coordinated to the lone pair of the other nitrogen. In alternative **e**, the position of the positive charge is not determined, *i.e.*, the positive charge may be spread anywhere within the three centre N–X–N bond. If **e** is symmetric with equal N–X distances, the interaction type might be considered as being comprised of two equal N···X halogen bonds. Similarly, the unsymmetrical alternatives, **c** and **d**, might also be considered to involve one classic covalent N–X bond, and one classic N···X halogen bond. The N–X–N interactions have often been related to the similar bonding seen in the trihalide ions.[166, 170] In addition, their

similarity with hydrogen bonds, where a central hydrogen is shared between two nitrogen donors, has also been noticed.[173]

So far only $[N–X–N]^+$ cations comprised of bromine(I) and iodine(I) are known. However, calculations by Sabin suggests that Py_2F^+ and Py_2Cl^+ cations might be stable enough to exist, and that, if they do, they are expected to have linear N–X–N bonds.[173] In Figure 15, a suggested molecular orbital model describing the favoured orbital overlap for the three-centre-four electron N–X–N bond of the Py_2X^+ cation is illustrated. The filled non-bonding orbital of the nitrogens overlap with one empty p orbital (p_z in Figure 15) of Br^+ or I^+.[166] For the N–I–N interaction, extra stabilisation may result from an efficient orbital overlap of a d orbital of I^+ and the nitrogen p-orbitals, which are involved in the aromatic system of the complexing pyridines.[163, 166]

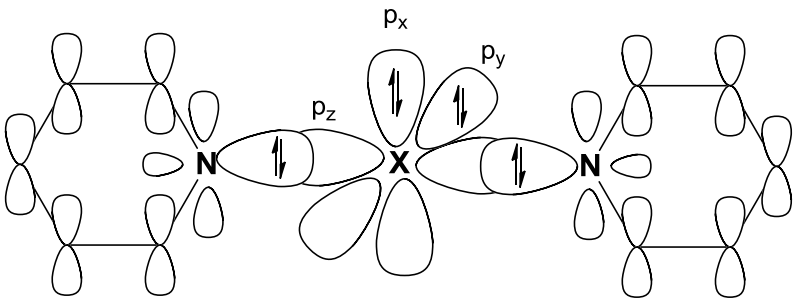

Figure 15. Molecular orbital model of the N–X–N interaction for the Py_2X^+ cation.

Some of the $[N–X–N]^+$ halonium complexes are used as synthetic reagents, acting as sources of electrophilic halogens. Of these complexes, the most commonly used electrophilic halogenation agent is bis(pyridine)iodonium tetrafluoroborate, IPy_2BF_4 (Figure 13), also referred to as Barluenga's reagent.[174] This is a very stable, mild, and powerful reagent with applications in a wide range of synthetic transformations involving I^+ transfer, such as iodination of unsaturated compounds (alkenes, alkynes and aromatics),[10, 175-176] halocyclisation reactions, oxidation of alcohols,[177] and glycosylation reactions.[178-179] Bis(*sym*-collidine)iodonium (IDCP) and bromonium perchlorates ($(coll)_2BrClO_4$) (Figure 13),[180-181] and, in particular, the corresponding hexafluorophosphates ($(coll)_2IPF_6$ and $(coll)_2BrPF_6$), are also often used as electrophilic halogenation agents, mainly in halocyclisation reactions.[12-13, 182-185] Other examples are halodecarboxylation,[186] halodephosphorylation,[187] and oxidation reactions.[188]

3 SYMMETRIC AND ASYMMETRIC STRUCTURES

For any molecular structure, *i.e.*, neutral molecule, ion, or complex, that is comprised of symmetrically arranged atoms, but has the possibility to exist as either a static, single symmetric structure, or as two equal, interconverting tautomers, there is one fundamental question to answer: is the structure being considered symmetric or asymmetric? Asymmetric in this case means that the atoms of the molecular structure in question are arranged unsymmetrically, and should not be confused with the term asymmetric used to describe chiral molecular structures. Some examples of such structures that could either be represented as single symmetric or asymmetric structures with two interconverting tautomers are depicted in Figure 16; hydrogen phthalate (**11**), *N*,*N'*-diphenyl-6-aminofulvene-2-aldimine (**12**), tetramethylethylenebromonium ion (**4b**), triiodide anion (**13**), and bis(pyridine)bromonium perchlorate (**14**). The first two examples, **11** and **12**, both represent structures with hydrogen bonding involved, the hydrogens being coordinated between two identical oxygen or nitrogen electron donors. In the symmetric structures (**11-*sym*** and **12-*sym***), the hydrogen involved in the hydrogen bond is centrally located with equal distance to each O or N electron donor. However, in the asymmetric structures (**11-*asym*** and **12-*asym***), the hydrogen is always closer to one of the electron donors. Halonium ions are typically described as cyclic, three-membered ring structures. The third example illustrates that the symmetric 1,2-bridged bromonium ion **4b-*sym*** might also be represented as an asymmetric structure (**4b-*asym***) comprised of two equilibrating β-bromocarbenium ions. The linear triiodide anion is an additional example of a structure that could be symmetric with the middle iodine centred (**13-*sym***) or asymmetric with two unequal I–I distances (**13-*asym***). The last example represents a $[N–Br–N]^+$ halonium complex, which might have the halogen either centrosymmetrically arranged (**14-*sym***) or closer to one of the nitrogens (**14-*asym***). In solution, the two tautomers of the asymmetric structures (Figure 16b) are continuously interconverting in an equilibrium process. On the other hand, for asymmetric structures in crystals the unsymmetrical arrangement of the interacting atoms is more fixed, and one of the possible tautomeric forms may be dominating.

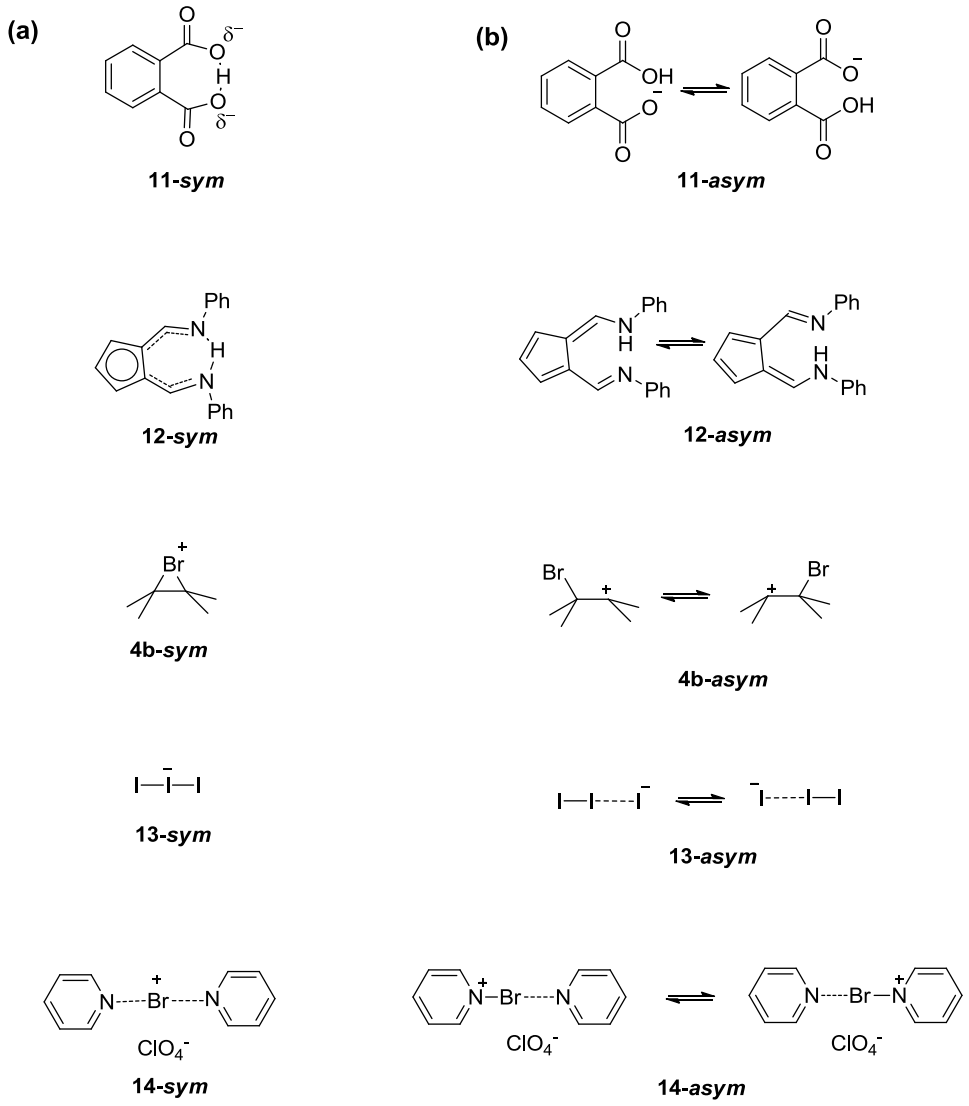

Figure 16. (a) Static, symmetric and **(b)** asymmetric structures of molecules and ions with symmetrically arranged atoms. Asymmetric structures in solution exist as two equilibrating tautomers.

3.1 SYMMETRIES IN SOLUTION

A method of classifying symmetric and asymmetric molecular structures in solution is based on the shape of the electrostatic energy potential well of the structure in question.[19] Asymmetric systems with two equilibrating tautomers follow a double-well energy potential, with the two equivalent energy minima separated by a high or low energy barrier. Considering a hypothetic asymmetric N–X–N bond of a $[N–X–N]^+$ halonium complex (Chapter 2, Section 2.3), one factor determining the height of the energy barrier is the distance between the identical nitrogen electron donors. Thus, if the N···N distance is large, the double-well has a high energy barrier, and if the nitrogens are close the energy barrier is low. The closer the nitrogens are to each other, the

stronger the bonding interaction between. When the nitrogens get close enough, the two energy minima merge into a single one, and the N–X–N bond gets symmetric, with the halogen in the middle. As a consequence, symmetric molecular structures have single-well energy potentials. In Figure 17, the three types of energy potential wells are pictured. For the illustration the asymmetric and symmetric N–X–N bonds are selected. To distinguish between the different types of energy potential wells of a certain molecular structure is not always easy. Particularly difficult is to differentiate between the double minima separated by a low energy barrier and a single minimum. However, usually, it is easy to distinguish an asymmetric high-barrier double well (Figure 17a) from the two other possible energy potential wells (Figure 17b, c), as the two equilibrating tautomers will give separate signals in an NMR spectrum.

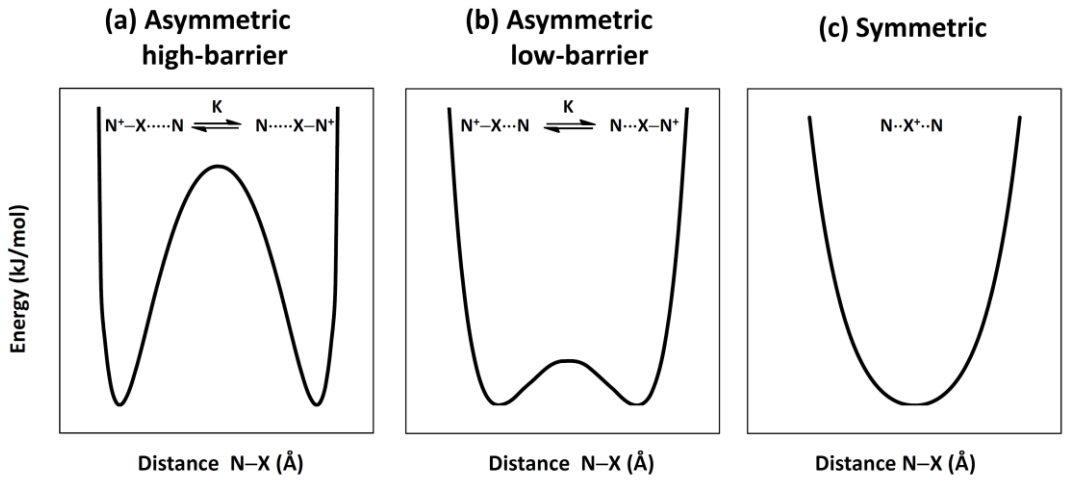

Figure 17. Electrostatic energy potential wells for an asymmetric **(a, b)** or symmetric **(c)** $[N–X–N]^+$ halonium complex; **(a)** double-well with high energy barrier, **(b)** double-well with low energy barrier, and **(c)** single well.

Equivalent tautomers, following a double-well energy potential, that are in a slow equilibrium on the NMR time-scale, give rise to two sets of sharp NMR signals, one for each tautomer.[189] If the equilibrium rate constant K increases, the two sets of signals come closer together. For an even faster equilibrium, the signals get broadened, and eventually overlap and coalesce. Finally, if the rate increases further, only one set of sharp averaged signals can be observed for both tautomers. As a result, both single symmetric structures and asymmetric structures with fast equilibrating tautomers give rise to one set of NMR signals, even at low temperatures. Figure 18 illustrates the ^{13}C NMR signals of one particular carbon pair for a symmetric structure and for the corresponding asymmetric structures with either slowly or rapidly equilibrating tautomers.

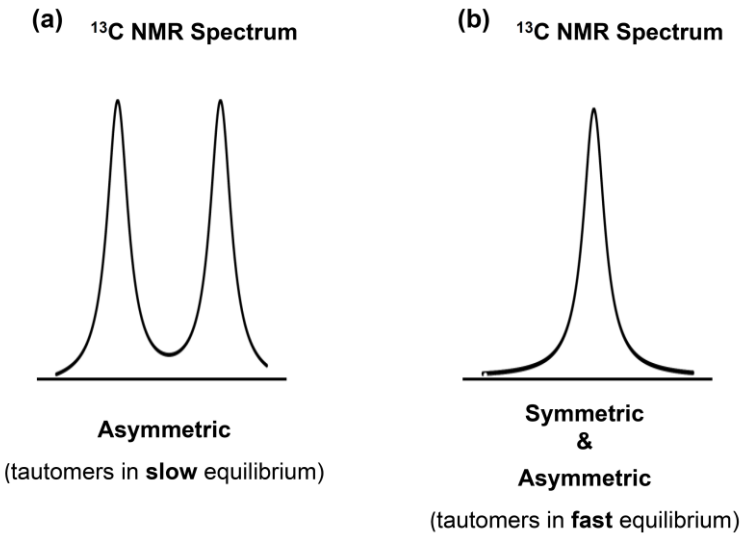

Figure 18. ^{13}C NMR signals for a matching carbon pair of **(a)** asymmetric structures with tautomers in slow equilibrium, and **(b)** symmetric or asymmetric structures with tautomers in fast equilibrium.

A method used to distinguish symmetric structures from asymmetric ones with rapidly interconverting tautomers in solution is Isotopic Perturbation of Equilibrium (IPE) NMR.[190-192] This method has been applied successfully to symmetry evaluations of *e.g.*, structures containing O–H–O and N–H–N hydrogen bonds,[193-197] carbocations,[198-202] halonium ions[203-204] and metal chelate complexes.[205] So far, only asymmetric hydrogen bonds have been revealed by IPE NMR.[193] Symmetric structures have been reported for the some carbocations[198, 206] and metal chelate complexes.[205] Hitherto, IPE NMR has never been used to evaluate the symmetry of $[N–X–N]^+$ halonium complexes. The methodology is described in detail in Chapter 5.

3.2 Symmetries in Crystals

The symmetries found in crystals seem to depend to a large extent on the molecular packing forces and on the counter ions, if present. Both symmetric and asymmetric structures of I_3^- ions have been observed in solids.[128, 154, 207-209] However, the corresponding Br_3^- ions are often found to be asymmetric.[207] X-ray studies of $[N–X–N]^+$ halonium complexes generally provide symmetric structures for the iodonium complexes,[167-169] whereas the bromonium complexes often show unsymmetrically arranged N–Br–N bonds.[166, 170-171] IR spectroscopic studies of the Py_2Br^+ cation with various counter ions indicated an asymmetric structure of the cation complexed with the counter ion ClO_4^- or Br_3^-, but a symmetric structure in complex with PF_6^- as counter ion.[159] This illustrates the influence of the counter ion on the symmetry properties in crystals. Several examples of crystalline, symmetric structures involving hydrogen bonds are reported.[210-212]

4 OBJECTIVES OF THIS THESIS

The overall goal of this thesis work has been to determine the symmetries of two different types of symmetrically substituted halonium complexes in solution, *i.e.*, investigate whether their molecular structure is symmetric or asymmetric. Both complex types are related to electrophilic halogenations; either as reagents or intermediates. A static, symmetric structure follows a single-well energy potential, whereas an asymmetric structure is comprised of two tautomers in rapid equilibrium, thus following a double-well energy potential. Symmetric structures are assumed to involve stronger interactions than the corresponding asymmetric structures.[19] The aims of each halonium complex type are described in the two sections below.

4.1 BIS(PYRIDINE)-BASED [N–X–N]$^+$ HALONIUM TRIFLATE COMPLEXES

This part of the thesis focuses on the symmetry evaluation of the [N–X–N]$^+$ halogen bond of three types of bis(pyridine)-based halonium triflate complexes. The three complexes studied are depicted in Figure 19; bis(pyridine)halonium triflate **16a,b**, 1,2-bis(pyridine-2-ylethynyl)benzenehalonium triflate **17a,b**, and 1,2-bis((4-methylpyridine-2-yl)ethynyl)benzene-halonium triflate **18a,b**, respectively. Only the static, symmetric structures are showed.

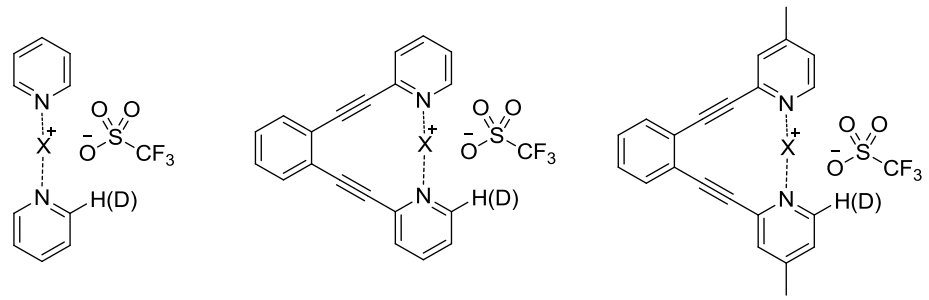

Figure 19. Static, symmetric bis(pyridine)-based [N–X–N]$^+$ halonium triflate complexes.

The specific aims of this study were the following:

1. Synthesis of the bromonium and iodonium triflate complexes **16a,b-18a,b**, and their corresponding mono-deuterated analogues **16a,b-*d*-18a,b-*d*** (Figure 19).
2. Evaluation of the symmetries of all [N–X–N]$^+$ complexes (**16a,b-18a,b**) in solution by analysing mixtures of non-deuterated and mono-deuterated complexes for each complex

type, using the specific NMR spectroscopic method Isotopic Perturbation of Equilibrium (IPE).

3. Evaluation of the structural influence on the symmetries by comparing the three different $[N–X–N]^+$ complex types with each other, comparing the bromonium and iodonium complexes separately. The major structural difference between **16** and **17** is the distance between the two pyridine rings; in **16** the distance can be adjusted, but in **17** it is restricted. The structural difference between **17** and **18** is the presence of the electron donating 4-methyl substituents in the pyridine rings of **18**.
4. Investigation of the influence of solvents of different polarities on the symmetries of the $[N–X–N]^+$ complexes by means of IPE NMR spectroscopy.
5. Determination of how strongly the negatively charged triflate ($CF_3SO_3^-$) counter ion coordinates to the $[N–X–N]^+$ complexes.
6. Evaluation and comparison of the experimentally determined symmetries with computational DFT calculations.

4.2 Ethylenehalonium Ions

This particular study addresses the symmetry of two classes of ethylenehalonium ions; ethylenehalonium ions **19a,b**, and dimethylethylenehalonium ion **20a,b**, respectively. Previously, it has been shown that both **19a,b** and **20a,b** are symmetric in solution under stable ion conditions. However, the technique previously used is not sensitive enough to differentiate between a static, symmetric and an asymmetric structure, originating from a rapid exchange of unsymmetrical tautomers faster than the NMR time-scale. The single symmetric structures of **19a,b** and **20a,b**, respectively, are shown in Figure 20.

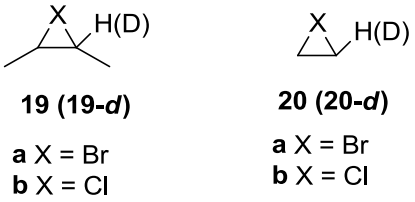

Figure 20. Symmetric ethylenehalonium ions

The specific aims of this investigation were the following:

1. Synthesis of mono-deuterated precursors of the bromonium ions (**19a-*d*** and **20a-*d***) and the chloronium ions (**19b-*d*** and **20b-*d***) of both ethylenehalonium classes (Figure 20).

2. Preparation of mixtures of non-deuterated (**19a,b** and **20a,b**) and mono-deuterated (**19a,b-*d*** and **20a,b-*d***) halonium ions, each class separately, from their precursors under stable ion conditions at low temperature.
3. Evaluation of the halonium ion symmetries by IPE NMR spectroscopy.

5 EQUILIBRIUM ISOTOPE EFFECTS

Equilibrium isotope effects are observable when the equilibrium constant, K, of a reaction is different for compounds that differ in isotope composition. When the bond to an isotopic atom is broken or formed during the reaction course, the isotope effect is referred as primary. The isotope effect is termed secondary when the isotopic bond is neither broken nor formed. In this thesis, all isotope effects are secondary ones.

5.1 DEUTERIUM ISOTOPE EFFECTS ON ^{13}C NMR SPECTRA

Isotopic substitution of a protium (^{1}H) with a deuterium (^{2}H) in a certain molecule gives rise to significant changes of its NMR spectra.[191, 213-215] Due to different Larmor frequencies of deuterium and proton (^{2}H 61.4 MHz, ^{1}H 400 MHz for a 400 MHz spectrometer),[216] the signals of the replaced proton by deuterium are removed from the ^{1}H NMR spectrum of the molecule. The magnetic properties of deuterium also affect the ^{13}C NMR spectra to a large extent. The signal-to-noise ratio is reduced due to several factors, *e.g.,* ^{13}C signal broadening resulting from the deuterium quadrupole moment, signal splittings from ^{13}C-^{2}H couplings, and reduced nuclear Overhauser enhancement as the result of proton removal. The most significant effects of deuterium substitution on the ^{13}C NMR spectra are caused by the nucleus mass difference between the two hydrogen isotopes, ^{1}H and ^{2}H. The different masses results in changes of the vibrational and rotational frequencies within the molecule, which in turn changes the average ^{13}C nuclear shieldings. The resulting chemical shift alterations caused by the nuclear motion changes are called isotope shifts.

The Born-Oppenheimer approximation provides a theoretical description of isotopic substitution on molecular properties, and the origination of isotope shifts.[217] According to this approximation, the electronic and nuclear motion of a molecule can be separated. The electronic energy depends on the nuclear charges, the nuclei location of the constituent atoms of the molecule, and on the number of the electrons present, but is independent of the masses of the nuclei. A function of the fixed position of the nuclei determines the electronic energy, and the resulting electronic energy surface is the same as the potential energy surface for the motion of the nuclei. Thus, the changes in nuclear average shielding and resulting isotope shifts are nuclear mass effects resulting from motion of nuclei of different masses (*e.g.,* ^{1}H and ^{2}H isotopes) on the same potential energy surface. Different nuclear masses have different zero-point vibrational levels in a potential energy

diagram; the heavier nucleus having the lowest zero-point energy. In Figure 21, the potential energy well showing the zero-point energy levels for C–H and C–D stretching vibrations is illustrated. Due to the anharmonicity of the vibrations, the average C–D bond is 0.003-0.005 Å shorter than the corresponding C–H bond.[218] This bond shortening is the main reason for the increased nuclear shielding effect observed upon deuterium substitution.

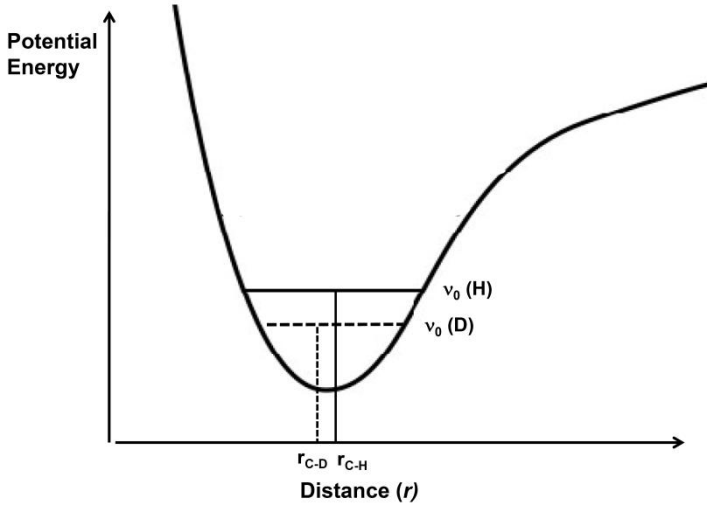

Figure 21. Potential energy well showing zero-point energy levels for C–H and C–D vibrations. The anharmonic nature of the vibrations makes the C–D bond shorter than the C–H bond ($r_{C\text{-}D} < r_{C\text{-}H}$).

5.1.1 Isotope Effects on NMR Chemical Shifts for Static Molecules

The observed isotope shifts, referred to as ${}^{n}\Delta_{obs}$, in a ^{13}C NMR spectrum is the difference between chemical shifts of molecules with and without deuterium, in accordance with Equation 1, where *n* is the number of bonds between the reporter carbon and the deuterium. For static molecules the observed isotope shifts are called intrinsic isotope shifts, ${}^{n}\Delta_0$.

$$ {}^{n}\Delta_{obs} = \delta_{C(D)} - \delta_{C(H)} \qquad \text{(Equation 1)} $$

Notable from observations of isotope shifts are some general trends concerning the magnitudes and sign of the intrinsic isotope shift.[213-214] Upon substitution with a heavier deuterium isotope the ^{13}C NMR signal of the nearby carbon, one or two bonds away from the deuterium, changes shifts towards lower frequencies, and becomes more shielded. This results in negative ${}^{1}\Delta_{obs}$ and ${}^{2}\Delta_{obs}$ isotope shifts. The magnitude of the isotope shift is dependent on how distant the deuterium

is from the reporter ^{13}C carbon. Hence, the one-bond isotope shifts are larger, in absolute values, than the two-bond or three-bond isotope shifts ($^{1}\Delta_{obs} > {}^{2}\Delta_{obs}$). The magnitude of the isotope shift is also more or less proportional to the number of equivalent atoms that have been substituted by isotopes, *i.e.*, the isotope shifts are additive ($^{1}\Delta_{obs}$ for $CD_3 \approx 3$ x $^{1}\Delta_{obs}$ for CD).[219] The one-bond isotope shifts are approximately in the range of 0.3 ppm per deuterium, and the two-bond isotope shifts are roughly 0.1 ppm per deuterium, typically one-third to one-quarter of the one-bond shifts.[213] Long-range isotope shifts, for carbons more than two bonds away from the deuterium are, if at all observable, generally very small but can be both positive and negative. However, they are also sensitive to secondary electronic factors related to the electronic transmission pathways within the molecule, such as π–delocalisation in aromatics or in highly conjugated systems.[220-221] These electronic factors are responsible for the signs of the long-range isotope shifts. Also noteworthy to mention are some general characteristics of the one-bond isotope shifts.[214] In general, the one-bond isotope shifts increase with increasing bond order and decreasing bond length between the reporter ^{13}C carbon and the deuterium. In addition, the magnitudes of the one-bond isotope shifts often correlate with the chemical shift of the reporter ^{13}C carbon; less shielded carbons normally have larger isotope shifts. Interactions between the C–D bond and the lone pairs of O, S or N atoms have also shown to influence the magnitude and sign of the isotope shifts.[221-223] Normally, the intrinsic isotope shifts are independent of temperature. However, changes in temperature might effect the nuclear geometry populations and average bond lengths by solution density and polarity changes.[224-227] Thus, a small temperature-dependence may be observable for intrinsic isotope effects.

5.1.2 Isotope Effects on NMR Chemical Shifts for Equilibrating Molecules

Equilibrium isotope effects are readily observed when isotopic substitution perturbs a degenerate equilibrium, inducing splitting of ^{13}C NMR signals of formerly chemically equivalent nuclei. Commonly studied equilibrium processes for which the degeneracy is broken upon deuterium substitution are carbocation rearrangement, and tautomerisation reactions. When isotopic substitution disturbs equilibria processes that are not degenerate, the resulting equilibrium isotope are more difficult to distinguish from the intrinsic isotope shifts. However, as equilibrium isotope effects are highly temperature dependent, they are, thus, possible to detect by observing isotope shift changes upon temperature changes. The equilibrium isotope shift, $^{n}\Delta_{eq}$, is generated from the difference between the observed isotope shift, $^{n}\Delta_{obs}$, and the intrinsic isotope shift $^{n}\Delta_{0}$, for the reporter carbon in question *via* Equation 2.

$$^{n}\Delta_{eq} = {}^{n}\Delta_{obs} - {}^{n}\Delta_{0} \qquad \text{(Equation 2)}$$

In addition, the equilibrium isotope shift can be obtained from Equation 3, which requires estimates of the equilibrium constant, K, and the chemical shift difference, Δ, between the individual tautomeric forms in a "frozen-out" dynamic process. The magnitude and sign of equilibrium isotope shifts varies. In principle, the larger constants and chemical shift differences, the larger equilibrium isotope shifts are provided. The temperature dependence of $^{n}\Delta_{eq}$ relates to the temperature dependence of equilibrium rate constant, K, in accordance with the thermodynamic Equation 4, where ΔG° is Gibbs energy in J/mol, R is the gas constant (8.314 J/mol·K), and T is the temperature in Kelvin.

$$\Delta_{eq} = \frac{\Delta(K-1)}{2(K+1)} \qquad \text{(Equation 3)}$$

$$\ln K = \frac{-\Delta G^{\circ}}{RT} \qquad \text{(Equation 4)}$$

For a rapid equilibrium process between equal tautomers of cations (where K = 1), isotopic substitution changes the value of the equilibrium rate constant and makes one of the directions of the equilibrium become preferential over the other (K > 1 for the favoured direction). The favoured direction is determined by the shape of the potential energy curves and the zero-point energy differences of the possible C–H and C–D vibrational levels of the two tautomers or cationic species of the equilibrium. As a rule of thumb, the heavier isotope prefers to make the stiffer bonds, preferring to accumulate in the potential energy minimum with the larger stretching and bending force constant, and the higher zero-point energy.[228-229] In general, deuterium prefers sp^3-hybridised centres to sp^2-centres, mainly because of the difference in the frequency of the out-of-plane bending vibrations.[191] On the same grounds, if there is a choice, deuteromethyl groups tend to be remote from the positively charged centre in carbocations.[191, 228] The reason for the one direction of the equilibrium being favoured over the other is illustrated in Figure 22.[191] The zero-point energy difference for the rearranging cation pair is lowest when the C-D carbon is sp^3-hybridised, and the C-H carbon sp^2-hybridised.

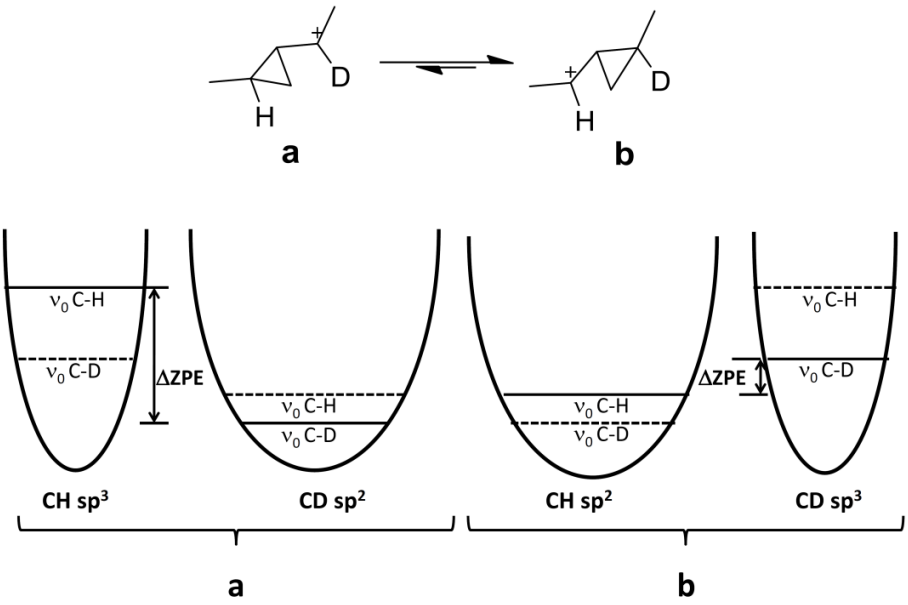

Figure 22. In the equilibrium **a** ⇌ **b**, H and D have two different bonding situations (sp^3 and sp^2). D accumulates in the position where the force constant, vibrational energy, and zero point energy are larger, providing the smallest difference in zero point energy (ΔZPE) between C–H and C–D. The equilibrium is driven to the right, where the hybridisations are sp^3 for C–D and sp^2 for C–H.[191]

It has been shown that deuterium introduction in amines increases their basicity.[193, 230] Thus, for the proton-transfer equilibrium between the pyridinium-d_5 cation and pyridine depicted in Scheme 7, the reaction is driven to the left.[231]

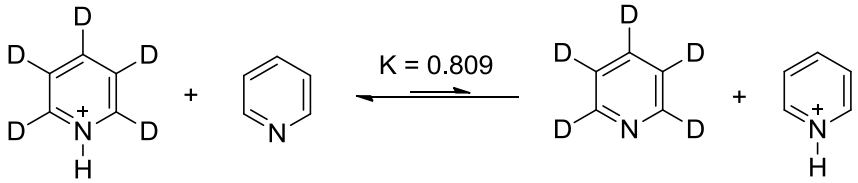

Scheme 7. Proton transfer between pyridinium-d_5 cation and pyridine. The reaction is driven to the left as pyridine-d_5 is more basic than non-deuterated pyridine.[231]

5.2 Isotopic Perturbation of Equilibrium NMR Spectroscopy

The NMR spectroscopic method Isotopic Perturbation of Equilibrium (IPE) is useful for the distinguishment between a single symmetric structure following a single-well energy potential, and equal, asymmetric structures in a rapid degenerate equilibrium following a double-well energy potential (Figure 17, Chapter 3, Section 3.1). As the name implies, the method is based on isotopic substitution, and the generation of equilibrium isotope effects to disturb a possible degenerate equilibrium process, and alter dynamically equivalent NMR chemical shifts. Saunders

and Kates developed IPE NMR to determine the presence of rapid equilibria in carbocations for which the symmetry was in doubt.[192, 206, 232] From the observed isotope shifts, ${}^{n}\Delta_{obs}$, in the ^{13}C NMR spectra of deuterated cyclohexyl and cyclopentyl cations it was concluded that both ions were best represented as single symmetric, delocalised ions, showing intrinsic isotope shifts only, and no obvious temperature dependence as observed for analogous, fast equilibrating cations.[192, 232] Ever since the first IPE NMR symmetry investigations, the method has been applied to a wide range of other chemical systems for which the symmetry has been in doubt.[191] Examples of molecular systems whose symmetry has been evaluated by IPE NMR include carbocations,[198, 201-202, 206, 232-233] conformational equilibria,[234-235] O–H–O and N–H–N hydrogen bonds in proton tautomeric systems,[193-197, 236-238] chelating symmetry of transition-metal complexes,[205, 239] symmetry of trithiapentalenes and analogous systems,[240] and 1,2-bridged halonium ions.[203]

The general requirements of IPE NMR are the analysis of mixtures of non-deuterated and deuterated molecules by ^{13}C NMR spectroscopy, and the measurements of isotope shifts, ${}^{n}\Delta_{obs}$, for the reporter carbons (Equation 1). An asymmetric introduction of deuterium isotopes is necessary for observation of equilibrium isotope effects. Commonly, the isotope shifts are measured over a broad temperature range to determine whether there is any temperature dependent equilibrium process taking place. The observation of large isotope shifts, often positive but not always, that are highly temperature dependent, is an indication of an asymmetric system, in rapid equilibrium; the isotope shifts observed are resulting from both intrinsic and equilibrium isotope effects (${}^{n}\Delta_{obs} = {}^{n}\Delta_{0} + {}^{n}\Delta_{eq}$). In general, for symmetric structures the isotope shifts are small, negative, and attenuate as the number of intervening bonds to the deuterium increase; only intrinsic isotope shifts are observed (${}^{n}\Delta_{obs} = {}^{n}\Delta_{0}$). Noteworthy to mention is that if the chemical shifts difference (Δ, Equation 3) between the reporter carbons of the two tautomeric forms in a "frozen out" equilibrium is small, the equilibrium isotope shifts will also be small. Consequently, the observed isotope shifts obtained from an asymmetric, equilibrating system might be very similar in both magnitude and sign to the isotope shifts expected for a corresponding single symmetric system.

The IPE NMR method has been chosen for evaluation of the symmetry of $[N–X–N]^{+}$ halogen bonds of bis(pyridine)-based halonium complexes, and of 1,2-bridged ethtylenehalonium ions described in this thesis (Chapter 6 and 7).

6 BIS(PYRIDINE)-BASED HALONIUM COMPLEXES (PAPER I & II)

6.1 BISPYRIDINE HALONIUM COMPLEXES - INTRODUCTION

The existence of solid salts of the bis(pyridine)iodine(I), Py_2I^+, and bis(pyridine)bromine(I), Py_2Br^+, cations has been known for a considerable time.[149-150, 152-153] In the 1950's, UV-Vis spectroscopical studies of iodine or iodinehalides showed significant spectral changes upon their addition to pyridine, which were interpreted as the formation of charge-transfer complexes.[241-242] In addition, conductivity studies indicated formation of ions.[243] In 1957, Popov and Plaum were the first to suggest that Py_2I^+ was possibly a cationic species in solution.[244] Since then, the identity of Py_2I^+ has been confirmed by vibrational spectroscopy (IR and Raman) in a variety of solvents.[155-157, 162] It is now widely accepted that the ionisation of pyridine-halogen complexes in solution occurs *via* the equilibrium $2(Py + IX) \rightleftharpoons 2Py{*}IX \rightleftharpoons Py_2I^+ + IX_2^-$ (X = I, Br or Cl).[161] Polar solvents and/or a decrease in temperature, due to increased dipolar ordering upon cooling, have shown to favour the ionisation.[161-162] Haque and Wood investigated Py_2I^+ and Py_2Br^+ cations with various negatively charged counter ions (BF_4^-, PF_6^-, and ClO_4^-) in solution by IR and Raman spectroscopy.[157] From the vibrational spectra it was concluded that the N–X interactions of the cations were strong, and that the N–I–N and N–Br–N interactions were linear, and had a centrosymmetric arrangement. It was also proposed that the coplanar arrangement of the pyridine rings found in the crystal for Py_2I^+ cation remains in solution.[157] Contemporary computational calculations implied that, the halogen atom oscillates between the two nitrogens following a flat, single-well energy potential.[245] Despite the preliminary indications summarised above, the symmetry of the N–X–N interaction of Py_2X^+ cations in solution has still not yet been studied in detail. Computational prediction proposes symmetric structures; however, no clear experimental evidence has yet been given.

There are a few reported applications of the solid $[N–X–N]^+$ complexes **16a** and **16b** reported. The $[N–Br–N]^+$ complex **16a** has previously been used as an electrophilic bromine source in mechanistic studies of Br^+ transfer to olefinic acceptors for halocyclisation reactions, and alkene bromination (Figure 23).[171] Very few examples of the use of the $[N–I–N]^+$ complex **16b** as a synthetic reagent and a source of electrophilic iodine are available. One such example is illustrated in Figure 24 below.[246] However, the tetrafluoroborate analogue (IPy_2BF_4) of **16b**, often

referred to as Barluenga's reagent, is a common electrophilic reagent, used in a wide range of organic synthesis applications involving I^+ transfers (Chapter 2, Section 2.3).[10, 174-175, 177]

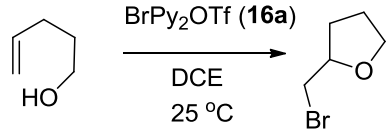

Figure 23. Halocyclisation of 4-penten-1-ol with $[N–Br–N]^+$ complex **16a** as reagent.[171]

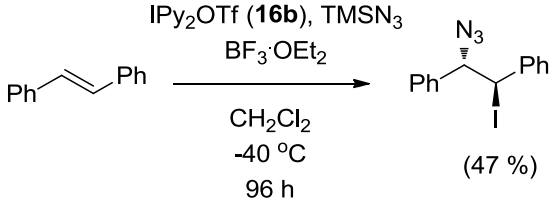

Figure 24. Azido-iodination reaction of an alkene with $[N–I–N]^+$ complex **16b** and $TMSN_3$ as reagents.[246]

An X-ray crystal structure of the $[N–Br–N]^+$ complex **16a** reveals a close to linear (178.4°) but asymmetric N–Br–N arrangement, the two N-Br distances being slightly unequal (2.075 and 2.107 Å), and the two pyridine rings slightly nonplanar.[171] No crystal structure of the corresponding $[N–I–N]^+$ complex **16b** has so far been reported. However, X-ray studies of crystalline $Py_2I^+ I_3^-$ and Barluenga's reagent $Py_2I^+ BF_4^-$ have been solved.[154, 247] Both $[N–I–N]^+$ complexes were found to be nearly planar and symmetric, with linear N–I–N arrangement, and equal N-I distances (2.164 Å for $Py_2I^+ I_3^-$ and 2.259 Å for $Py_2I^+ BF_4^-$).

6.2 1,2-Bis(Pyridin-2-ylethynyl)Benzene-Halonium Complexes

- Introduction

The ability of 1,2-bis(pyridinyl-2-ethynyl)benzene **21** to act as a coordinating ligand of metals is widely recognised, and several complexes have been characterised by X-ray crystallography. Examples of silver(I) (**23**),[248] palladium(II) (**24** and **25**),[248-250] Cu(I) (**26**)[251] and Cu(II) (**27**)[252] complexes with one or two molecules of the coordinating dipyridyl ligand **21** are depicted in Figure 25. In all complexes shown, the metal is centrally located between the two pyridine nitrogens with a close to linear N–M–N angle (M = metal). Introduction of electron donating methyl groups in the *para*-positions of ligand **21** proved to have a stabilising effect on palladium(II) chloride complexes in terms of reactivity. Complex **24b** with the *para*-dimethylated **22** as ligand was therefore considered to be more stable than **24a**.[249]

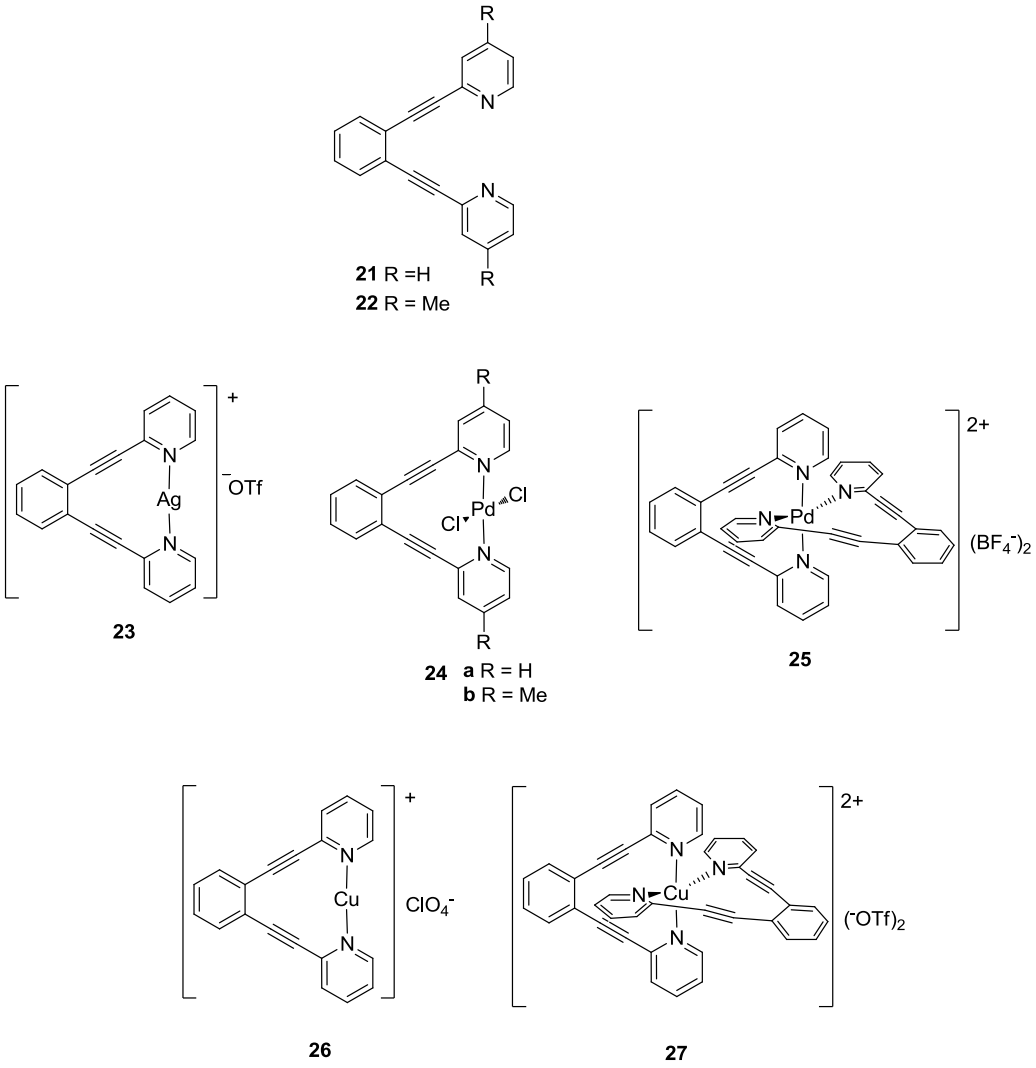

Figure 25. Metal complexes with 1,2- bis(pyridinyl-2-ethynyl)benzenes (**21** and **22**) as chelating ligands.[248-252]

Based on the chelating properties of ligand **21**, and on the N-Br distances reported for related $[N–Br–N]^+$ bromonium complexes,[166, 170] Brown and co-workers assumed that an electropositive bromine(I) would coordinate perfectly between the pyridines of **21**. Their assumption proved to be right, and they successfully prepared the bromonium triflate complex **17a**, which was utilized in mechanistic studies of Br^+ transfer to a variety of olefinic acceptors (*e.g.*, 4-pentenoic acid, cyclohexene, and Ad=Ad) by UV or NMR spectroscopy (Figure 26).[171] Attempts to obtain the crystal structure of **17a** however failed.[171]

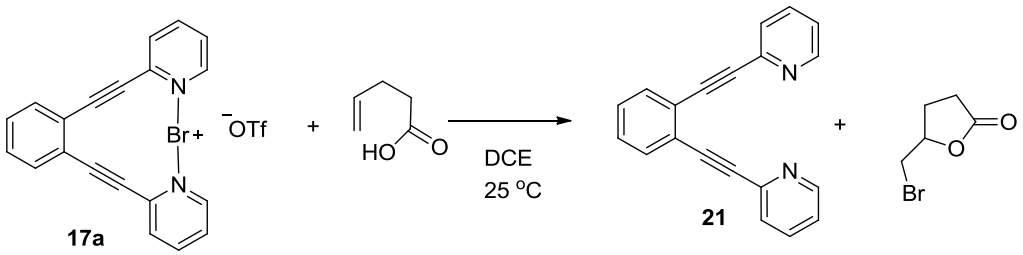

Figure 26. Halolactonisation of 4-pentenoic acid with $[N–Br–N]^+$ complex **17a** as reagent.[171]

6.3 Symmetry Investigation –Description

The main goal of this particular study was to determine the symmetry of the $[N–I–N]^+$ and $[N–Br–N]^+$ bonding interactions in the triflate complexes **16a,b**, **17a,b** and **18a,b** in solution. In a symmetric arrangement, the halogen is centrally located with equal distances to both nitrogens (Figure 27a), whereas in an asymmetric arrangement the halogen is jumping between the nitrogens in a fast equilibrium, always being closer to one of the two nitrogens (Figure 27b). A single symmetric structure is represented by a single-well energy potential, whereas asymmetric, rapidly equilibrating structures are represented by a double-well energy potential (Chapter 3, Section 3.1). If the equilibrium is degenerate, single symmetric structures and fast interconverting tautomers are indistinguishable on the NMR time-scale as both give one single set of signals in their corresponding NMR spectra. All $[N–X–N]^+$ complexes included in this thesis were observed to be single symmetric or rapidly equilibrating asymmetric structures in a degenerate equilibrium as indicated by single set of signals in their NMR spectra.

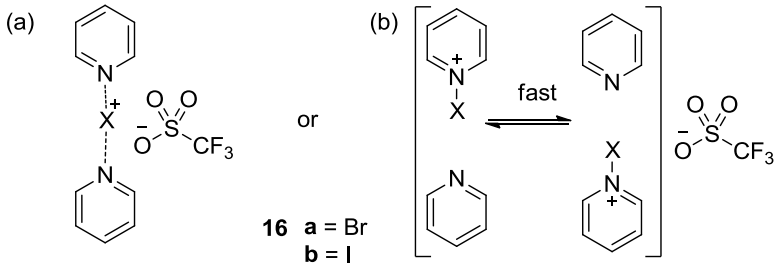

Figure 27. (a) Symmetric and **(b)** asymmetric $[N–X–N]^+$ bonding interaction illustrated for $[N–X–N]^+$ halonium triflate complexes **16a,b**.

The symmetry of the $[N–X–N]^+$ complexes is, most likely, to be influenced by the chemical environment surrounding them. Polar solvents might benefit the asymmetric $N^+–X^{\cdots}N$ arrangement, which is more polar due to the concentration of positive charge on one of the nitrogens than the corresponding symmetric $N^{\cdots}X^{+\cdots}N$ arrangement having the positive charge

more delocalised. For the same reason, symmetric $N^{\cdots}X^{+\cdots}N$ geometry might be preferred in non-polar solvents. The counter ion might also influence the symmetry of the $[N–X–N]^+$ complexes. Depending on its coordination and ion pairing ability, the counter ion might induce either symmetric or asymmetric arrangement of the N–X–N bonding interaction. In addition, the distance between the two electron donating pyridine nitrogens might be crucial for the symmetry of the $[N–X–N]^+$ complexes. In the bispyridine complexes **16a,b** the N–N distance can be varied, and adjusted to the most favourable interaction. On the other hand, for the $[N–X–N]^+$ complexes of the 1,2-bis(pyridinyl-2-ethynyl)benzene ligands, **17a,b** and **18a,b**, respectively, the N–N distance is restrained. Reasonable to assume, the formation of symmetric N–X–N bonding interaction would, therefore, be somewhat more difficult for the two latter complexes **17a,b** and **18a,b** with their N–N distances being restricted. Symmetric hydrogen bonds are suggested to be more stable and stronger than their asymmetric analogues.[19, 253] Originating from their proposed similarity,[254] symmetric N–X–N bonds may be stronger than the corresponding asymmetric bonds too. The strength of the N–X–N interaction is assumed to be related to the electron density on the nitrogens. Therefore, comparison of the nitrogen electron densities between the different $[N–X–N]^+$ complexes might provide insights in the required characteristics of a molecular structure to give a strong N–X–N bonding interaction.

The fact that the halogen of the $[N–X–N]^+$ cations is located between two identical electron donors, and with the pyridine rings being coordinated in a linear fashion, suggests that the $[N–X–N]^+$ interaction may involve halogen bonding, consisting of either two identical N···X halogen bonds, or one classic covalent N–X bond, and one classic N···X halogen bond. The former category of halogen bonding represents a symmetric interaction and the latter an asymmetric interaction. The symmetry of hydrogen bonds for similar molecular systems comprised of identical electron donors has been extensively studied in solution with IPE NMR spectroscopy.[193] Consequently, as halogen bonds are analogous to hydrogen bonds,[5, 18] the IPE NMR spectroscopic method, was chosen for the symmetry evaluation of the $[N–Br–N]^+$ complexes **16a-18a** and the $[N–I–N]^+$ complexes **16b-18b**, respectively. Since the IPE NMR technique relies on the observation of isotope shifts, deuterated and non-deuterated isotopologues of all $[N–X–N]^+$ halonium complexes (**16a,b-18a,b**) were required. To observe a large isotope effect, it is preferable to introduce a deuterium substituent close to the site of the interaction. Deuteration increases the electron density as the shorter C–D bond has shown to be more electron

donating than a C–H bond.[230, 255] In aliphatic amines, Perrin and co-workers have observed that deuteration synperiplanar to the electron lone pair of the nitrogen increases its basicity.[230, 255] The basicity of the aromatic nitrogen of pyridine is, also, expected to be increased upon such deuteration. Hence, by introducing a deuterium on the carbon closest to the nitrogen of one of the pyridine rings, the basicity of this nitrogen is expected to increase.[230, 256] This will perturb any equilibrium processes the nitrogens may be involved in. The non-deuterated and mono-deuterated $[N–X–N]^+$ complex isotopologue pair (**16a,b-18a,b**) included in the IPE NMR symmetry studies are depicted in Figure 28.

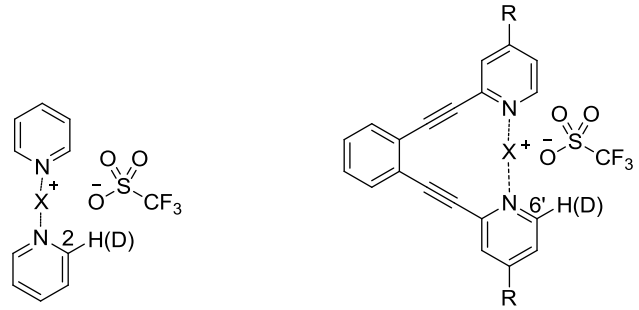

16 (16-*d*) a X = Br
b X = I

17 (17-*d*) a X = Br, R = H
b X = I, R = H
18 (18-*d*) a X = Br, R = Me
b X = I, R = Me

Figure 28. Non-deuterated $[N–X–N]^+$ complexes (**16a,b-18a,b**), and mono-deuterated $[N–X–N]^+$ complexes (**16a,b-*d*-18a,b-*d***),

The corresponding non-deuterated and mono-deuterated $[N–H–N]^+$ complexes (**27a,b-30a,b**) were included as references of asymmetric rapid equilibrating systems (Figure 29a). Included were also non-deuterated and mono-deuterated free pyridine (**31**), and the free chelating ligands **21** and **22**, respectively, as references for static symmetric structures (Figure 29b). The references were included to make the symmetry evaluations more reliable as isotope effects in themselves may be difficult to interpret just from the magnitude or temperature dependence, especially, if the ^{13}C chemical shift difference (Δ, Equation 3) between the two tautomeric forms ($N–X^+$ and free N:) is small.

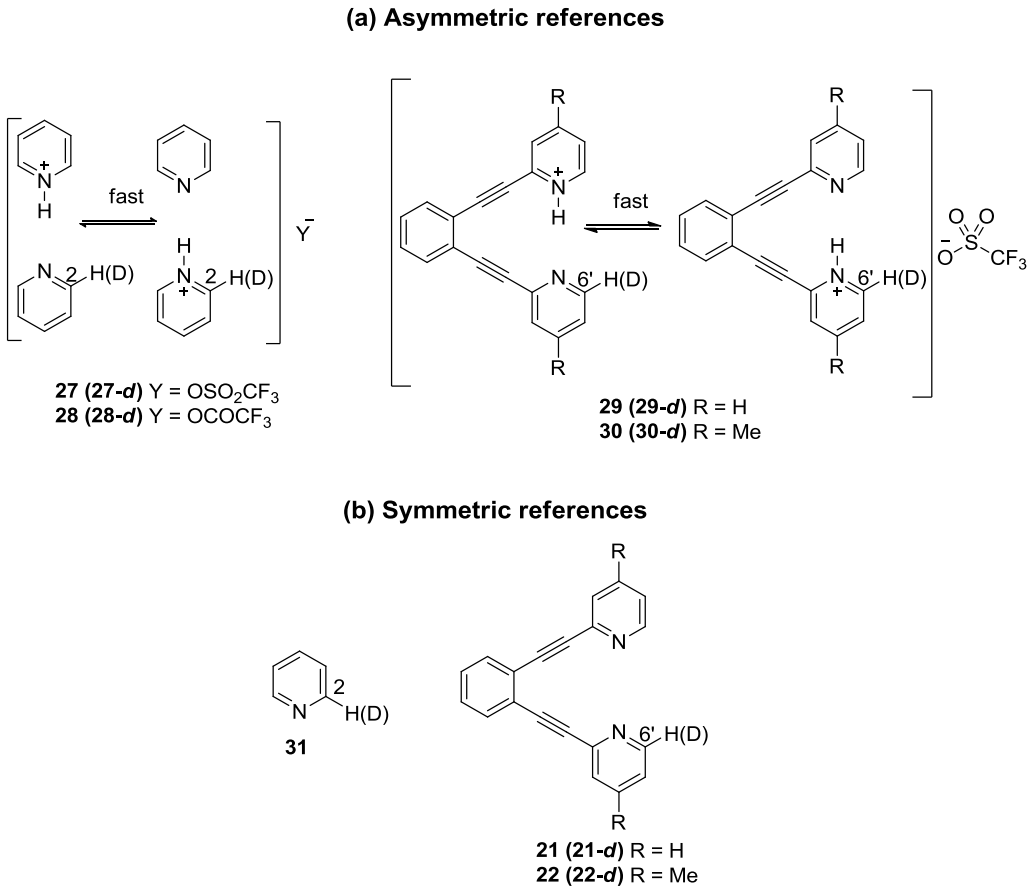

Figure 29. (a) Non-deuterated and mono-deuterated asymmetric reference $[N–H–N]^+$ complexes **27a,b-*d*-30a,b-*d***), and **(b)** symmetric, references (**31**, **21**, **22** and **31-*d***, **21-*d***, **22-*d***).

To investigate the effect of environment polarity, the symmetries for complexes **16a,b-18a,b** and their references were explored in two aprotic solvents; CD_2Cl_2 (dichloromethane $\varepsilon = 8.9$)[257] and CD_3CN (acetonitrile $\varepsilon = 37.5$),[257] respectively. As the counter ion was shown to influence the symmetry of $[N–X–N]^+$ complexes in crystals, it might also be of importance for the symmetry of $[N–X–N]^+$ complexes in solution.[159] Therefore, included in this study were also the investigations of the ion pairing ability of the anionic triflate ($CF_3SO_3^-$) counter ion by ^1H and ^{19}F diffusion NMR spectroscopy for the $[N–X–N]^+$ complexes **16a,b** and **17a,b**, and their asymmetric references $[N–H–N]^+$ complexes **27** and **29**.

As mentioned above, the electron density around the nitrogens of the $[N–X–N]^+$ bonding interaction might affect the interaction strength. To evaluate the influence of the differences in electron density distribution of the pyridine rings on the symmetry of $[N–X–N]^+$ complexes, ^{15}N NMR chemical shifts were determined by ^1H-^{15}N-HMBC experiments. For the same reason, the

^{13}C NMR chemical shifts for the pyridine carbons of the $[N–X–N]^+$ complexes and their references were also compared.

6.4 Synthesis of $[N–X–N]^+$ Complexes and Their References

6.4.1 $[N–X–N]^+$ Complexes and Symmetric References

The syntheses of non-deuterated and mono-deuterated $[N–X–N]^+$ complexes, **16a,b** and **16a,b-*d***, are depicted in Scheme 8. Deuterium was introduced at the C2-position of one of the pyridine rings. As the IPE NMR method is based upon the analysis of mixtures of non-deuterated and deuterated molecules, it was advantageous to prepare the $[N–X–N]^+$ complex **16a,b** as isotopologue mixtures. A synthetic protocol described by Brown and co-workers for the synthesis of **16a** was followed for the halogenations reactions.[171] Approximately equal amounts of pyridine (**31**) and 2-deuteropyridine (**31-*d***) were mixed together with silver triflate, to first generate the corresponding silver(I) complexes. Subsequent addition of Br_2 or I_2 resulted in precipitation of silver halide (AgBr or AgI), and formation of the isotopologue mixture of **16a**, **16a-*d***, and **16a-*d*$_2$**, or **16b**, **16b-*d***, and **16b-*d*$_2$** in high yields. 2-Deuteropyridine (**31-*d***) was either bought from a commercial supplier, or synthesised from 2-bromopyridine (**32**) using two portions of excess Zn dust in D_2SO_4/D_2O at 90 °C.[258]

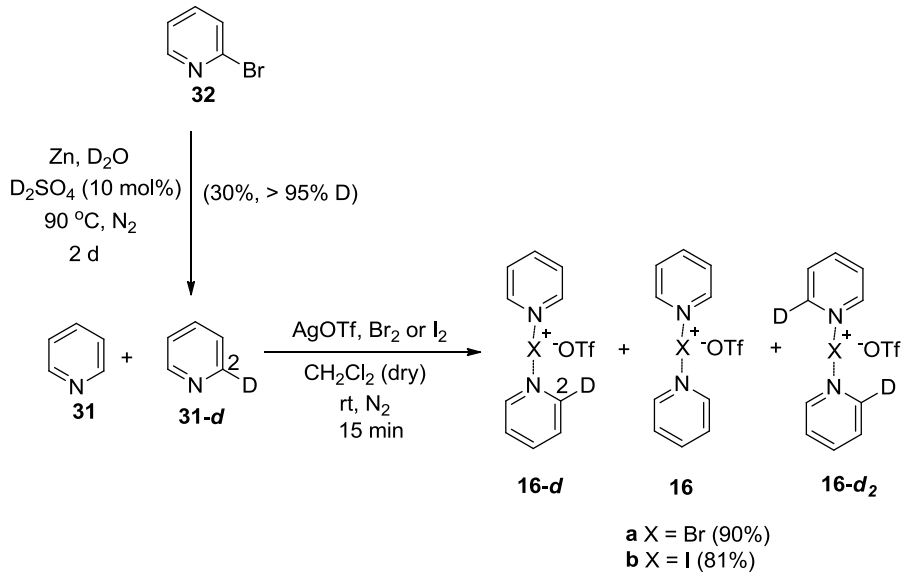

Scheme 8. Synthesis of isotopologue mixtures of $[N–X–N]^+$ complexes **16a** and **16b**.

The $[N–X–N]^+$ complexes **17a,b** and **18a,b** and their mono-deuterated analogues **17a,b-*d*** and **18a,b-*d*** were synthesised in accordance with the routes depicted in Scheme 9 and Scheme 10, respectively. Deuterium was introduced selectively at the C6'-position, next to the nitrogen

interaction site, to cause as large isotope effect as possible. For the syntheses of $[N–X–N]^+$ complexes **17a,b** and **18a,b** a modified version of the protocol previously reported by the group of Brown was followed.[171] With this new procedure (Scheme 9), the Sonogashira coupling reaction[259-260] of 1,2-diiodobenzene (**33**) with ethynylpyridine (**34**) or 2-ethynyl-4-methylpyridine (**35**) was carried out under microwave-assisted conditions,[261] which shortened the reaction time for the generation of di-coupled **21** and **22** considerably. Under microwave heating at 120 °C, 9-10 minutes only were sufficient for the reactions to go to completion, *i.e.*, much shorter time than the 8 hours' reaction time reported by Brown and co-workers.[171] Both di-coupled **21** and **22** were isolated in high yields. 2-Ethynyl-4-methylpyridine (**35**) was synthesised in two steps from 2-chloro-4-methylpyridine (**36**) *via* microwave-assisted Sonogashira coupling with TMS-acetylene, followed by TMS-deprotection with potassium fluoride.[262] Treatment of **21** or **22** with silver triflate, furnished their corresponding silver(I) complexes, which directly upon formation were reacted with either Br_2 or I_2 to generate the $[N–X–N]^+$ complexes **17a,b** or **18a,b** in moderate yields.

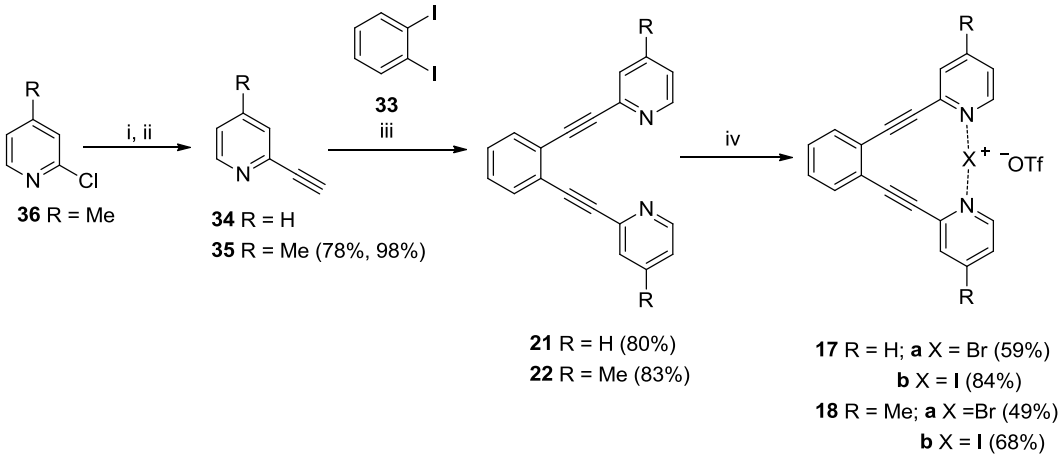

Scheme 9. *Reagents and conditions: (i)* TMS-acetylene, $Pd(PPh_3)_2Cl_2$, CuI, PPh_3, Et_2NH, DMF, MW, 120 °C, 27 min;*(ii)* KF, MeOH, rt, 16 h; *(iii)* 2,3 equiv. **34** or **35**, $Pd(PPh_3)_2Cl_2$, CuI, Et_2NH, DMF, MW, 120 °C, 9-10 min;*(iv)* Br_2 or I_2, AgOTf, dry CH_2Cl_2, rt, N_2, 15 min.

The synthetic protocol for the generation of the mono-deuterated $[N\text{-}X\text{-}N]^+$ analogues **17a,b-*d*** and **18a,b-*d*** is shown in Scheme 10. The synthesis was initiated by a microwave-assisted Sonogashira coupling reaction with 1,2-diiodobenzene (**33**) and ethynylpyridine (**34**) or 2-ethynyl-4-methylpyridine (**35**). To produce the mono-coupled products (**37** or **38**) in adequate yields, **33** was added in excess and microwave irradiation was allowed to proceed for 4 minutes

only. Despite the short reaction time, in addition to the mono-coupled products (**37** or **38**), the corresponding di-coupled products **21** and **22** were isolated in 44 % and 27% yield, respectively.

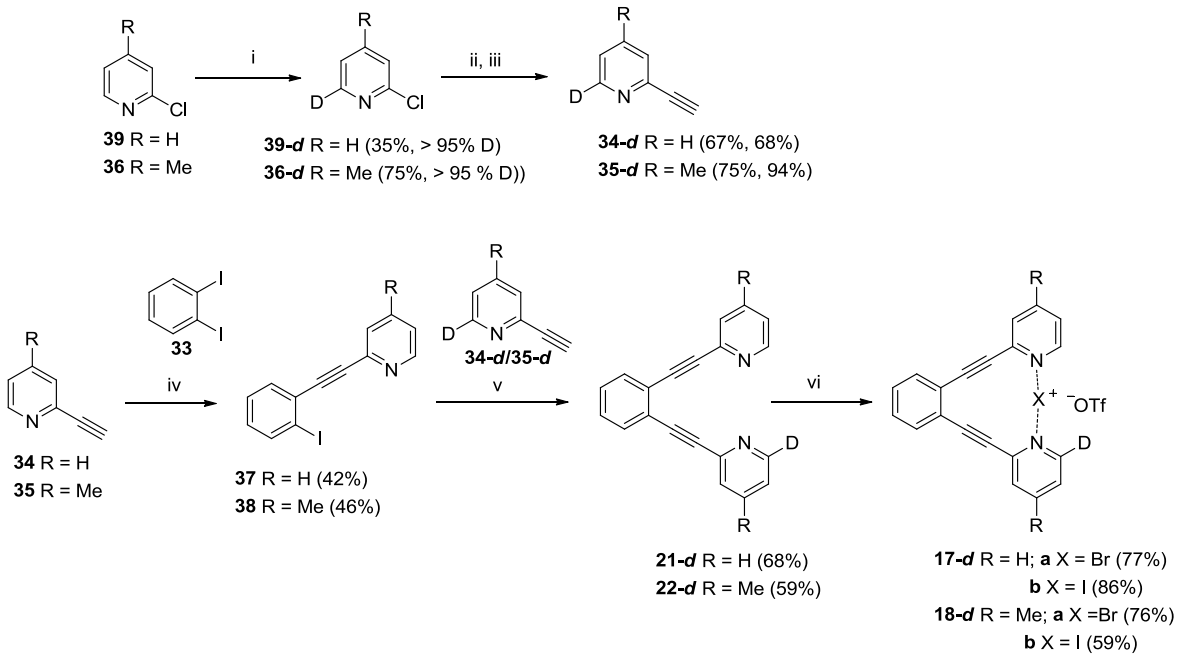

Scheme 10. *Reagents and conditions: (i)* 1. *n*-BuLi-LiDMAE, dry *n*-hexane, -78 °C, N_2; 2. MeOD, -78 °C – 0 °C, 30 min; *(ii)* TMS-acetylene, $Pd(PPh_3)_2Cl_2$, CuI, PPh_3, Et_2NH, DMF, MW, 120 °C, 27 min; *(iii)* KF, MeOH, rt, 16 h; *(iv)* 0.7 equiv. **34** or **35**, $Pd(PPh_3)_2Cl_2$, CuI, Et_2NH, DMF, MW, 120 °C, 4 min; *(v)* 1.5 equiv. **34-*d*** or **35-*d***, $Pd(PPh_3)_2Cl_2$, CuI, PPh_3, Et_2NH, DMF, MW, 120 °C, 13 min; *(vi)* Br_2 or I_2, AgOTf, dry CH_2Cl_2, rt, N_2, 15 min.

For regioselective introduction of deuterium, *n*-BuLi-LiDMAE mediated lithiation at the C6 position of 2-chloropyridine (**39**) was chosen.[263-264] Gros and co-workers explained the selectivity of the deuteration by formation of aggregates (**40**) between *n*-BuLi-LiDMAE and **39** as illustrated in Scheme 11. Chelation of two lithiums by the pyridine nitrogen, the chlorine at the C2 position, and the oxygen and nitrogen of DMAE promotes selective H6 proton abstraction by *n*-BuLi and generation of the stabilized intermediate **41**. Subsequent introduction of an electrophilic species, MeOD in this case, directs the electrophilic addition towards the C6 carbon. In absence of DMAE, the *ortho*-directing chlorine would direct the lithiation towards the C3 position, thus making the electrophilic addition to the C3 carbon to be the most favoured. This would result in a deuterium three bonds away from the nitrogen instead of two bonds away at C6, which is presumably more beneficial for the planned IPE NMR studies as the largest isotope effects are expected close to the main interaction site.

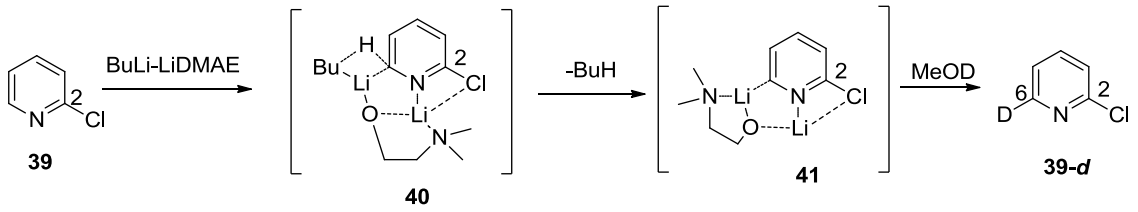

Scheme 11. BuLi-LiDMAE-mediated regioselective deuteration of 2-chloropyridine.[263-264]

Using the procedure for the deuteration described above, 2-chloro-6-deuteropyridine (**39-*d***) and its 4-methyl analogue **36-*d*** were both afforded with high regioselectivity; > 95% deuterium substitution in accordance with ^{1}H NMR spectra of the crude products. To prevent deuterium substitution at the 4-methyl group of **36**, addition of MeOD at low temperature (-78 °C) was necessary. Due to higher volatility, **39-*d*** was isolated in much lower yield than **36-*d*** (35% versus 75%). Mono-deuterated **34-*d*** and **35-*d*** were afforded from a two-step reaction sequence, starting with a microwave-assisted Sonogashira coupling reaction between **39-*d*** or **36-*d*** and TMS-acetylene, followed by TMS-deprotection with potassium fluoride. Originating from the volatility of the products careful isolation was necessary. A second Sonogashira coupling reaction using microwave heating of **34-*d*** or **35-*d*** and mono-coupled **37** or **38**, furnished the desired mono-deuterated **21-*d*** and **22-*d*** in moderate yields, 68% and 59%, respectively. The $[N–X–N]^+$ complexes **17a,b-*d*** and **18a,b-*d*** were prepared in moderate to high yields, as described above, from their corresponding silver(I) triflate complexes, which were reacted with either Br_2 or I_2.

6.4.2 Asymmetric $[N–H–N]^+$ Complex References

The preparation of isotopologue mixtures of the asymmetric reference $[N–H–N]^+$ complexes **27/27-*d*** and **28/28-*d*** (Figure 29a) was accomplished by mixing pyridine (**31**) and 2-deuteropyridine (**31-*d***) in CD_2Cl_2 in the NMR tube, then adding TfOH or TFA portionwise, and adjusting the ^{13}C chemical shifts until the mixture contained pyridines/acid in a 2:1 ratio. The ^{13}C chemical shifts of the 2:1 complexes were determined by titrations of pyridine (**31**) with TfOH or TFA to the end point, *i.e.*, the point where **31** was fully protonated, and the ^{13}C chemical shifts did not change any further.[256] Care was needed to be taken when preparing the samples of $[N–H–N]^+$ complexes, especially for the triflate complex mixture **27/27-*d***. Both **27** and **28** have limited solubility in CD_2Cl_2, **27** being even less soluble than **28**. If too concentrated samples are prepared, there is an apparent risk for precipitation to occur.

The corresponding reference samples of the $[N–H–N]^+$ complexes **29/29-*d*** or **30/30-*d*** (Figure 29a) were prepared in a similar way, by careful portionwise addition of TfOH to an NMR tube with a mixture of **21**/**21-*d*** or **32/32-*d*** in CD_2Cl_2, and by adjusting the ^{13}C chemical shifts until the mixture contained a 1:1 ratio of the corresponding 1,2-bis(pyridinyl-2-ethynyl)benzenes/acid. The ^{13}C NMR chemical shifts of the 1:1 complexes were determined from previous titrations of **21** or **32** with TfOH to the end point as described previously. Due to the low solubility of the $[N–H–N]^+$ complexes in CD_2Cl_2, the methylated complexes **32/32-*d*** in particular being poorly soluble, diluted samples were studied to avoid precipitation.

6.5 NMR EXPERIMENTS

6.5.1 IPE NMR Experiments for Symmetry Evaluation

For determination of the isotope effects caused by unsymmetrical deuterium substitution by IPE NMR, all ^{13}C NMR spectra were acquired at 126 MHz with broadband ^1H and inverse-gated ^2H decoupling. Without simultaneous ^2H decoupling, the C–D ^{13}C NMR signals are split into triplets and/or are broadened due to J_{CD} couplings, which makes the isotope shifts difficult to measure. The lack of the nuclear Overhauser enhancement also decrease the sensitivity of the C–D signals if not ^2H-decoupled. The advantage with using ^2H decoupling is illustrated in Figure 30, showing overlapped $^{13}C\{^1H\}$ and $^{13}C\{^1H,^2H\}$ NMR spectra of a mixture of pyridine (**31**) and 2-deuteropyridine (**31-*d***), with expansions around the C2, C6 (Figure 30a) and C5, C3 carbon (Figure 30b) signals. Without ^2H decoupling, the C–D signals are split into triplets (red spectrum), whereas with simultaneous ^2H decoupling the signals are sharper and appear as singlets (blue spectrum), which, in turn, makes the isotope effects ($^n\Delta_{obs}$) measurable with a higher accuracy.

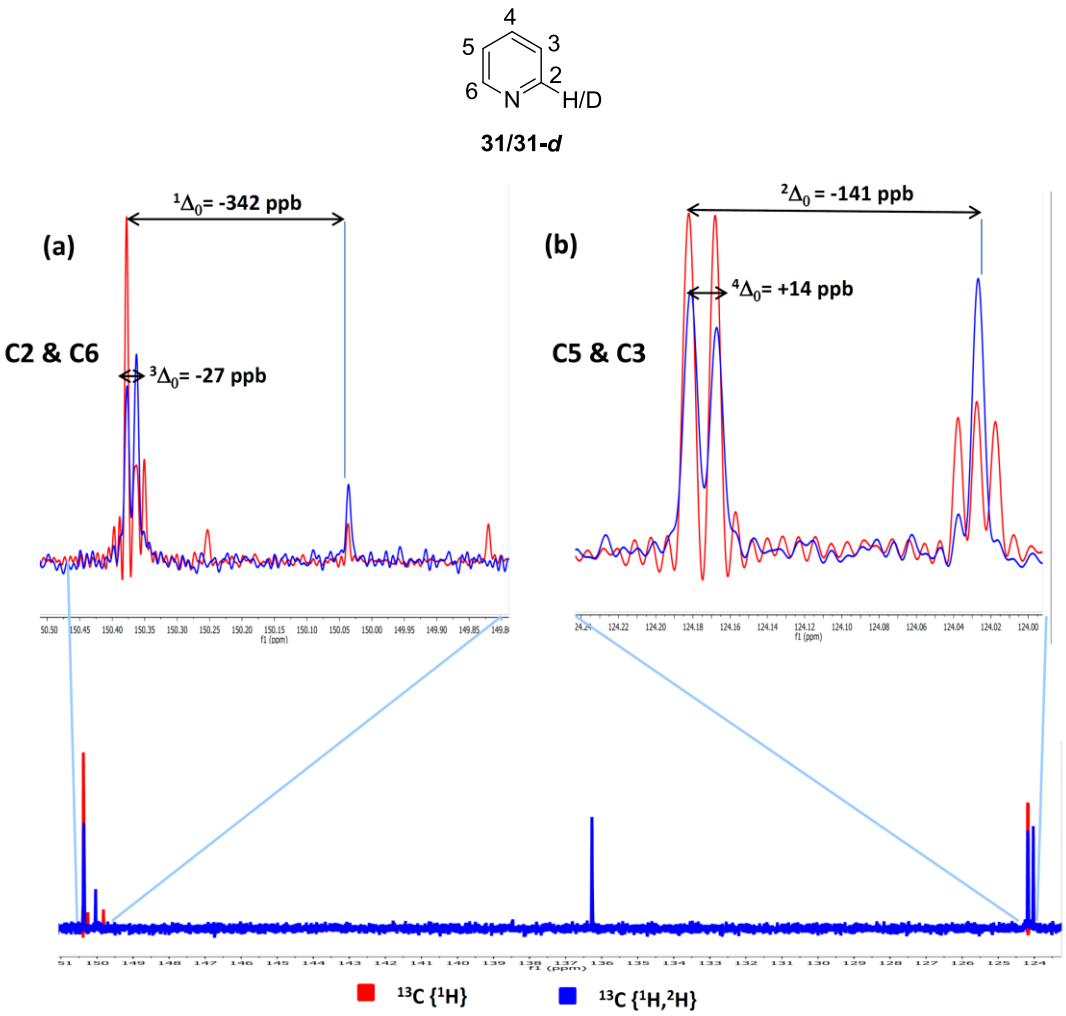

Figure 30. ^{13}C NMR spectra of a mixture of **31** and **31-*d*** in CD_2Cl_2 at 126 MHz; {^{1}H} spectrum in red and {^{1}H,^{2}H} spectrum in blue**. (a)** Expansion around the C2 and C6 signals; **(b)** expansion around the C3 and C5 signals.

6.5.1.1 Bispyridine [N–X–N]$^+$ Halonium Complexes

The acquired isotope effects ($^n\Delta_{obs}$) for isotopologue mixtures of [N–X–N]$^+$ complexes **16a/16a-*d*/16a-*d*$_2$** and **16b/16b-*d*/16b-*d*$_2$**, and mixtures of the references, asymmetric [N–H–N]$^+$ complexes **27/27-*d*** and **28/28-*d***, and symmetric **31/31-*d***, respectively, in CD_2Cl_2 and CD_3CN solutions at 25 °C are summarised in Table 1. The isotope effects acquired for the symmetric reference mixture **31/31-*d*** provide estimates for the intrinsic isotope shifts ($^n\Delta_0$). Noteworthy to mention is that in the di-deuterated [N–X–N]$^+$ complexes, **16a-*d*$_2$** and **16b-*d*$_2$**, the both pyridine rings are identical, and thus a rapid equilibrium, if present, will not be disturbed by the symmetric presence of deuterium isotopes. For that reason, only intrinsic isotope shifts ($^n\Delta_0$) can be observed for the di-deuterated isotopologues with IPE NMR spectroscopy. Furthermore, the calculated

isotope effects for all $[N–X–N]^+$ complexes and their references for CD_2Cl_2 solutions have been added to Table 1. For the $[N–X–N]^+$ and $[N–H–N]^+$ complexes, the structures used in the calculations were geometry optimised models of hypothetical, symmetric and asymmetric structures.

Table 1. Measured ^{13}C NMR isotope shifts, $^n\Delta_{obs}$, in ppb at 126 MHz for CD_2Cl_2 and CD_3CN solutions at 25 °C. Included are also the calculated† isotope shifts (in *italics*) for symmetric and asymmetric structures for CD_2Cl_2 solutions.

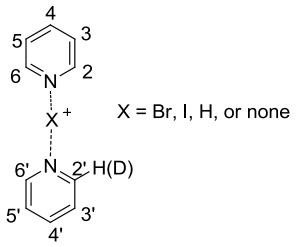

Structure	$[N–X–N]^+$ X	Solvent	$^1\Delta_{obs}$ δ(C2'-C2)	$^2\Delta_{obs}$ δ(C3'-C3)	$^3\Delta_{obs}$ δ(C4'-C4)	$^4\Delta_{obs}$ δ(C5'-C5)	$^3\Delta_{obs}$ δ(C6'-C6)
31	-	CD_2Cl_2	-341	-140	0	+14	-15
		Calculated	*-358*	*-154*	*+2*	*+1*	*-21*
		CD_3CN	-333	-141	0	+14	-17
16a	Br	CD_2Cl_2	-307	-139	+17	0	-29
		Symmetric	*-301*	*-141*	*-6*	*-2*	*-19*
		Asymmetric	*-304*	*-144*	*+41*	*-5*	*-23*
		CD_3CN	-309	-141	+18	0	-31
16b	I	CD_2Cl_2	-336	-145	+20	0	-30
		Symmetric	*-310*	*-146*	*-8*	*-3*	*-17*
		Asymmetric	*-307*	*-151*	*+8*	*-10*	*-18*
		CD_3CN	-345	-148	+21	0	-30
27	H	CD_2Cl_2	-333	-126	+45	+20	-52
		Symmetric	*-270*	*-145*	*-33*	*-2*	*-13*
		Asymmetric	*-308*	*-120*	*+63*	*+23*	*-43*
28	H	CD_2Cl_2	-325	-130	+34	+13	-47

†The calculations were carried out by Assoc. Prof. Jürgen Gräfenstein

Notable from Table 1 is that the $^1\Delta_{obs}$ and $^2\Delta_{obs}$ values, for the carbons one and two bonds away from the deuterium, are negative and of comparable magnitudes for the symmetric and asymmetric reference (**31** and **27**), the values for the asymmetric $[N–H–N]^+$ complex **27** being only slightly less negative than the intrinsic values estimated from single symmetric **31**. This

confirms the expectations that the equilibrium isotope shifts, Δ_{eq}, are small for this type of complexes, resulting from a very small difference of the nitrogen basicities and, hence, small equilibrium rate constant ($K \leq 1.01$) of the tautomerisation ($[N^{+}–H^{\cdots}N] \rightleftharpoons [N^{\cdots}H–N^{+}]$ for the asymmetric references), and from small ^{13}C NMR chemical shift differences (Δ, Equation 3, Chapter 5, Section 5.1.2) between the two tautomeric states ($\Delta \sim 8$ ppm for the protonated (N^{+}-H) and non-protonated (N:) states at C2).[256] This makes the differentiation between single symmetric structures or asymmetric, fast equilibrating structures for the $[N–X–N]^{+}$ complexes **16a,b** not straightforward. Due to their larger magnitude, the $^{1}\Delta_{obs}$ and $^{2}\Delta_{obs}$ values suffer least from measurements errors, and, therefore, give the most accurate information. However, the magnitude and sign of the smaller isotope effects, 3-4 bonds away from the deuterium, might also be informative. In this case, both **[**$N–X–N]^{+}$ complexes **16a,b** show more similarities with the symmetric reference **31** than with the rapid equilibrating reference **27**, based on both the larger isotope effects ($^{1}\Delta_{obs}$ and $^{2}\Delta_{obs}$) together with the smaller isotope effects ($^{3}\Delta_{obs}$ and $^{4}\Delta_{obs}$). For this reason, the $[N–X–N]^{+}$ complexes **16a,b** may possibly be considered as single symmetric structures. The smaller value of the one-bond isotope shift ($^{1}\Delta_{obs}$) for the bromine complex **16a** than for the corresponding iodine complex **16b** and pyridine **31**, might be an effect of the different shieldings of their C2 carbons caused by different, intrinsic chemical characteristics of bromine and iodine, as the $^{1}\Delta_{obs}$ values have shown to relate to the chemical shift of the reporter ^{13}C carbon with the less shielded carbons having the larger isotope shifts.[214] The C2 chemical shifts are 150.5 ppm for **31**, 150.0 ppm for $[N–I–N]^{+}$ complex **16b**, and 147.0 ppm for $[N–Br–N]^{+}$ complex **16a**. The high similarities of the measured isotope effects for the two solvents of different polarity, CD_2Cl_2 and CD_3CN, respectively, suggests that the changes in polarity does not effect the symmetry of the $[N–X–N]^{+}$ complex **16a,b**. They are likely to be symmetric structures even in polar acetonitrile. The asymmetric reference $[N–H–N]^{+}$ complex **28**, with trifluoroacetate ($CF_3CO_2^{-}$) as counter ion shows comparable isotope shifts in both magnitude and sign to the corresponding triflate ($CF_3SO_3^{-}$) complex **27**. From the calculated isotope shifts included in Table 1, it is impossible to draw any conclusions whether the $[N–X–N]^{+}$ complexes **16a,b** are symmetric or asymmetric, fast equilibrating structures. Only the asymmetry of the $[N–X–N]^{+}$ complex **27** could be confirmed by the calculations. However, noteworthy is the proximity of the theoretical calculated isotope shifts to the measured experimental isotope shifts in both magnitude and sign. In Figure 31, expansions of the resulting ^{13}C NMR spectra, acquired in CD_2Cl_2 at 25 °C, around the C2/C2'/C6/C6' and C3/C3'/C5/C5'

regions for both $[N–X–N]^+$ complexes **16a,b** are depicted, showing the observed isotope effect for each carbon pair. Notable in Figure 31 are the broadened peaks in the ^{13}C NMR spectra (a) of the bromonium complex **16a** in comparison with the spectra (b) of the iodonium complex **16b**.

(a)

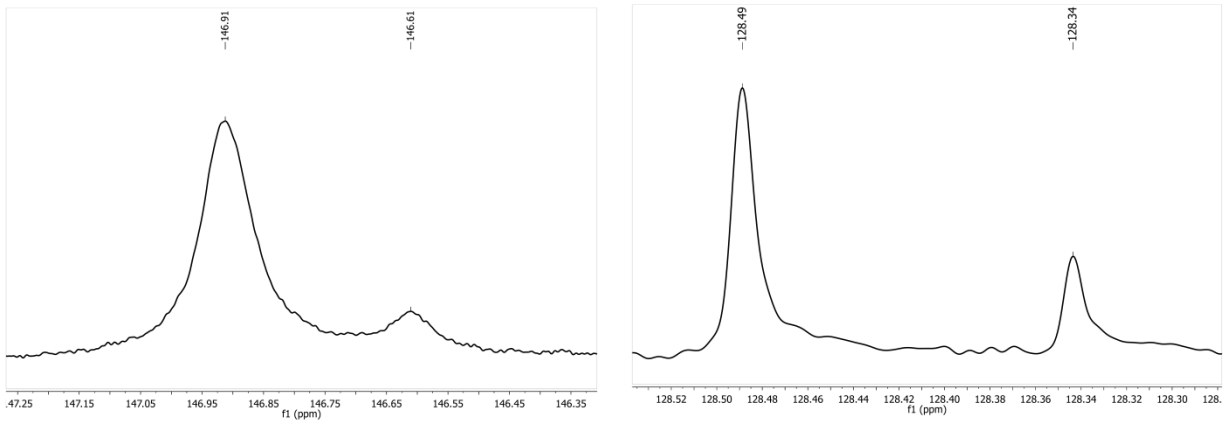

(b)

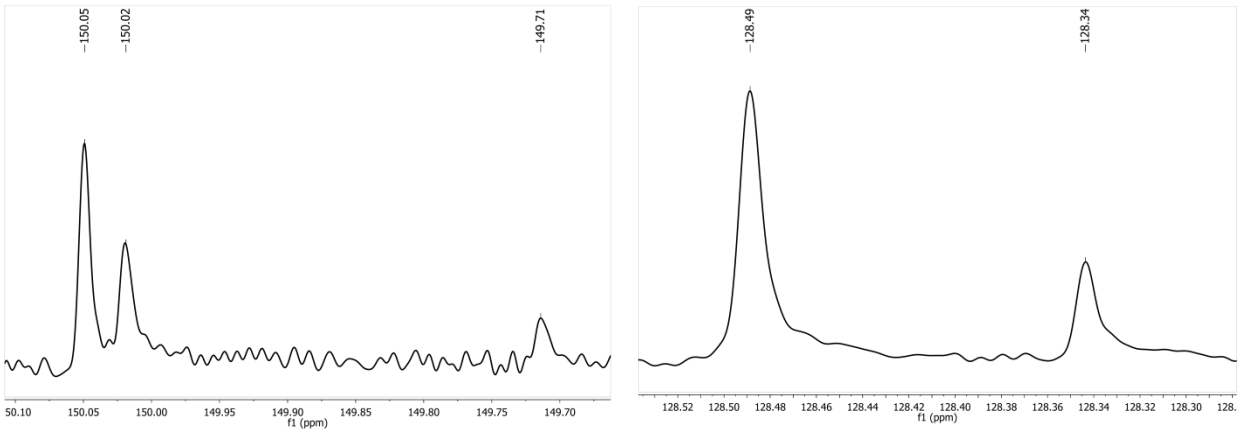

Figure 31. Expansions of ^{13}C $\{^1H,^2H\}$ NMR spectra of **(a)** $[N–Br–N]^+$ complex **16a**, and **(b)** $[N–I–N]^+$ complex **16b** in CD_2Cl_2 at 25 °C. To the left: C6/C6' and C2/C2' carbon signals with $^3\Delta_{obs}$ and $^1\Delta_{obs}$ isotope shifts. To the right: C5/C5' and C2/C2' carbon signals with $^2\Delta_{obs}$ isotope shifts.

For a reliable distinguishment between single symmetric and asymmetric, fast equilibrating structures, the temperature dependence of the isotope effects was studied for CD_2Cl_2 solutions. For asymmetric structures, significant effects on the isotope shifts were expected, as $^n\Delta_{eq}$ is highly temperature dependent. On the contrary, for symmetric structures, and for pyridine, no effects were expected. In Table 2, the acquired temperature coefficients of the isotope effects, *i.e.*, the slopes of $^n\Delta_{obs}$ versus reciprocal temperature plots for each carbon pair, are depicted. In Figure 32, the matching charts for each carbon pair are displayed. The $[N–X–N]^+$ complexes **16a,b** and pyridine (**31**) were studied in the temperature interval 25 °C to -80 °C, whereas the asymmetric

$[N–H–N]^+$ complexes in the intervals 25 °C to -40 °C for **28**, and 25 °C to 0 °C for **27** depending on the limitations in their solubility. Included in Table 2 are also the temperature coefficients of the bromonium complex **16a** in CD_3CN.

Table 2. Temperature coefficients in ppm × K of the ^{13}C NMR isotope shifts for CD_2Cl_2 solutions. The R^2 value from each plot is shown in parenthesis (in *italics*).

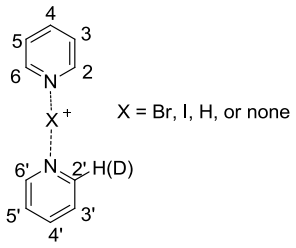

Structure	$[N–X–N]^+$ X	Solvent	$^1\Delta_{obs}$ δ(C2'-C2)	$^2\Delta_{obs}$ δ(C3'-C3)	$^3\Delta_{obs}$ δ(C4'-C4)	$^4\Delta_{obs}$ δ(C5'-C5)	$^3\Delta_{obs}$ δ(C6'-C6)
31	-	CD_2Cl_2	-4.8 *(0.945)*	-4.8 *(0.941)*	0	+1.9 *(0.970)*	-2.1 *(0.940)*
16a	Br	CD_2Cl_2	-3.1 *(0.936)*	-6.4 *(0.942)*	+0.5 *(0.980)*	0	-2.5 *(0.943)*
		CD_3CN	-4.7 *(0.949)*	-12.1 *(0.983)*	+8.1 *(0.989)*	0	*-5.1* *(0.848)*
16b	I	CD_2Cl_2	-4.5 *(0.957)*	-6.4 *(0.944)*	+0.6 *(0.940)*	0	-2.6 *(0.968)*
27	H	CD_2Cl_2	-6.1 *(0.967)*	-9.8 *(1.000)*	-4.5 *(0.992)*	-5.8 *(0.976)*	-6.5 *(0.992)*
28	H	CD_2Cl_2	-5.6 *(0.991)*	-6.2 *(0.972)*	+8.3 *(0.952)*	+4.0 *(0.919)*	-6.8 *(0.949)*

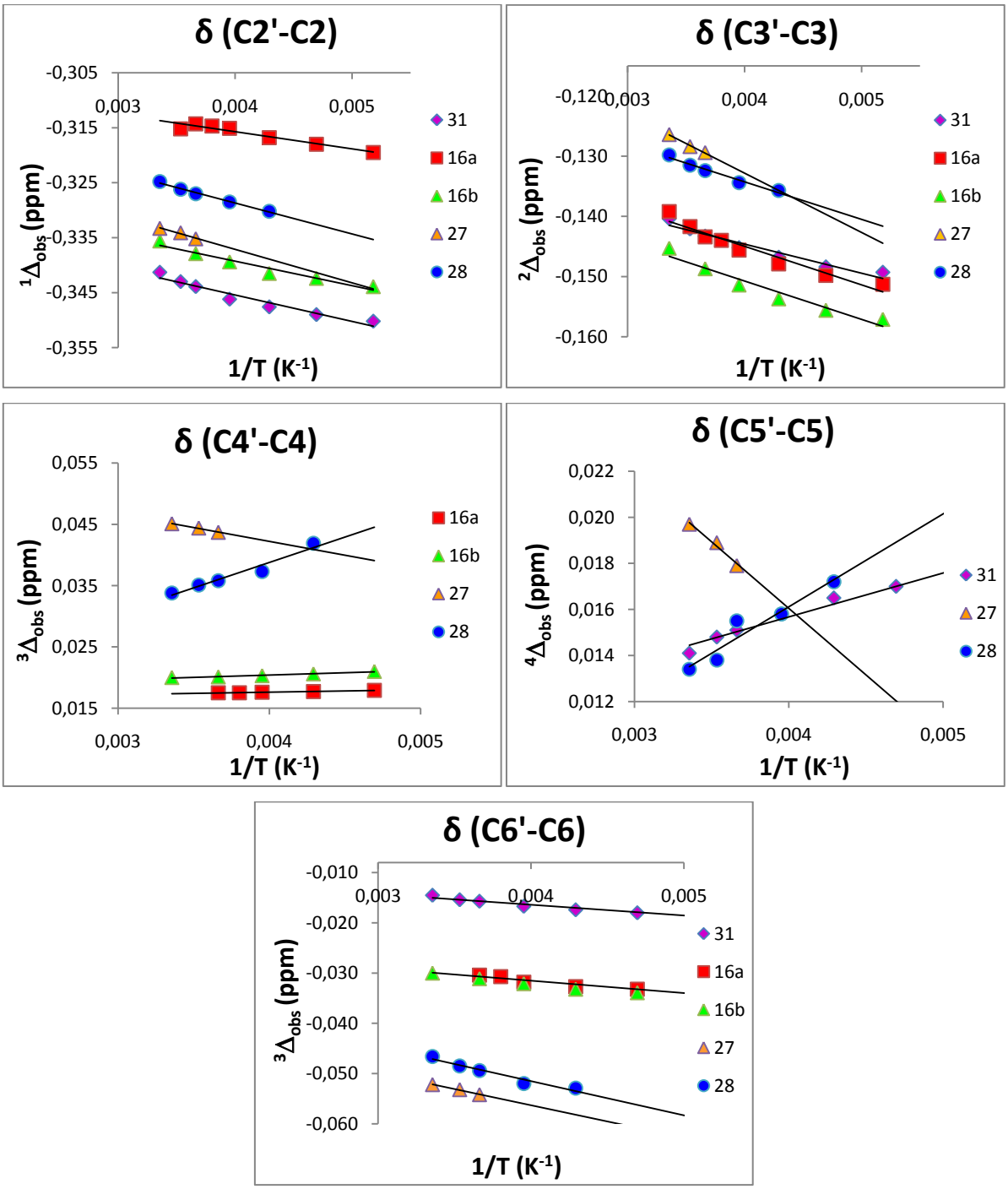

Figure 32. Isotope shifts ($^{n}\Delta_{obs}$) versus reciprocal temperature plots for each carbon pair for the symmetric reference **31**(violet), **[**N–Br–N]$^{+}$ complex **16a** (red), **[**N–I–N]$^{+}$ complex **16b** (green), and asymmetric **[**N–H–N]$^{+}$ complexes **27** (orange) and **28** (blue).

The isotope effects of pyridine (**31**), the reference for the intrinsic isotope effects ($^{n}\Delta_{0}$) was observed to be temperature dependent. This might be explained by the temperature-dependence of solvent polarity; the dielectric constants (ε) are known to increase with decreasing temperature.[161, 265-266] Hence, altered polarity of the solvent could effect the electron density of

the nitrogen lone pair *via* changes in dipolar interactions, which, in turn, could influence the magnitude of the isotope shifts.[214, 224] Table 3 shows that the temperature coefficients for the **[**N–X–N]$^+$ complexes **16a,b** are very similar to the temperature coefficients for pyridine (**31**), both in magnitude and in sign. The magnitude of the alteration of $^n\Delta_{obs}$ with temperature seems to depend on the number of intervening bonds to the deuterium isotope, the temperature coefficients being largest for $^1\Delta_{obs}$ and $^2\Delta_{obs}$, respectively. For the asymmetric systems, **[**N–H–N]$^+$ complexes **27** and **28**, on the other hand, the temperature coefficients are significantly larger for most isotope shifts, which is also to be expected for fast equilibrating tautomers. Noteworthy is that the degree of $^n\Delta_{obs}$ change with temperature for the asymmetric references **27** and **28** varies, and the temperature coefficients differ in sign for both $^3\Delta_{obs}$ and $^4\Delta_{obs}$ of the C4/C4' and C5/C5' carbons, respectively. This variation might be an effect of different coordination of the triflate ($CF_3SO_3^-$) and trifluoroacetate ($CF_3CO_2^-$) counter ions. Importantly, the alteration of $^n\Delta_{obs}$ with temperature for **27** and **28** show an additional dependence on the distance of the reporter carbons to the nitrogen. In fact, in absolute values the temperature coefficients are largely symmetric around the N-C4 axis, which is indicative of the involvement of the nitrogen in an equilibrium process. In contrast, for pyridine (**31**) and the **[**N–X–N]$^+$ complexes **16a,b**, the magnitude of the temperature coefficient for each $^n\Delta_{obs}$ is independent on the distance of the reporter carbons to the nitrogens. This is an indication that the nitrogens of **31** and **[**N–X–N]$^+$ complexes **16a,b**, respectively, do not take part in any equilibrium whatsoever. Hence, the conclusion can be drawn that both the **[**N–X–N]$^+$ complexes **16a,b** are best represented as single, symmetric structures.

The temperature coefficients for the **[**N–Br–N]$^+$ complex **16a** for CD_3CN solution are all of the same sign, but their magnitudes are significantly larger than the temperature coefficients obtained for the less polar CD_2Cl_2 solution (Table 2). The difference in temperature dependency might either be an effect of the polarity differences, or an indication of symmetry differences between the two solvents, *i.e.*, the structure of **16a** being single symmetric in dichloromethane but asymmetric in acetonitrile. To determine whether the larger magnitudes of the temperature coefficients for CD_3CN solutions are caused by a change in solvent polarity or alternation of symmetry, IPE and VT NMR studies must, of course, also be conducted for CD_3CN solutions of the single symmetric and asymmetric references. It has previously been proposed that the Pyr_2Br^+ ClO_4^- complex reacts with the solvent molecules themselves in acetonitrile solutions, forming pyridinium ions and free pyridine.[160] Thus, the high temperature coefficients for CD_3CN solution might also be the consequence of **16a** reacting with the solvent.

Noteworthy to comment is that the isotope effects ($^2\Delta_{obs}$) of the C3/C3' carbons, are overall most effected by temperature changes. Recently, Perrin and co-workers observed that the C3/C5 carbons of pyridine are influenced most by deuterium substitution; the isotope effect per deuterium was largest for pyridine-3,5-d_2 than for pyridine-2,6-d_2 despite the deuterium substitution being closest to the nitrogen in the latter isotopologue.[256] However, this observation could not be explained by the available theories.

The ^{13}C NMR spectra of **[**N–Br–N]$^+$ complex **16a** for CD_2Cl_2 solution showed significant peak broadening at the higher temperatures (10 °C to 25 °C), whereas at lower temperatures the peaks turned sharper. In Figure 33 the ^{13}C {^{1}H,^{2}H} NMR spectra of the C6/C6' and C2/C2' carbon signals at -40 °C and 25 °C are shown. The observed temperature dependence of the peak broadening is explainable by the quadrupolar relaxation caused by of bromine.[267] At reduced temperatures the relaxation rates increase, which make the quadrupolar couplings to collapse, and, thus, the peaks get sharper at lower temperatures.[268] No peak broadening was observed for the corresponding **[**N–I–N]$^+$ complex **16b**.

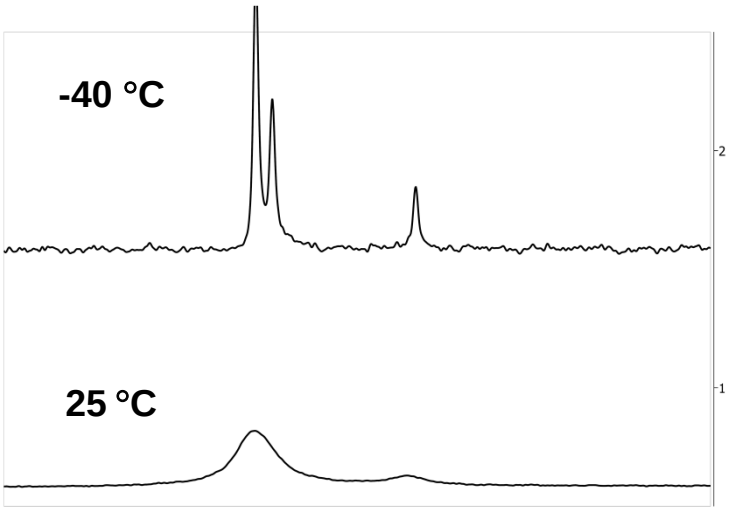

Figure 33. Observed line-brodening for the C6/C6' and C2/C2' carbon signals in ^{13}C {^{1}H,^{2}H} NMR spectra of [N–Br–N]$^+$ complex **16a** at 25 °C for CD_2Cl_2 solution. At -40 °C the $^3\Delta_{obs}$ and $^1\Delta_{obs}$ isotope shifts are perfectly resolved.

6.5.1.2 1,2-Bis(pyridine-2-ylethynyl)benzene [N–X–N]$^+$ Halonium Complexes

The 1,2-bis(pyridine-2-ylethynyl)benzene-based [N–X–N]$^+$ complexes **17a,b** and **18a,b** proved to be somewhat less stable in CD_2Cl_2 and CD_3CN solutions than the corresponding bispyridine [N–X–N]$^+$ complexes **16a,b**. The [N–I–N]$^+$ complex **17b** was stable in solution for days,

whereas the $[N–Br–N]^+$ complex **17a** turned out to be significantly less stable. It was revealed that **17a** was decomposing into its corresponding protonated complex in contact with moisture. This was confirmed by addition of H_2O or TfOH, which both made the ^1H NMR signals of the bromonium complex **17a** decrease, whereas the signals of the protonated complex increased and got slightly shifted, verifying their pH dependence. Despite careful preparation of the $[N–Br–N]^+$ complex **17a**, with anhydrous condition and inert atmosphere, the protonated complex was always present upon isolation. Thus, the synthesis described by Neverov *et al.* could not be reproduced.[171] It should be noted that the reported ^{13}C NMR assignment of $[N–Br–N]^+$ complex **17a** is deficient in the quaternary carbon peaks.[171]

The *para*-dimethylated $[N–X–N]^+$ complexes **18a,b** were also sensitive to moisture, as indicated by the presence of their protonated complexes in their NMR spectra. The bromonium complex **18a** was significantly less stable than the corresponding iodonium complex **18b**. However, in comparison with the analogous complex **17a**, the bromonium complex **18a** proved to be much more stable in solution, most likely due to the stabilising effect of its electron donating *para*-methyl groups. The dimethylated $[N–X–N]^+$ complexes **18a,b** was considerably less soluble than the analogous complexes **17a,b**. Consequently, longer experimental times were needed for observation of the ^{13}C isotope shifts generated from the **18a**/**18a-*d*** and **18b**/**18b-*d*** mixtures.

In Table 3, the measured isotope effects ($^n\Delta_{obs}$) acquired for the mixtures of non-deuterated and mono-deuterated $[N–Br–N]^+$ complexes **17a/17a-*d*** and **18a/18a-*d***, the $[N–I–N]^+$ complexes and **17b**/**17b-*d*** and **18b**/**18b-*d***, their asymmetric $[N–H–N]^+$ references **29/29-*d*** and **30**/**30-*d***, and their symmetric references **21/21-*d*** and **32/32-*d*** at 25 °C for CD_2Cl_2 solutions are summarised. Included in Table 3 are also the obtained isotope shifts for CD_3CN solutions of the isotopologue mixtures of the $[N–I–N]^+$ complex **17b/17b-*d*** and the corresponding symmetric reference **21/21-*d***.

Table 3. Measured ^{13}C NMR isotope shifts, $^{n}\Delta_{obs}$, in ppb at 126 MHz for CD_2Cl_2 and CD_3CN solutions at 25 °C.

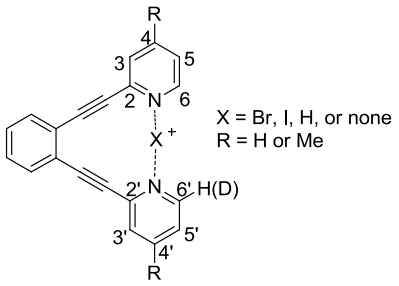

Structure	X, R	Solvent	$^{1}\Delta_{obs}$ δ(C6'-C6)	$^{2}\Delta_{obs}$ δ(C5'-C5)	$^{3}\Delta_{obs}$ δ(C4'-C4)	$^{4}\Delta_{obs}$ δ(C3'-C3)	$^{3}\Delta_{obs}$ δ(C2'-C2)
21	-, H	CD_2Cl_2	-333	-135	+15	+13	-17
		CD_3CN	-326	-138	+10	+11	-17
17a	Br, H	CD_2Cl_2	-315	-138	+23	0	-24
17b	I, H	CD_2Cl_2	-334	-145	+24	0	-28
		CD_3CN	-328	-145	+20	0	-29
29	H, H	CD_2Cl_2	-299	-133	+21	0	-31
32	-, Me	CD_2Cl_2	-331	-132	+12	+13	-14
18a	Br, Me	CD_2Cl_2	-310	-135	+21	0	-24
18b	I, Me	CD_2Cl_2	-328	-140	+24	0	-21
30	H, Me	CD_2Cl_2	-300	-132	+15	0	-11

For the 1,2-bis(pyridine-2-ylethynyl)benzene-based $[N–X–N]^+$ complexes **17a,b** and **18a,b** and their symmetric (**21** and **32**) and asymmetric (**29** and **30**) references, the one-bond and two-bond isotope shifts ($^{1}\Delta_{obs}$ and $^{2}\Delta_{obs}$) are negative and of similar magnitudes. In addition, the small three-bond and four-bond isotope shifts ($^{3}\Delta_{obs}$ and $^{4}\Delta_{obs}$) are also of similar magnitudes and signs for all compounds. The fact that the $^{1}\Delta_{obs}$ and $^{2}\Delta_{obs}$ isotope shifts for the asymmetric $[N–H–N]^+$ complexes **29** and **30** are only slightly less negative than the intrinsic values estimated from the $^{1}\Delta_{obs}$ and $^{2}\Delta_{obs}$ isotope shifts of the corresponding symmetric references **21** and **32** (the same $^{2}\Delta_{obs}$ values for **30** and **32**), indicates that the equilibrium isotope effects are very small for the 1,2-bis(pyridine-2-ylethynyl)benzene systems. As for the bispyridine $[N–X–N]^+$ complexes **16a,b**, the $^{1}\Delta_{obs}$ isotope shifts for the iodonium complexes, **17b** and **18b**, are close to the estimated intrinsic values (from **21** and **32**), and of larger magnitudes than for the corresponding bromonium complexes, **17a** and **18a**. The similarity of the isotope effects observed for the $[N–I–N]^+$ complex **17b** for CD_2Cl_2 and CD_3CN solutions, may be indicative for its remaining symmetry even in a solvent having higher polarity.

To determine the symmetries of the $[N–X–N]^+$ complexes **17a,b** and **18a,b**, the temperature dependence of the isotope effects was studied by IPE NMR in combination with VT NMR at low temperatures for CD_2Cl_2 solutions. In Table 4, the resulting temperature coefficients of the isotope effects, obtained from the slopes of ${}^n\Delta_{obs}$ versus reciprocal temperature plots for each carbon pair, are shown. In Figure 34, the matching charts for each carbon pair of the 1,2-bis(pyridine-2-ylethynyl)benzene $[N–X–N]^+$ complexes **17a,b** and their references **29** and **21** are depicted. The matching charts for the *para*-dimethylated analogues are shown in Figure 35. The $[N–I–N]^+$ complex **17b** and 1,2-bis(pyridine-2-ylethynyl)benzene (**21**) were studied in the temperature interval 25 °C to -60 °C, whereas the $[N–Br–N]^+$ complex **17a** and the asymmetric reference $[N–H–N]^+$ complex **29** were studied in the interval 25 °C to -40 °C, depending on the limitations in solubility. Because of the even lower solubilities of the *para*-dimethylated analogues, their temperature dependence was studied in the temperature intervals 25 °C to -60 °C for symmetric reference **32**, 25 °C to -40 °C for $[N–I–N]^+$ complex **18b** and asymmetric reference $[N–H–N]^+$ complex **30**, and 25 °C to -25 °C for $[N–Br–N]^+$ complex **18a**.

For the 1,2-bis(pyridine-2-ylethynyl)benzene structures, Table 4 shows comparable temperature coefficients, related to the deuterium distance, both for the single symmetric, static reference **21** and the corresponding $[N–X–N]^+$ complexes **17a,b**, which implies that the structure of both the bromonium and iodonium complexes is symmetric in dichloromethane. The asymmetric reference, $[N–H–N]^+$ complex **29**, shows, as expected for equilibrating tautomers, significantly larger temperature coefficients for all observable isotope shifts. Notable is also the large temperature coefficients with opposite sign for the C2'/C2 carbon pair of $[N–H–N]^+$ complex **29**, which further supports the asymmetry of the complex. The isotope effects of an equilibrating system both depend on the distance of the reporter carbon from the deuterium isotope and from the nitrogens, which have most involvement in the equilibrium process.

Table 4. Temperature coefficients in ppm × K of the ^{13}C NMR isotope shifts for CD_2Cl_2 solutions. The R^2 value from each plot is shown in parenthesis (in *italics*).

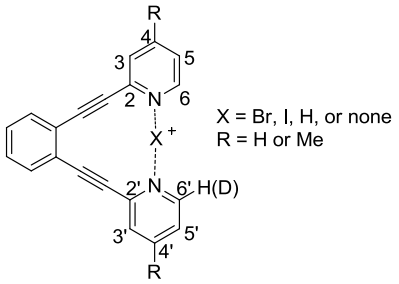

Structure	X, R	Solvent	$^{1}\Delta_{obs}$ δ(C6'-C6)	$^{2}\Delta_{obs}$ δ(C5'-C5)	$^{3}\Delta_{obs}$ δ(C4'-C4)	$^{4}\Delta_{obs}$ δ(C3'-C3)	$^{3}\Delta_{obs}$ δ(C2'-C2)
21	-, H	CD_2Cl_2	-5.1 *(0.934)*	-6.7 *(0.930)*	-2.8 *(0.982)*	+1.8 *(0.989)*	-2.1 *(0.912)*
17a	Br, H	CD_2Cl_2	-6.7 *(0.972)*	-9.2 *(0.990)*	-2.7 *(0.952)*	0	-[a]
17b	I, H	CD_2Cl_2	-7.4 *(0.944)*	-6.5 *(0.974)*	-2.4 *(0.968)*	0	-2.7 *(0.958)*
29	H, H	CD_2Cl_2	-10.0 *(0.987)*	-10.8 *(0.994)*	-3.5 *(0.906)*	0	+15.0 *(0.902)*
22	-, Me	CD_2Cl_2	-6.8 *(0.975)*	-6.9 *(0.994)*	-[a]	+2.8 *(0.966)*	-[a]
18a	Br, Me	CD_2Cl_2	-12.0 *(0.905)*	-9.7 *(0.947)*	-[a]	0	-[a]
18b	I, Me	CD_2Cl_2	-10.9 *(0.982)*	-10.4 *(0.984)*	-[a]	0	-[a]
30	H, Me	CD_2Cl_2	+7.2 *(0.987)*	-8.5 *(0.939)*	-[a]	0	-12.1 *(0.994)*

[a] The temperature coefficients could not be accurately determined.

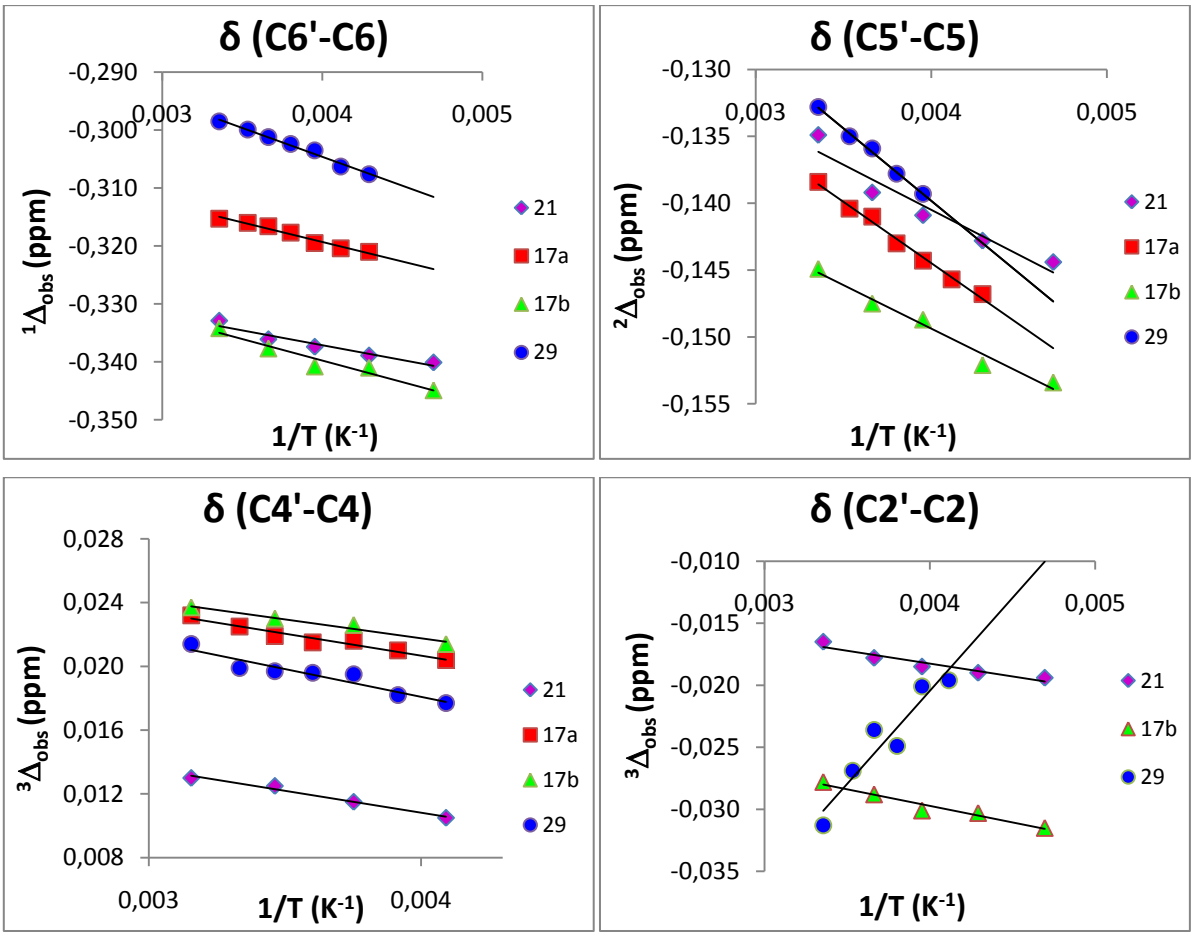

Figure 34. Isotope shifts ($^{n}\Delta_{obs}$) versus reciprocal temperature plots for the C6'/C6, C5'/C5, C4'/C4 and C2'/C2 carbon pairs for the symmetric reference **21** (violet), [N–Br–N]$^{+}$ complex **17a** (red), **[**N–I–N]$^{+}$ complex **17b** (green), and asymmetric **[**N–H–N]$^{+}$ complex **29** (blue)

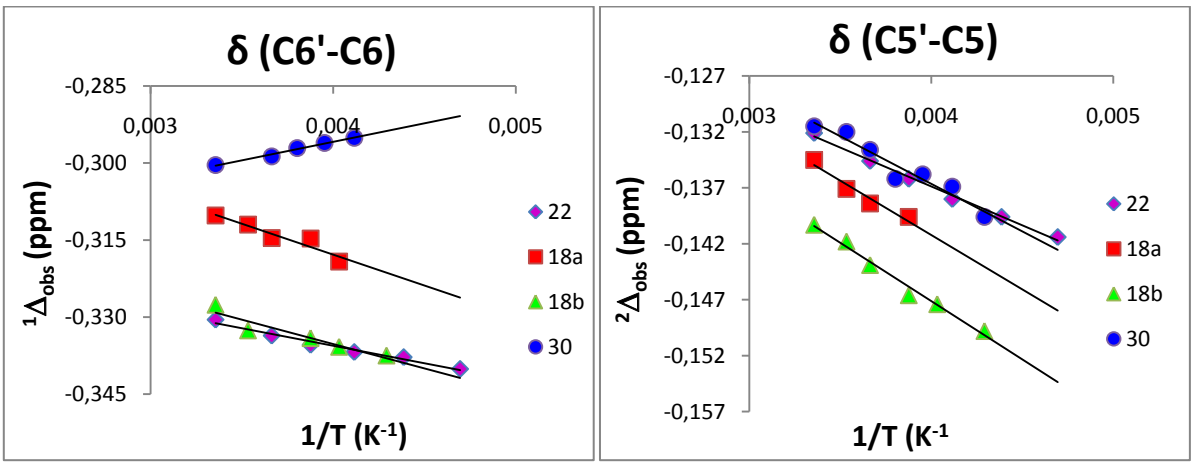

Figure 35. Isotope shifts ($^{n}\Delta_{obs}$) versus reciprocal temperature plots for the C6'/C6 and C5'/C5 carbon pairs for the symmetric reference **22** (violet), **[**N–Br–N]$^{+}$ complex **18a** (red), **[**N–I–N]$^{+}$ complex **18b** (green), and asymmetric **[**N–H–N]$^{+}$ complex **30** (blue).

As for pyridine (**31**), a significant temperature dependency of the isotope shifts is noted for both the single symmetric, static references of the conformationally restrained analogues; 1,2-bis(pyridine-2-ylethynyl)benzene (**21**) and its *para*-dimethylated analogue **22**, respectively. An explanation for this observation, as suggested previously, might be the changes of solvent polarity with temperature.[265-266]

The temperature coefficients obtained for the $[N–X–N]^+$ complexes **18a,b** are very similar, which indicates that the symmetry of both complexes is similar. As the temperature coefficients of the static, symmetric *para*-dimethylated reference **22** are larger in magnitude as compared to its non-methylated analogue **21**, it is not surprising that the temperature coefficients of the $[N–X–N]^+$ complexes **18a,b** also are larger in magnitude as compared to their analogues complexes **17a,b**. Table 4 also shows that temperature coefficients for the ${}^{1}\Delta_{obs}$ and ${}^{2}\Delta_{obs}$ isotope shifts, in general, are somewhat larger for the $[N–X–N]^+$ complexes than for their corresponding static, symmetric references. Unexpectedly, the temperature coefficients for the ${}^{1}\Delta_{obs}$ and ${}^{2}\Delta_{obs}$ isotope shifts of the equilibrating, asymmetric $[N–H–N]^+$ complex **30** are lower in magnitude as compared to the corresponding $[N–X–N]^+$ complexes **18a,b**. However, the opposite sign of the one-bond isotope shift of $[N–H–N]^+$ complex **30** may imply that its symmetry differs from the symmetry of the $[N–X–N]^+$ complexes **18a,b**. Thus, the different direction of the slopes of the ${}^{1}\Delta_{obs}$ isotope shifts, shown in Figure 35, suggests that the $[N–X–N]^+$ complexes **18a,b** may be better described as single symmetric structures. The large temperature coefficient obtained for the ${}^{3}\Delta_{obs}$ isotope shifts of the C2'/C2 carbon pair, close to the nitrogens, may also support that the $[N–H–N]^+$ complex **30** is comprised of asymmetric tautomers in rapid equilibrium.

Noteworthy to mention is that, as observed for the bispyridine analogues **16a,b**, the ^{13}C NMR signals of the **[**$N–Br–N]^+$ complexes **17a** and **18a** for CD_2Cl_2 solutions were significantly broader for the higher temperatures studied than for the lower temperatures. This broadening effect was not observed for the corresponding **[**$N–I–N]^+$ complexes **17b** and **18b**.

6.5.2 Diffusion NMR Experiments for Evaluation of Counter Ion Interaction

Diffusion NMR spectroscopy is applicable for estimating the degree of ion pairing of salts in solution.[269-270] The diffusion coefficient, *D*, is an estimate of relative molecular volumes. As the

molecules become larger, their radii increases, and they generally move slower in solution. This results in smaller *D* values. The *D* value is given from the Stokes-Einstein relation (Equation 5):

$$D = \frac{kT}{6\pi\eta r_H} \qquad \text{(Equation 5)}$$

where k is the Boltzmann constant, T is the absolute temperature, η the viscosity and r_H the hydrodynamic radius. A significant simplification with Equation 5 is that it assumes a spherical shape for the molecules in question. In reality, few molecules are shaped as perfect spheres.

For cations and anions of different size, observation of similar *D* values indicates a high degree of ion pairing. Advantageous is if the diffusion characteristics of the cation and anion of a salt can be measured separately. As the triflate anions ($CF_3SO_3^-$) of the $[N–X–N]^+$ complexes **16a,b** and **17a,b** contain fluorines, it was possible to determine the *D* values of both the $[N–X–N]^+$ cations and their triflate anions separately, with ^1H and ^{19}F diffusion NMR experiments, respectively. The results obtained from ^1H and ^{19}F NMR spectroscopic diffusion studies for CD_2Cl_2 solutions of $[N–X–N]^+$ complexes **16a,b** and **17a,b**, and their references, asymmetric $[N–H–N]^+$ complexes **27** and **29** and symmetric molecules **31** and **21**, respectively, are shown in Table 5.

Table 5. ^1H and ^{19}F NMR translational diffusion coefficients (D)[†] for CD_2Cl_2 solutions at 25 °C.

Structure	**$[N–X–N]^+$ X**	***D* (^{1}H)** ($\times 10^{-10}$ m^2/s)	***D* (^{19}F)** ($\times 10^{-10}$ m^2/s)
31	-	30.6	-
16a	Br	13.9	8.8
16b	I	14.0	15.0
27	H	20.3	14.4
21	-	14.5	-
17a	Br	10.7	10.4
17b	I	10.7	11.7
29	H	11.7	10.7

[†]The diffusion NMR experiments were performed by Dr Ulrika Brath

The comparable diffusion coefficients (*D*), resulting from the ^1H and ^{19}F Diffusion NMR experiments, of the corresponding $[N–I–N]^+$ cation and triflate anion of the $[N–I–N]^+$ complexes **16b** and **17b**, respectively, reveals a tight ion pairing within the complexes (Table 5). Despite the

close coordination of the triflate anion to the $[N–I–N]^+$ cation, the symmetric arrangement of the $N^{\cdots}I^{+\cdots}N$ bond is not disturbed. Thus, the triflate might either be symmetrically coordinated with equal distances to the two nitrogens of the pyridine rings, or unsymmetrically coordinated and still not able to break the strongly stabilised symmetric $N^{\cdots}I^{+\cdots}N$ bonding interaction. The higher *D* values of the bispyridine $[N–X–N]^+$ complexes **16b**, as compared to the 1,2-bis(pyridine-2-ylethynyl)benzene $[N–X–N]^+$ complexes **17b**, originate from their smaller size, and thus, smaller available surface for the solvent to interact with. The smaller size and absence of counter ion make the symmetric references **31** and **21** to diffuse faster than their corresponding $[N–X–N]^+$ complexes as expected. For the asymmetric $[N–H–N]^+$ complex **29**, the similar *D* values for the cation and the anion indicate a tight ion pairing in CD_2Cl_2. The fact that the asymmetric $[N–H–N]^+$ complex **27** can either behave as a 2:1 complex of pyridine/TfOH (**27**) or as a 1:1 complex (**43**) with exchange to free pyridine (**31**), as illustrated in Figure 36, might explain the higher *D* value for the cation than for the anion. The *D* value for the cation represents an average value of the rapidly exchanging free and complexed pyridine, diffusing with different rates.

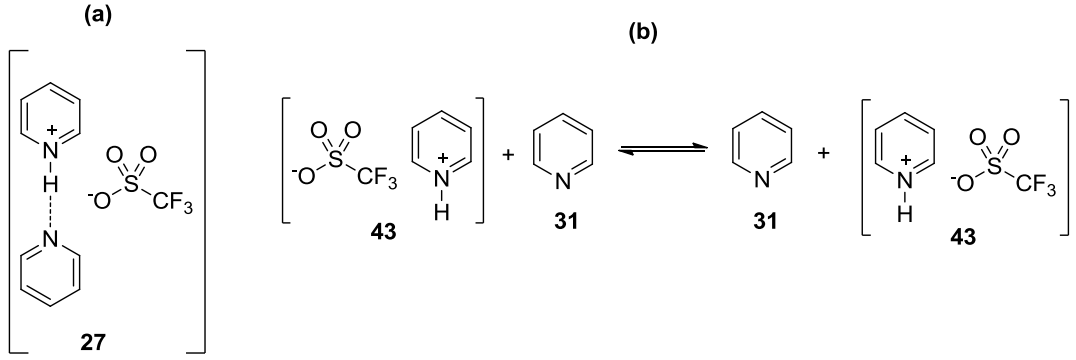

Figure 36. Asymmetric bispyridine $[N–H–N]^+$ triflate complex as a **(a)** 2:1 complex **27** or **(b)** as a 1:1 complex **43** in exchange with free **31**.

6.5.3 ^{15}N and ^{13}C NMR Chemical Shifts as Electron Density Indicators

The ^{15}N NMR chemical shift is a sensitive indicator of the electron density of a nitrogen.[271] Therefore, the ^{15}N NMR chemical shifts were determined for the $[N–X–N]^+$ complexes **16a,b** and **17a,b** and their corresponding symmetric references **31** and **21**, and asymmetric references, the $[N–H–N]^+$ complexes **27** and **29** by ^1H-^{15}N HMBC experiments for CD_2Cl_2 solutions at 25 °C. For each structure a single nitrogen signal was detected, supporting the proposal of single symmetric or fast equilibrating asymmetric structures. As observed also from the ^{13}C NMR experiments at 25 °C, the signals were significantly broader for the $[N–Br–N]^+$ complexes **16a** and **17a** than for the other compounds, explainable by the quadrupolar characteristics of ^{79}Br and

^{81}Br.[267] The ^{15}N NMR chemical shifts obtained are shown in Table 6. Included in the same table are the ^{13}C NMR chemical shifts of the pyridine ring carbons (α, β, and γ) of all $[N–X–N]^+$ complexes and their symmetric and asymmetric references.

Table 6. ^{15}N NMR chemical shifts† and ^{13}C NMR chemical shifts (ppm) of the pyridine ring carbons for CD_2Cl_2 solutions at 25 °C.

Structure	**$[N–X–N]^+$ X**	**δ ^{15}N**	**C-α_1 δ ^{13}C** C2[a] or C6[b]	**C-β_1 δ ^{13}C** C3[a] or C5[b]	**C-γ δ ^{13}C** C4	**C-β_2 δ ^{13}C** C5[a] or C3[b]	**C-α_2 δ ^{13}C** C6[a] or C2[b]
31	-	-67.0	150.5	124.2	136.3	124.2	150.5
16a	Br	-142.9	147.0	128.3	142.7	128.3	147.0
16b	I	-175.1	150.0	128.5	142.7	128.5	150.0
27	H	-134.1	146.3	126.2	141.9	126.2	146.3
21	-	-64.5	150.6	123.6	136.7	128.3	143.7
17a	Br	-141.2	148.5	126.9	142.5	131.3	140.5
17b	I	-165.0	151.3	127.0	142.7	130.9	143.1
29	H	-137.9	147.0	126.0	142.9	130.0	142.9
22	-	-	150.4	124.7	148.0	129.3	143.6
18a	Br	-	147.5	127.7	155.6	131.4	139.9
18b	I	-	150.4	127.9	155.9	131.4	142.6
30	H	-	147.2	126.8	155.1	130.2	138.8

[a] Structures **31**, **16a,b** and **27** (see numbering in **Table 1** and **2**, Section 6.5.1).

[b] Structures **21**, **17a,b**, **29**, **22**, **18a,b** and **30** (see numbering in **Table 3** and **4**, Section 6.5.1).

† The ^{1}H-^{15}N HMBC NMR experiments were performed by Dr Ulrika Brath

In comparison with free pyridine (**31**), the ^{15}N NMR chemical shifts became more shielded upon complexation with either a positive halogen (**16a,b**) or a proton (**27**), indicating increased electron densities on the nitrogen. A possible explanation is that the aromatic electrons are pushed towards the nitrogens due to the positive charge nearby. Table 6 shows that the change in shift increased in the order H < Br < I. A larger chemical shift change might be interpreted as a stronger interaction. Thus, the significantly larger chemical shift change for the $[N–I–N]^+$ complex **16b** suggests that the N–I^+–N binding interaction is strong, and may have a covalent character. The fact, that the ^{15}N shift of **16b** is comparable with the ^{15}N shift of *N*-methylpyridinium iodide (^{15}N δ = -180.5 ppm) further supports a covalent character of the N–I^+–N bond. The same trend is observed for the 1,2-bis(pyridine-2-ylethynyl)benzene complexes, $[N–X–N]^+$ complex **17a,b** and $[N–H–N]^+$ complex **29** in comparison with the free

ligand **21**. However, the 10 ppm higher ^{15}N chemical shift of $[N–I–N]^+$ complex **17b** as compared to **16b** implies a weaker $N–I^+–N$ binding interaction for **17b**. This might be the consequence of the restricted flexibility of the 1,2-bis(pyridine-2-ylethynyl)benzene ligand, providing a non-optimal N–N distance for formation of a stronger $N–I^+–N$ interaction. For the $[N–I–N]^+$ complex **16b**, on the other hand, the N–N distance of the two coordinating pyridines can be adjusted to furnish the most favourable $N–I^+–N$ interaction.

There are some general trends observed for the changes in ^{13}C NMR shifts on complexation (Table 6). In comparison with the free nitrogen bases (**31**, **21** and **22**), the ^{13}C shifts of the C–H α-carbons are decreased upon bromonium and proton complexation (**16a-18a**, **27**, **29** and **30**). The shifts of the β and γ pyridine carbons get less shielded, revealing a decrease in electron density. In fact, the ^{13}C NMR shifts of the $[N–Br–N]^+$ and $[N–H–N]^+$ complexes for each of the three bispyridine-based structures are very similar. For the iodonium complexes (**16b-18b**), on the other hand, the ^{13}C NMR signals of C–H α-carbons remain or move to higher shifts upon complexation. The electron densities of the β- and γ-carbons also get reduced on iodonium complexation; their ^{13}C NMR shifts get less shielded with magnitudes comparable with the corresponding shifts of the $[N–Br–N]^+$ and $[N–H–N]^+$ complexes. The shifts of the C–C α-carbons, close to the triple bonds, of the two $[N–I–N]^+$ complexes **17b** and **18b** , only become slightly more shielded as compared with the free nitrogen bases, significantly less shielded than the C–C α-carbons of the corresponding $[N–Br–N]^+$ and $[N–H–N]^+$ complexes (**17a**, **18a**, **29** and **30**).

The evident ^{15}N shift and α-carbon ^{13}C shift differences between the $[N–I–N]^+$ complexes and their corresponding $[N–Br–N]^+$ and $[N–H–N]^+$ complexes, imply that the interactions within the complexes may be of different types. The interaction type of the bromonium complexes might be similar to the interaction type of the proton complexes, *i.e.*, with the positive bromine only loosely coordinated between the nitrogens in the $N–Br^+–N$ bond. Previously, it has been reported that more shielded shifts of the α-carbons in comparison to free pyridine on protonation or formation of 1:1 pyridine/halogen complexes are caused by changes in bond order and/or higher excitation energies.[164, 272-273]

6.6 Computational Geometry Optimisation[†]

To confirm the experimentally determined symmetries, the geometry of the $[N–X–N]^+$ cations of **16a,b** and **17a,b** and the $[N–H–N]^+$ cations of the corresponding asymmetric references **27** and **29** were evaluated by theoretical computational methods. Geometry optimisations were performed on the DFT level applying a dichloromethane solvent model (B3LYP level, LACVP* basis set). The calculations predicted single symmetric geometries for all $[N–X–N]^+$ complexes included (**16a,b** and **17a,b**). As expected, they also confirmed the asymmetric geometries of the $[N–H–N]^+$ complexes **27** and **29**. No consideration was taken to the triflate counter ion in the calculations. The theoretically derived optimal distances of the structures included in the theoretical study are shown in Figure 37 and 38. For the $[N–X–N]^+$ complexes **16a,b**, the optimal N–X distances are slightly longer when the halogen is coordinated between two pyridines than when bound to one pyridine only, the N–I distances being longer than the N–Br distances as expected as iodine is much bigger than bromine (Figure 37). Both the N–Br and the N–I distances in the $[N–X–N]^+$ complexes are shorter than the sum of the van der Waals radii (N–Br 3.40 Å; N–I 3.53 Å)[123] but close to the distances of common N–X covalent bonds (N–Br 1.9 Å; N–I 2.1 Å).[124]

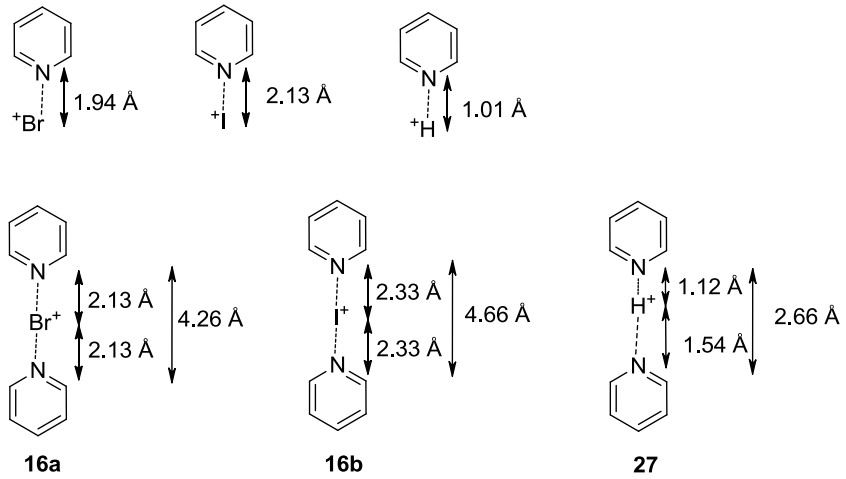

Figure 37. Optimised geometries and N–X, N–H, and N–N distances for $[N–X–N]^+$ complexes **16a,b** and $[N–H–N]^+$ complex **27**.

For the 1,2-bis(pyridine-2-ylethynyl)benzene complexes, $[N–X–N]^+$ complexes **17a,b**, depicted in Figure 38, the N–X distances are also shorter than the sum of the van der Waals radii of the

[†] The calculations were performed by Assoc. Prof. Máté Erdélyi

corresponding atoms, but only slightly longer than the typical distances of corresponding covalent bonds. The N–Br distances of **17a** are somewhat longer in comparison with the distances of **16a**. However, the N–I distances of the $[N–I–N]^+$ complexes **17b** and **16b** are almost identical, which implies that the $N–I^+–N$ interaction of **17b** is optimal. The 0.06 Å longer N-Br bond lengths of $[N–Br–N]^+$ complex **17a** as compared to **16a** may explain its experimentally observed, lower stability. In comparison with the free ligand **21**, the N–N distances of both $[N–X–N]^+$ complexes **17a,b** are shorter, the pyridine rings being more squeezed together when coordinating the smaller bromine than the iodine. This suggests that the symmetric $N–X^+–N$ interaction results in an energy gain sufficiently strong to compensate for the distortion of favoured geometry of the free ligand **21**, with the N–N distance being longer.

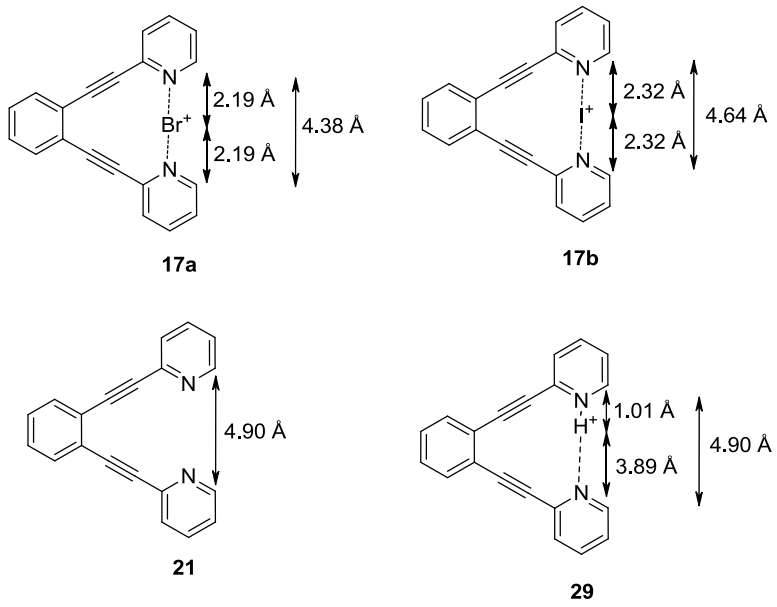

Figure 38. Optimised geometries and N–X, N–H, and N–N distances for $[N–X–N]^+$ complexes **17a,b** and $[N–H–N]^+$ complex **29** and free ligand **21**. The DFT calculations were performed at the B3LYP/LACVP* level for dichloromethane solution.

The symmetric geometries of the $[N–X–N]^+$ complexes **17a,b** were further confirmed by relaxed potential energy surface (PES) calculations, scanned for geometry with varying N–X distances on 0.05 Å steps at the B3LYP/LACVP* level. The calculations resulted in single-well energy potential curves for both complexes, with the N–Br distances 2.19 Å (N–N 4.38 Å) for $[N–Br–N]^+$ complex **17a**, and the N–I distances 2.32 Å (N–N 4.64 Å) for $[N–I–N]^+$ complex **17b**. The PES scan of the $[N–H–N]^+$ complex **29** resulted in a double-well potential curve. The

resulting potential energy curves from the PES scans of $[N–Br–N]^+$ complex **17a** and $[N–H–N]^+$ complex **29** are depicted in Figure 39.

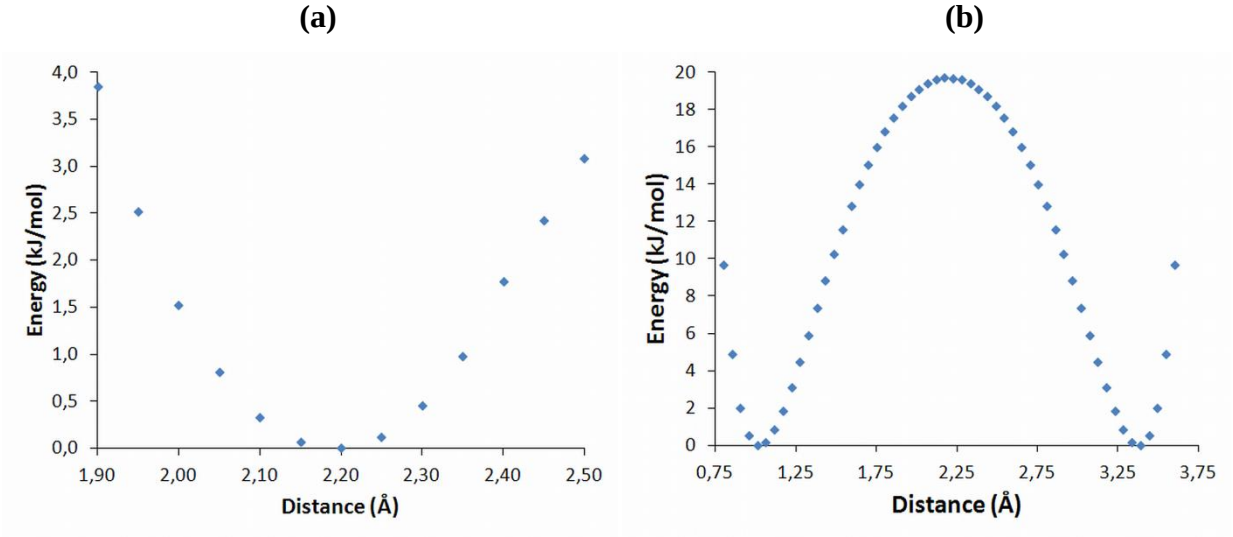

Figure 39. The relaxed potential energy surface scans of **(a)** $[N–Br–N]^+$ complex **17a**, resulting in a single-well potential curve, and **(b)** $[N–H–N]^+$ complex **29**, resulting in a double-well potential. The DFT calculations were performed with variation of N–I and N–H distances in 0.05 Å steps at the B3LYP/LACVP* level.

6.7 Conclusions and Outlook

The IPE NMR studies provide a strong indication that the $[N–X–N]^+$ complexes **16a,b-18a,b** evaluated are best represented as single symmetric structures in dichloromethane. Furthermore, the isotope shifts obtained for the $[N–X–N]^+$ complexes **16a,b** and **17b** for CD_3CN solutions at 25 °C suggest that their symmetric $N–X^+–N$ interactions are retained in the more polar solvent acetonitrile. For confirmation that so is the case, the temperature dependency of the isotope shifts needs to be investigated by IPE NMR in combination with VT NMR for CD_3CN solutions.

N–H–N hydrogen bonds are asymmetric in solution,[193] but have been reported to be symmetric in crystals.[274-276] For the $[N–X–N]^+$ halonium complexes the results from the IPE NMR experiments presented above imply that the analogous $N–X^+–N$ halogen bonds prefer a symmetric arrangement in solution. Interestingly, in crystals, unsymmetrical N–Br–N arrangement were often observed.[170-171] In contrast, related $[N–I–N]^+$ iodonium complexes are commonly found to be symmetric in the solid state with equal N–I distances.[167-169] The fact that the preferred symmetries of N–H–N hydrogen bonds and $N–X^+–N$ halogen bonds seem to differ in solution

implies that there are distinct differences between the two types of interactions. The higher stability of the symmetric N–X^+–N halogen bond as compared to the corresponding symmetric N–H–N hydrogen bond in solution might originate from a more advantageous orbital overlap between the nitrogen lone pairs and one of the p orbitals of I^+ or Br^+ in the 3-centre-4-electron N–X–N bond[166] as compared to the overlap of the nitrogen lone pairs with the smaller s orbital of H^+.

In accordance with the NMR studies, the iodonium complexes seem to be more stable than the corresponding bromonium complexes. For the two 1,2-bis(pyridine-2-ylethynyl)benzene systems, this is revealed by the faster decomposition of the $[N–Br–N]^+$ complexes (**17a** and **18a**) as compared to the $[N–I–N]^+$ complexes (**17b** and **18b**). The ^{15}N NMR shifts also imply that the N–X–N interactions are strongest in the $[N–I–N]^+$ complexes, indicated by their significantly larger changes in magnitude on iodonium complexation than on bromonium complexation. The stronger interaction of the iodonium complexes might be explainable by the larger size and higher polarisability of iodine as compared to bromine. It might also be a consequence of extra advantageous orbital overlaps; efficient σ-overlap of an empty iodine p orbital and the filled non-bonding orbital of the nitrogens, and, additionally, an efficient orbital overlap of a filled d orbital of I(I) and the nitrogen p-orbitals involved in the aromatic system of the pyridine rings.[163, 166] Furthermore, the N–X–N bonds appears to be strongest for the bispyridine complexes (**16a,b**), where the N–N distances can be adjusted to provide the most favourable interaction.

From the ^1H and ^{19}F diffusion NMR measurements it was concluded that the negatively charged triflate ($CF_3SO_3^-$) counter ions are tightly coordinated to the positively charged $[N–X–N]^+$ halonium cations. In crystals, close interaction of the counter ion often results in an unsymmetrical arrangement of the N–X–N bonding interaction, with the two N–X distances being unequal. However, it appears that despite the tendency of the triflate counter ions to be tightly bound in the $[N–X–N]^+$ complexes (**16a,b** and **17a,b**) in dichloromethane solutions, they are not capable of destabilising the strong, centrosymmetric arrangement of the N–X–N bonds.

For completion of the symmetry investigation of the bis(pyridine)based $[N–X–N]^+$ halonium complexes in dichloromethane and acetonitrile solutions, some further experiments are required. For dichloromethane solutions, the degree of ion pairing of the triflate and the cation of the *para*-dimethylated 1,2-bis(pyridine-2-ylethynyl)benzene $[N–X–N]^+$ complexes **18a,b**, and their ^{15}N

chemical shifts for evaluation of the $N–X^+–N$ interaction strength needs to be included. To confirm that the symmetries are the same in both dichloromethane and the more polar acetonitrile solvents, IPE NMR measurements of all $[N–X–N]^+$ complexes at a broader temperature interval are necessary also for acetonitrile solutions. These experiments will be completed in a near future. Furthermore, desirable is to obtain the crystal structures for all $[N–X–N]^+$ halonium complexes included in this investigation, for comparison of their symmetry in solution and in crystals.

To gain a broader understanding of the influence of environment factors on the symmetry of bis(pyridine)based $[N–X–N]^+$ halonium complexes, it is desirable to extend the investigation, and include other solvents and counter ions. In addition, interesting would be to, if possible, study the symmetry of the analogous bis(pyridine)based $[N–Cl–N]^+$ chloronium complexes. Most likely, the $[N–Cl–N]^+$ complexes are much less stable as compared to the iodonium and bromonium complexes, and they are probably best represented as asymmetric, structures in fast equilibrium. It would also be interesting to elucidate the influence of different electronic effects on the $[N–X–N]^+$ halonium complex symmetry, by introducing functional groups in the pyridine rings with either electron donating of electron withdrawing properties. A long-term goal may be to assess $[N–X–N]^+$ halonium complexes with different structural features and different electronic properties as electrophilic halogenations agents in halocyclisation or other alkene halogenations reactions.

7 ETHYLENE HALONIUM IONS

(PAPER III)

7.1 BACKGROUND

The breakthrough for determining the today widely accepted structure of halonium ions was Olah and Bollinger's direct characterisation by ^{1}H and ^{13}C NMR spectroscopy of cyclic, symmetric 1,2-bridged tetramethylethylenehalonium ions under superacidic conditions.[49] Subsequently, Olah and co-workers also characterised a series of methyl-substituted ethylenehalonium ions, as well as the non-substituted parent ethylenehalonium ions, under the same conditions.[277-280] In accordance with the NMR spectroscopic analyses, of both chemical shifts and J_{CH} coupling constants, the symmetrically substituted (tetramethyl and 1,2-dimethyl) and non-substituted ethylenechloronium, bromonium, and iodonium ions were all consistent with symmetric structures. However, no evidence was provided for the existence of cyclic fluoronium ions; instead the NMR spectral data of the tetramethylated ion were consistent with an equilibrium of rapidly, *via* successive 1,2-methyl shifts, interconverting β-fluorocarbenium ions.[281] Due to the temperature-dependency of the ^{13}C NMR shifts of the unsymmetrically substituted ethylenebromonium ions (2-methyl and 2,2-dimethyl), Olah *et al.* suggested equilibrium mixtures of both unsymmetrically bridged ions, *i.e.*, with unequal C–Br bond lengths, and open-chain β-bromocarbenium ions with the positive charge located at the tertiary carbon.[279] It was also suggested that the tetramethylethylenehalonium ions also might involve mixtures of bridged and open-chain ions; with the carbenium ion character being larger in the bromonium and chloronium ions than in the iodonium ion as iodine can accommodate positive charge better than chlorine and bromine.[279, 282] However, scalar couplings and chemical shifts, that are both time averaged phenomena, do not allow reliable differentiation between a static structure and a rapid equilibrating mixture. Hence, the suggestion of Olah is somewhat hypothetic as his data does not provide basis for the conclusions he made. In fact, the symmetrically substituted ethylenehalonium ions might better be described as equivalent, asymmetric β-halocarbenium ions in rapid degenerate equilibrium on the NMR time-scale. If that would be true, their time-averaged NMR signals would be indistinguishable from a symmetric halonium ion (Figure 40).

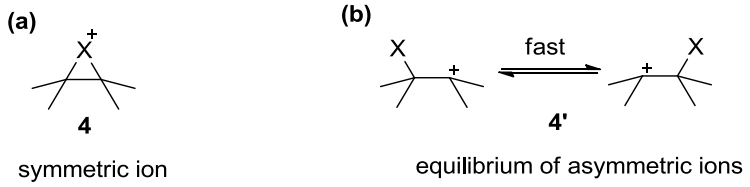

Figure 40. (a) Symmetric 1,2-bridged halonium ion (**4**); and **(b)** asymmetric β-halocarbenium ions (**4'**) in fast equilibrium.

The X-ray crystal structures of the stable 1,2-bridged, symmetrically substituted adamantylideneadamantanebromonium and -iodonium ions (Figure 6, Chapter 2) reveals that the C–X bond distances are slightly unequal and that the extent of asymmetry is dependent on the counter anion (*e.g.* N–Br = 2.116 and 2.194 Å for **10a**; N–Br = 2.118 and 2.136 Å for **10c**).[36, 283] This indicates that the halonium ion is sensitive to its environment, and that formation of ion-pair in solution may influence its symmetry. Most computationally calculated data for the halonium ion structure imply that symmetrically alkylsubstituted ethylenechloronium and –bromonium ions are best represented as cyclic, symmetric ions, and that the corresponding unsymmetrically substituted ions also are closed structures but with their C–X bond distances being unequal.[284-288] Generally, the β-halocarbenium ions have not been studied in detail, as they have been regarded as transitory structures only. The β-bromocarbenium ion has been estimated to be approximately 15 kcal/mol higher in energy than the corresponding symmetric bromonium ion (Figure 40).[284] By calculating the positive charge distribution within the ethylenebrominium ion when interacting with its counter anion, Cossi and co-workers have showed that the positive charge redistributes based on the placement of the counter ion.[289] Hence, their results provide theoretical evidence that supports the suggestion that the chemical environment may influence the symmetry of halonium ions.

The probability that symmetrically substituted halonium ions may involve fast interconverting β-halocarbenium ions in a degenerate equilibrium instead of cyclic halonium ions, encouraged Ohta and co-workers to investigate the symmetry of tetramethylethylenebromonium and chloronium ions, **4a** and **4b**, respectively, by IPE NMR spectroscopy.[203] From the two- and three-bond ^{13}C NMR isotope shifts ($^{2}\Delta_{obs}$ and $^{3}\Delta_{obs}$), observed for the ^{13}C NMR spectra of mixtures of non-deuterated and unsymmetrically deuterated ions generated under stable ion conditions (SbF_5/SO_2 at -60 °C),[49] the conclusion was drawn that both halonium ions are best represented by equilibria of β-halocarbenium ions (Scheme 12). The observation of large deshielded (+1.50 ppm for **4a'-*d*$_6$**

and +1.42 ppm for **4b'-*d*$_3$**) and shielded (-2.11 ppm for **4a'-*d*$_6$** and -1.90 ppm for **4b'-*d*$_3$**) isotope shifts for the quaternary carbons indicated the presence of equilibrium isotope shifts (Δ_{eq}). The upfield, shielded shifts were obtained from two-bond intrinsic and equilibrium isotope shifts $6(^2\Delta_0 - \Delta_{eq})$ for **4a'-*d*$_6$** and $3(^2\Delta_0 - \Delta_{eq})$ for **4b'-*d*$_3$**). The higher shifts resulted from three-bond intrinsic and equilibrium isotope shifts ($6(^3\Delta_0 + \Delta_{eq})$ for **4a'-*d*$_6$** and $3(^3\Delta_0 + \Delta_{eq})$ for **4b'-*d*$_3$**).

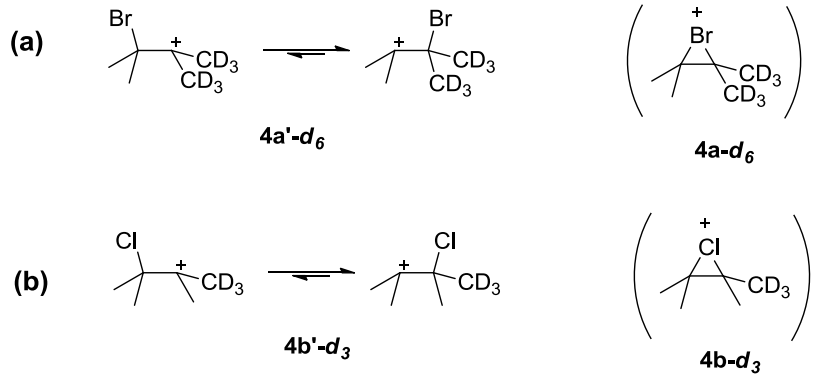

Scheme 12. The cyclic tetramethylethylenebromonium and –chloronium ions, **4a-*d*$_6$** and **4b-*d*$_3$**, respectively, represented as asymmetric **(a)** β-bromocarbenium ions, **4a'-*d*$_6$**, and **(b)** β-chloro-carbenium ions, **4b'-*d*$_3$**, in rapid equilibria.[49]

Moreover, from the observation of dynamic changes of the ^{13}C signals and isotope effects in the temperature interval of -60 °C to -80 °C, evidence of 1,2-methyl shifts in the β-halocarbenium ions was provided (Scheme 13).[203]

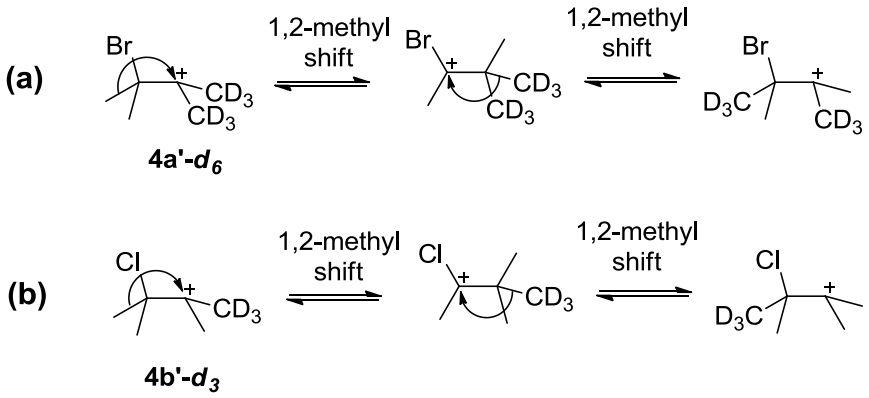

Scheme 13. Successive 1,2-methyl shifts in β-halocarbenium ions, via α-halocarbenium ions; **(a)** β-bromocarbenium ions (**4a'-*d*$_6$**), and **(b)** β-chlorocarbenium ions (**4b'-*d*$_3$**).

Theoretical investigations of the symmetrically alkylsubstituted ethylenehalonium ions in presence of SO_2, used as solvent used in the IPE NMR studies, revealed that SO_2 can act as a nucleophile and, *via syn*-addition, produce covalently bound ion-SO_2 complexes that are

comparable in energy with the cyclic halonium ions, but more stable than the corresponding β-halocarbenium ions (Scheme 14).[290] On the basis of the theoretical evidence of solvent binding,[290] in combination with the results of the IPE NMR studies,[203] Ohta and co-workers suggested that the previously reported characterisation of cyclic halonium ions in SO_2 needs to be reinterpreted. Instead, it was proposed that the cyclic halonium ions should be characterised as rapidly equilibrating ion-SO_2 complexes, with the positive charge located on sulphur (Scheme 14)

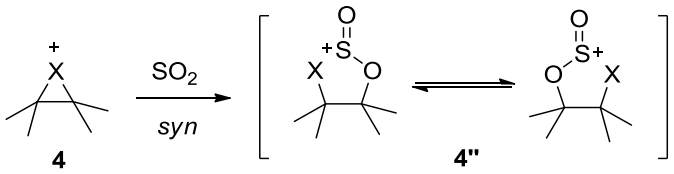

Scheme 14. Formation of equilibrating ion-SO_2 complexes by nucleophilic SO_2 addition.[290]

7.1.1 Effects of Alkyl Substitution on Halonium Ion Symmetry

As alkyl substitution at a carbenium ion centre stabilises the positive charge *via* hyperconjugation,[291] it is reasonable that tertiary β-halocarbenium ions, as the ones described in Scheme 12, are more stabilised by alkyl substituents than the corresponding symmetric halonium ions. Therefore, halonium ions based on 2-butene, the 1,2-dimethylethylenehalonium ions (**19**, Figure 20, Chapter 4), are viable candidates for symmetric 1,2-bridged halonium ions. If formation of β-halocarbenium ions occurs, they should be less stabilised as they are cations of secondary nature. The non-substituted ethylenehalonium ions (**20**, Figure 20, Chapter 4) should exhibit even stronger tendency to form a symmetric, cyclic halonium ion, as primary β-halocarbenium ions are unlikely to be stable.

The main goal of this particular study was to investigate the influence of alkyl substituents on the symmetry of halonium ions. For this purpose the IPE NMR method was chosen for evaluation of the symmetries of the 1,2-dimethylethylenebromonium and chloronium ions (**19a,b**), and the ethylenbromonium and chloronium ions (**20a,b**), respectively.

7.2 Dimethylethylene Bromonium and Chloronium Ions

7.2.1 Introduction and Aims

Olah and co-workers generated the 1,2-dimethylethylenebromonium ions from either *meso*- and *dl*-dibromobutanes (**44**), or *erythro*- and *threo-dl*-1-bromo-2-fluorobutanes (**45**) under stable ion

conditions, in accordance with Scheme 15.[278, 292] A mixture of the *cis* and *trans* bromonium ions (**19a**) in a 3:7 ratio was formed, independent of which diastereomer of the starting material was used. Upon warming the diastereomeric bromonium ion mixture to -40 °C for 5 min, isomerisation, *via* proposed 1,2-hydride and 1,2-methyl shifts in open carbenium ion intermediates, to the 1,1-dimethylethylenebromonium ion (**46**) was observed.[292]

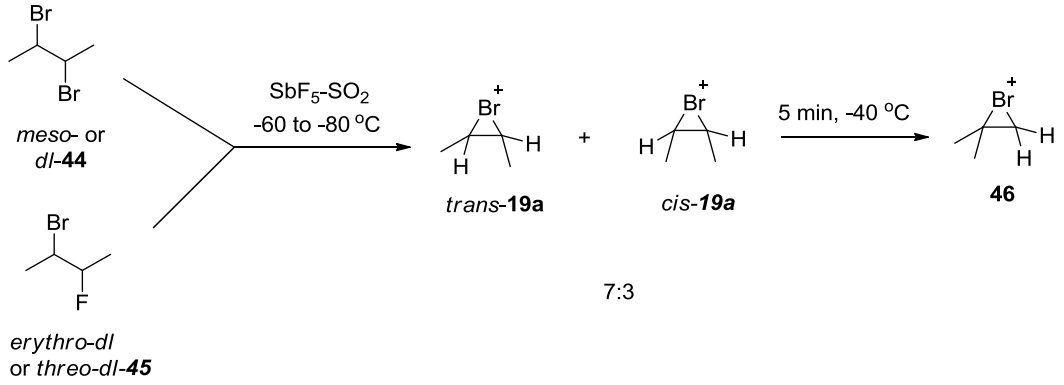

Scheme 15. Preparation of *cis*- and *trans*-1,2-dimethylethylenebromonium ions **19a** under stable ion conditions.[278, 292]

In similar attempts to prepare the corresponding chloronium ions from *meso*- and *dl*-dichlorobutanes (**47**), or *erythro*- and *threo-dl*-1-fluoro-2-chlorobutanes (**48**) under similar ionisation conditions, Olah and co-workers observed immediate rearrangement to chlorocarbenium ions, interpreted as a 2:3 mixture of dimethylchloromethyl- and methylethylchlorocarbenium ions (**49** and **50**) (Scheme 16).[292]

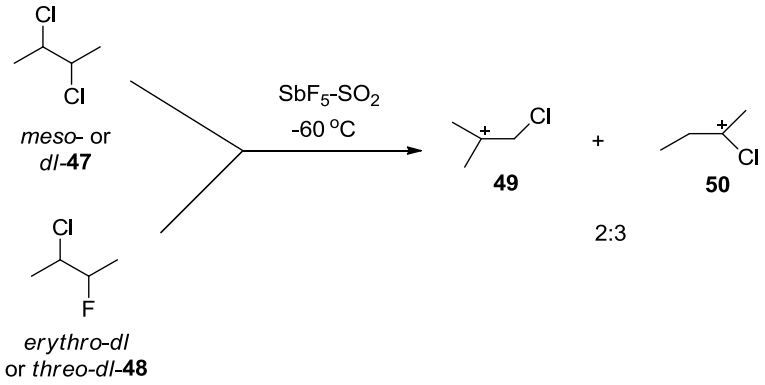

Scheme 16. Formation of dimethylchloromethyl- and methylethylchlorocarbenium ions (**49** and **50**).[292]

The main goal of this study was to evaluate the symmetries of the 1,2-dimethylethylenebromonium (**19a**) and -chloronium ions (**19b**) by IPE NMR spectroscopy. Based on Olah's reported preparation methods shown in Scheme 15 and 16, it was decided to attempt to generate the bromonium ions **19a** and chloronium ions **19b** from diastereomeric

mixtures of *meso*- and *dl*-dibromobutanes (**44**) and dichlorobutanes (**47**), respectively, using similar SbF_5-SO_2 conditions, but keeping the temperature lower, at -80 °C, to prevent rearrangements to occur. In order to evaluate the symmetries of the ions with IPE NMR spectroscopy (Figure 41), syntheses of both non-deuterated (**44** and **47**) and, asymmetrically deuterium substituted *meso*- and *dl*-2,3-dihalobutane precursors (**44-*d*** and **47-*d***) were required.

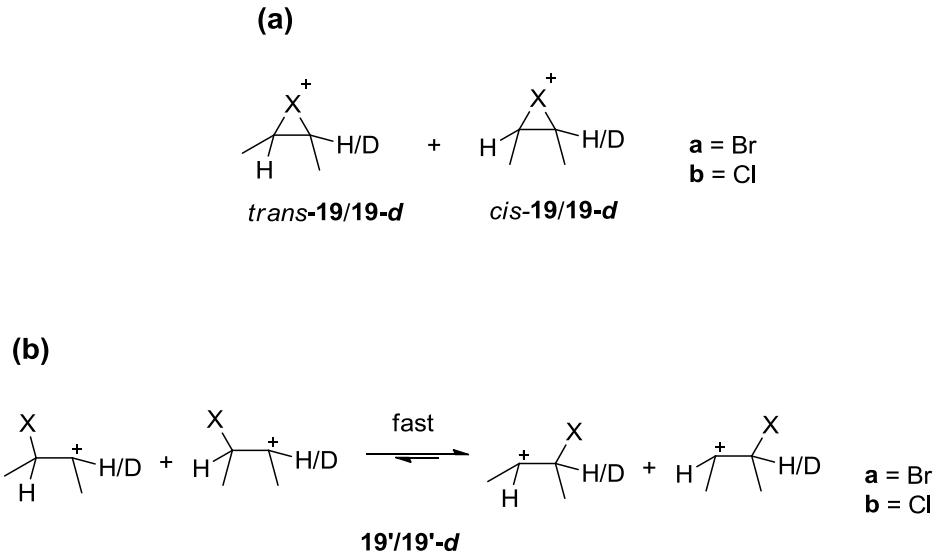

Figure 41. (a) Symmetric 1,2-dimethylethylenehalonium ions **19**/**19-*d*** and **(b)** their corresponding fast equilibrating, asymmetric β-halocarbenium ions **19'**/**19'-*d***.

7.2.2 Synthesis

For the synthesis of non-deuterated (**44**) and mono-deuterated *meso*- and *dl*-2,3-dibromobutanes (**44-*d***) a protocol for regioselective transformation of an α-chloro ketone into alkenes and mono-deuterated alkene developed by Barluenga and co-workers was followed (Scheme 17).[293] By using either $LiAlH_4$ or $LiAlD_4$ as reducing agent, both 2,3-dibromobutanes **44** and their mono-deuterated analogues **44-*d*** could be prepared. The $LiAlH_4/AlCl_3$ combination has proved to be appropriate for selective reduction of the carbonyl group in α-chloro carbonyl compounds.[294] Following carbonyl reduction of α-chloro ketone **51**, subsequent addition of lithium powder provides intermediate **52** *via* a Li-Cl exchange, which is, upon hydrolysis, followed by β-elimination to furnish a 1:1 diastereomeric mixture of *cis*- and *trans*-2-butenes (**53**). By trapping the low-boiling alkenes in a solution of Br_2 in excess, dibromination occurs. When following the synthetic route depicted in Scheme 17, the 2,3-dibromobutanes **44** could be isolated in 57% yield as a 1:1 diastereomeric mixture after purification by vacuum distillation. The corresponding mono-deuterated analogues **44-*d*** were isolated as a mixture of stereoisomers in 30% yield.

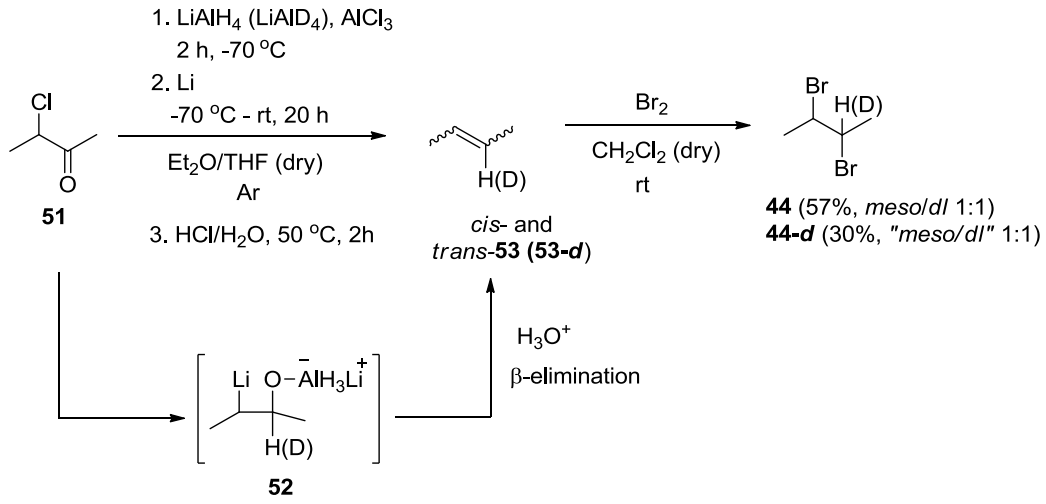

Scheme 17. Synthesis of non-deuterated and mono-deuterated 2,3-dibromobutanes **44** and **44-*d***, respectively, from α-chloro ketone **51**.[293]

Non-deuterated and mono-deuterated *meso*- and *dl*-2,3-dichlorobutanes (**47** and **47-*d***) were synthesised in accordance with a similar protocol, starting with the preparation of *cis*- and *trans*-2-butenes following Barluenga's procedure.[293] In this case, the volatile alkenes (**53** or **53-*d***) were trapped in a solution of ICl in excess. Two consecutive additions of chlorine to the 2-butenes by ICl furnished the desired 2,3-dichlorobutanes (**47** or **47-*d***).[295] In Scheme 18, the synthetic route is shown. The second chlorine addition with ICl as reagent proved to be very slow. Thus, a large excess of ICl (3-4 equivalents) and heating at 50 °C for ~24 h was necessary to drive the reaction to completion. Due to the difficulties in finding optimal reaction conditions, and the difficulties to get rid of the remaining ICl, I_2 and/or I_3^- formed during the chlorination step by work-up with aqueous $Na_2S_2O_3$ solution, the 1:1 diastereomeric mixture of 2,3-dichlorobutanes **47** was isolated in 8% yield following purification by vacuum distillation. The corresponding mono-deuterated 2,3-dichlorobutanes **47-*d*** were isolated as a mixture of stereoisomers in 42% yield, following the route in Scheme 18.

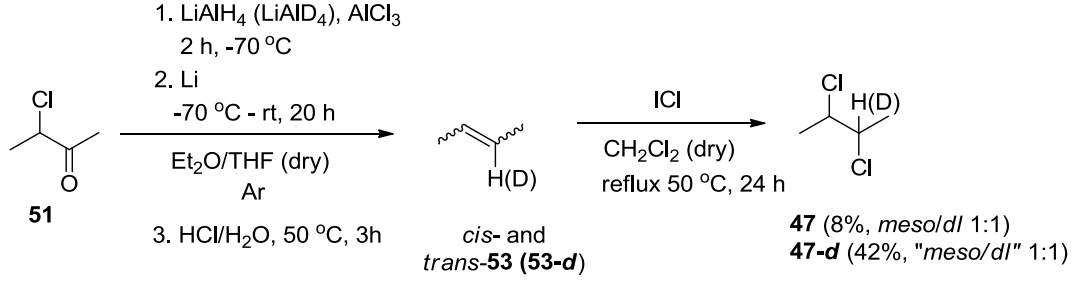

Scheme 18. Synthesis of non-deuterated and mono-deuterated 2,3-dichlorobutanes **47** and **47-*d***, respectively, from α-chloro ketone **51**.[293, 295]

The first addition of ICl to the *cis*- and *trans*-alkenes (**53**) to form the corresponding *erythro*- and *threo*-2-chloro-3-iodobutane diastereomers (**54**) occurs fast. The second reaction with ICl is, however, much slower. The stereospecific transformation for this second chlorination step by ICl suggested by Schmid and Gordon is depicted in Scheme 19.[295] The sequence starts with a complexation of ICl and 2-chloro-3-iodobutane (**54**). Upon this activation, the neighboring chlorine can participate in the reaction by forming a chloronium ion (**55**). An *anti*-attack of the chloronium ion by Cl^- results in stereoselective formation of the 2,3-dichlorobutane; the *erythro*-2-chloro-3-iodobutane **54** forms only the *meso*-2,3-dichlorobutane **47**, wheras *threo*-**54** forms *dl*-**47**. Thus, replacement of iodine by chlorine occurs with retention of configuration.

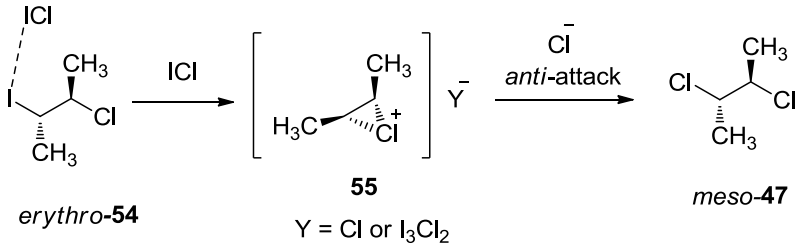

Scheme 19. Stereoselective chlorination of 2-chloro-3-iodobutane **54** by ICl *via* a chloronium cation intermediate **55**. Starting from the *erythro*-diastereomer of **54** provides the *meso*-diastereomer of 2,3-dichlorobutane **47**.[295]

7.2.3 NMR Experiments

Sample concentrations of non-deuterated and mono-deuterated 2,3-dihalobutane precursors (**44/44-*d*** and **47/47-*d***) used in the NMR experiments were in general 50 mg/mL. When preparing the ionised mixtures directly in the NMR tubes, the samples were kept at approximately -80 °C (dry-ice/ethanol bath) under a stream of argon. Careful preparation is important as the samples readily take in moisture from the atmosphere, and as the ions generated rapidly rearrange or decompose upon heating. For the symmetry evaluation of the 1,2-dimethylethylenebromonium ion **19a** a 1:1 mixture of diastereomeric 2,3-dibromobutanes **44** and **44-*d*** was ionised using superacidic SbF_5-SO_2 conditions. For the corresponding IPE NMR studies of the 1,2-dimethylethylenechloronium ion **19b** a 1:3 mixture of diastereomeric **47** and **47-*d*** was used. The symmetries were evaluated in the temperature range -80 °C to -40 °C for bromonium ion **19a** and at -80 °C for chloronium ion **19b**.

7.2.3.1 Symmetry of the 2,3-Dimethylethylenebromonium Ion

Similar to Olah's observations, when treating a 1:1 mixture of *meso*- and *dl*-2,3-dibromobutanes **44** with antimony pentafluoride in liquid SO_2 at -80 °C ionisation to the *trans*- and *cis*-2,3-

dimethylethylenebromonium ions *trans*-**19a** and *cis*-**19a** in a 3:1 ratio occurred, in accordance with ^{1}H and ^{13}C NMR spectra. Upon warming to -40 °C, rearrangement to the corresponding 1,1-dimethylethylenebromonium ion **46** was also observed (Scheme 20). The ^{1}H and ^{13}C NMR spectra of ionisation products of non-deuterated **44** at -80 °C and -40 °C, respectively, are shown in Figure 42.

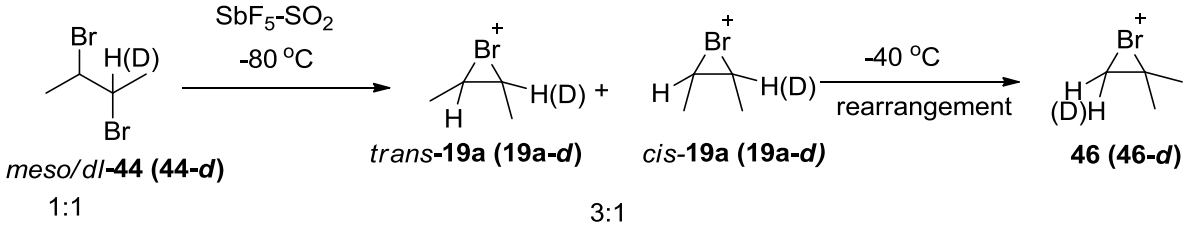

Scheme 20. Ionisation of 2,3-dibromobutanes **44** under stable ion conditions.

The assignment of the ^{1}H and ^{13}C signals of *trans*-**19a**, *cis*-**19a** and rearranged **46** is shown in Table 7 and 8. Included in the tables are Olah's assignments for comparison.[277-279, 296]

Table 7. ^{1}H NMR assignments of ionisation products from 2,3-dibromobutanes **44**. Olah's assignments are shown in *italics*.[277-278]

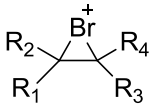

Structure	R_1	R_2	R_3	R_4	δ R_1 (ppm)	δ R_2 (ppm)	δ R_3 (ppm)	δ R_4 (ppm)
***trans*-19a**	CH_3	H	H	CH_3	2.57 (m)[a]	6.69 (m)[a]	6.69 (m)[a]	2.57 (m)[a]
					2.61 (m)[c]	*6.72 (m)*[c]	*6.72 (m)*[c]	*2.61 (m)*[c]
***cis*-19a**	CH_3	H	CH_3	H	2.59(m)[a]	6.88 (m)[a]	2.59 (m)[a]	6.88 (m)[a]
					2.61 (m)[c]	*6.92 (m)*[c]	*2.61 (m)*[c]	*6.92 (m)*[c]
46	CH_3	CH_3	H	H	3.34 (s)[b]	3.34 (s)[b]	5.46 (s)[b]	5.46 (s)[b]
					3.32 (s)[d]	*3.32 (s)*[d]	*5.55 (s)*[d]	5.55 (s)[d]

[a] ^{1}H NMR spectrum at 300 MHz at -80 °C with external acetone-d_6 as reference.
[b] ^{1}H NMR spectrum at 300 MHz at -40 °C external acetone-d_6 as reference.
[c] ^{1}H NMR spectrum at 60 MHz at -60 °C with external TMS as reference.[278]
[d] ^{1}H NMR spectrum at 60 MHz at -70 °C with internal TMS as reference.[277]

(a) ^{1}H NMR spectra at 300 MHz

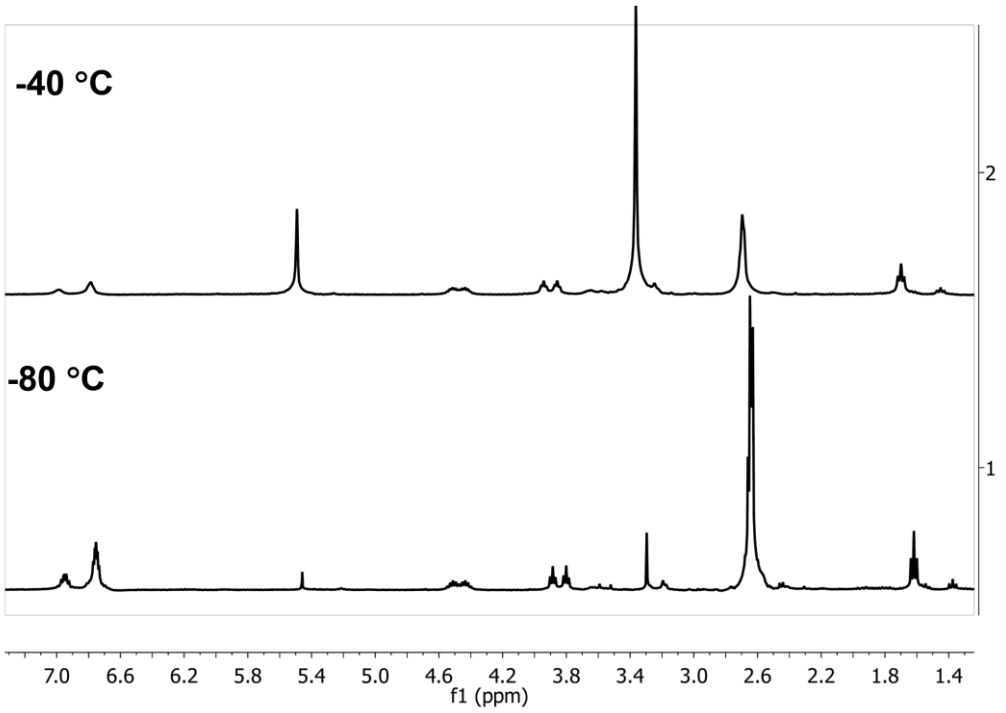

(b) ^{13}C NMR spectra at 75 MHz

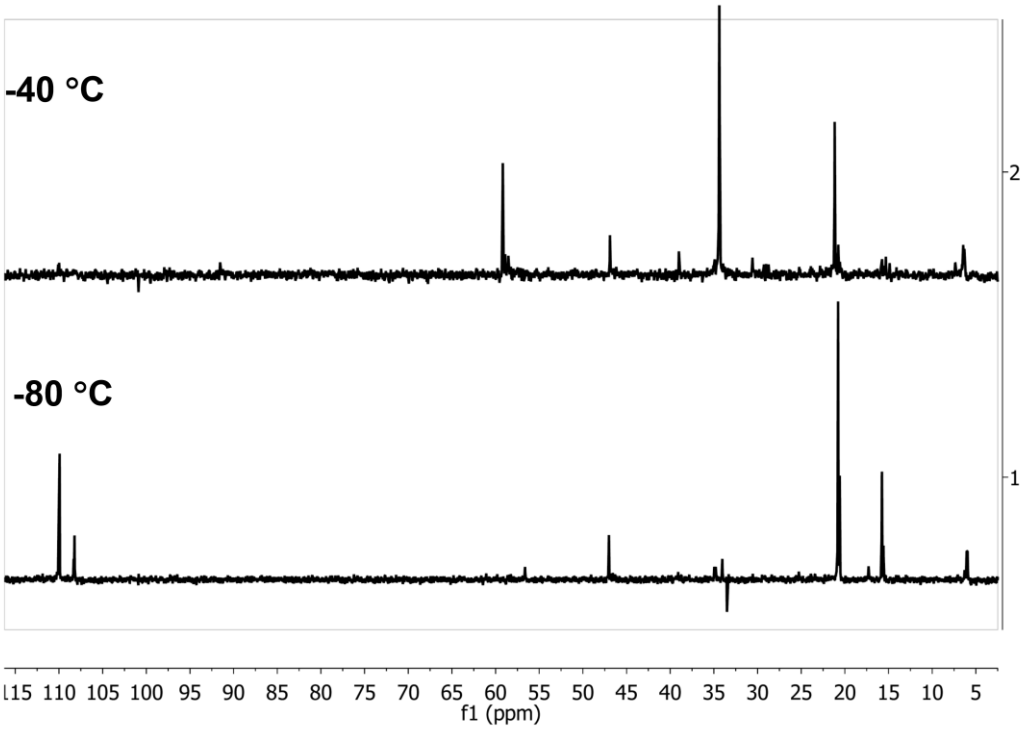

Figure 42. (a) ^{1}H NMR spectra and **(b)** ^{13}C NMR spectra of the ionisation products of *meso*- and *dl*-**44** (1:1) at -80°C and -40°C, respectively.

Table 8. ^{13}C NMR assignments of ionisation products from 2,3-dibromobutanes **44**. Olah's assignments are shown in *italics*.[279, 296]

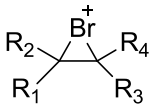

Structure	R_1	R_2	R_3	R_4	δ C-2 (ppm)	δ C-3 (ppm)	δ CH_3 (C-2) (ppm)	δ CH_3 (C-3) (ppm)
***trans*-19a**	CH_3	H	H	CH_3	109.9[a]	109.9[a]	20.8[a]	20.8[a]
					110.9[c]	*110.9*[c]	*22.4*[c]	*22.4*[c]
***cis*-19a**	CH_3	H	CH_3	H	108.2[a]	108.2[a]	15.8[a]	15.8[a]
					108.8[c]	*108.8*[c]	*17.4*[c]	*17.4*[c]
46	CH_3	CH_3	H	H	204.4[b]	59.2[b]	34.4[b]	-
					211.4[d]	*50.5*[d]	*35.4*[d]	-

[a] ^{13}C NMR spectrum at 75 MHz at -80 °C with external acetone-d_6 as reference.
[b] ^{13}C NMR spectrum at 75 MHz at -40 °C with external acetone-d_6 as reference.
[c] ^{13}C NMR spectrum at 15 MHz at -60 °C with internal TMS as reference.[279, 296]
[d] ^{13}C NMR spectrum at 15 MHz at -40 °C with internal TMS as reference.[296]

Notable in the NMR spectra depicted in Figure 42 is the presence of additional peaks not reported by Olah and co-workers. The ^1H-^1H coupling pattern of these peaks are comparable with those observed for the open chlorocarbenium ions **49** and **50** shown in Scheme 16: septet and triplet for **49** (J = 5 Hz), and singlet, quartet and triplet for **50** (J = 6 Hz). An expansion of the ^1H NMR spectrum at -80 °C (taken after the sample had been warmed to -40 °C) is depicted in Figure 43. As indicated by preliminary ^1H-^1H COSY, ^{13}C-^1H HETCOR and DEPT experiments, the multiplet at 4.31-4.52 ppm is suggested to contain four overlapped protons; two diastereotopic CH-protons (double septet) that are coupled to two diastereotopic CH_3-groups at 3.82 ppm and 3.74 ppm (double triplet, J = 5.0 Hz), and two CH_2-protons that are coupled to one CH_3-group at 1.56 ppm (triplet, J = 5.7 Hz). This indication of diastereotopic CH and CH_3 protons, and the similarity with the ^1H-^1H coupling pattern of chlorocarbenium ions **49** and **50**, led to the two structure proposals **56** and **57** illustrated in Figure 44. A suggestion for the mechanism of formation of **56** is through nucleophilic addition of SO_2 to the open, tertiary β-bromocarbenium ion, followed by cyclisation to a five-membered ring *via* bromine electron lone pair interacting with the resulting positively charged sulfur. The chiral nature of the sulfinyl group of the resulting sulfoxide, as illustrated in Figure 45, results in the diastereotopic character of the CH_2-protons and the CH_3-groups. To confirm the structures, more thorough NMR analyses are required.

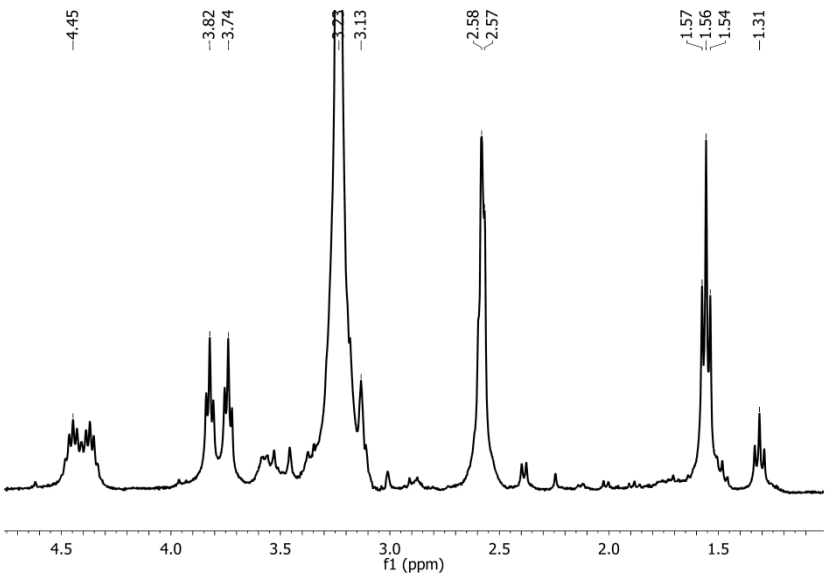

Figure 43. Expansion of the ^{1}H NMR spectrum obtained at 300 MHz at -80°C showing the peaks of the suggested rearranged ions **56** and **57** generated from *meso*- and *dl*-**44** (1:1) under SbF_5-SO_2 condition, after previous warming to -40°C.

56 **57**

Figure 44. Suggested structures of the rearranged cations **56** and **57** formed upon treatment of the ionised mixture of *meso*- and *dl*-**44** (1:1) under SbF_5-SO_2 condition at -40 °C; **56** being formed by nucleophilic addition of SO_2 to the rearranged 1,1-dimethylethylenebromonium ion **46** or its corresponding open β-bromocarbenium ion.

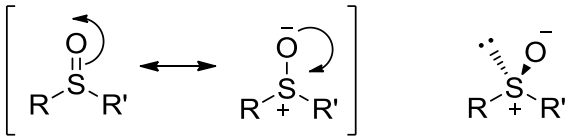

Figure 45. Resonance in the sulfinyl group. When R and R' represents two different organic groups, the sulfinyl group becomes chiral due to the lone pair of electrons that resides on the sulfur atom. As for sp^3 carbons, the molecular geometry of the chiral sulfinyl group is tetrahedral.

The observed isotope shifts, $^{2}\Delta_{obs}$ and $^{3}\Delta_{obs}$, obtained from the IPE NMR experiments of the ionised 1:1 mixture of the diastereomeric bromonium ions **19a** and **19a-*d*** for the temperatures -80 °C to -40 °C are shown in Figure 46 and summarised in Table 9.

(a) $^{13}C\{^{1}H\}$ NMR spectra at 75 MHz; expansion 108.0 to 110.2 ppm

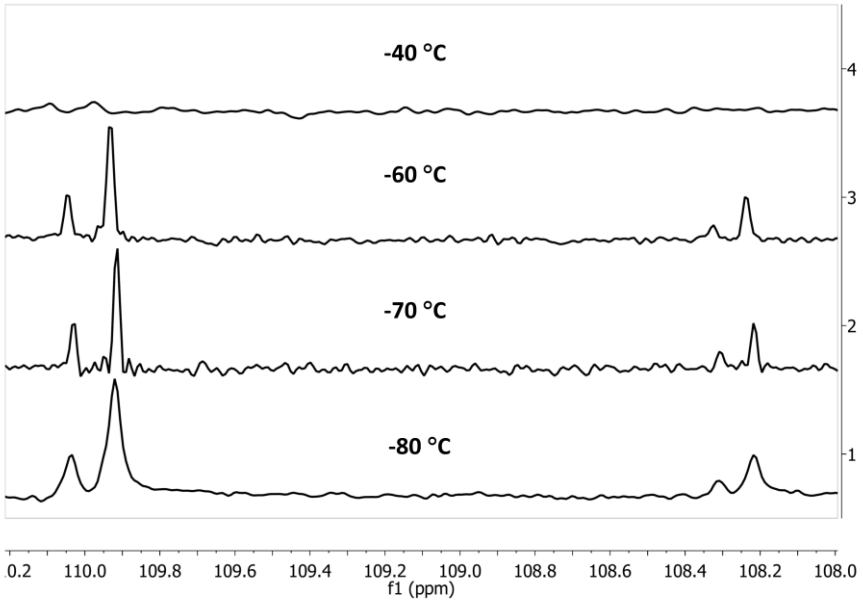

(b) ^{13}C $\{^{1}H\}$ NMR spectra at 75 MHz; expansion 15.4. to 20.8 ppm

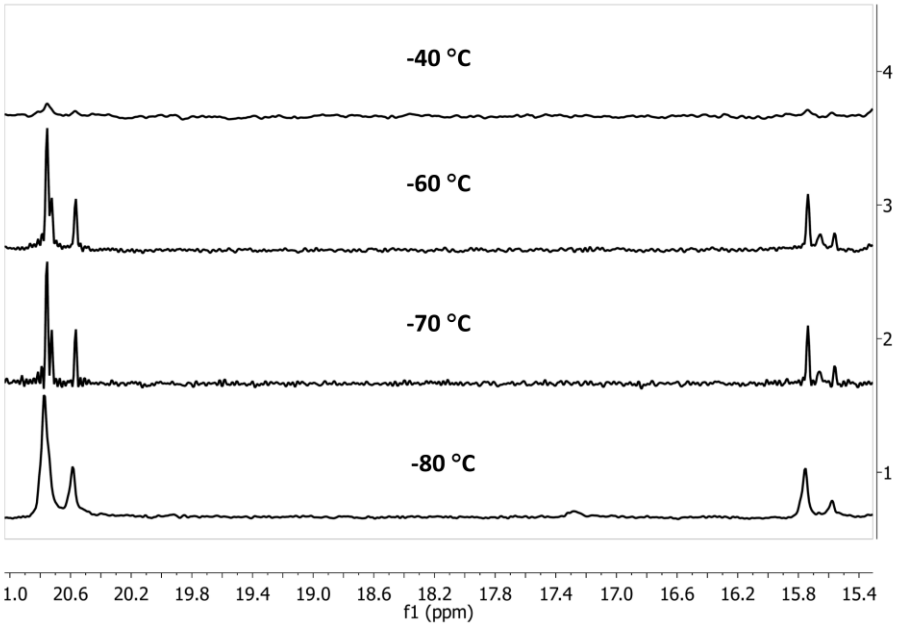

Figure 46. Expansions of ^{13}C $\{^{1}H\}$ NMR spectrum of *cis*- and *trans*-**19a**/**19a-*d*** bromonium ions; left ^{13}C signals of *trans*-**19a**/**19a-*d***, right ^{13}C signals of *cis*-**19a**/**19a-*d***. **(a)** CH/CD carbons with positive isotope shifts; **(b)** CH_3 carbons with negative isotope shifts.

In Figure 46, the major signal pairs (left) come from the *trans* isomer of **19a**, whereas the minor ones (right) come from *cis*-**19a**; (a) CH and CD carbons, and (b) CH_3 carbons. Unfortunately, the one-bond isotope shifts could not be observed, probably due to a strong $^{1}J_{CD}$ coupling and the absence of nuclear Overhauser enhancement upon broadband ^{1}H decoupling.

Table 9. Measured ^{13}C NMR isotope shifts, $^{2}\Delta_{obs}$ and $^{3}\Delta_{obs}$, of bromonium ion isomers *trans*-**19a/19a-*d*** and *cis*-**19a/19a-*d***, in ppb at 75 MHz at -80 °C to -60 °C.[a]

	***trans*-19a**			***cis*-19a**		
Temp.	CH	CH_3	CH_3	CH	CH_3	CH_3
(°C)	$^{2}\Delta_{obs}$ (ppb)	$^{2}\Delta_{obs}$ (ppb)	$^{3}\Delta_{obs}$ (ppb)	$^{2}\Delta_{obs}$ (ppb)	$^{2}\Delta_{obs}$ (ppb)	$^{3}\Delta_{obs}$ (ppb)
-80	+117	-189	-	+99	-177	-
-70	+115	-190	-32	+90	-177	-32
-60	+114	-189	-31	+87	-176	-31

[a] $^{13}C\{^{1}H\}$NMR spectra with external acetone-d_6 as reference.

In accordance with Table 9, all two-bond isotope effects, $^{2}\Delta_{obs}$, obtained from the IPE NMR experiment are consistent with a combination of intrinsic and equilibrium isotope shifts ($^{2}\Delta_{o}$ + Δ_{eq}). Previously reported two-bond intrinsic shifts, $^{2}\Delta_{o,}$ are approximately -0.1 ppm.[213] The $^{n}\Delta_{obs}$ values indicate that there might be a small temperature dependence of the isotope shifts, which support the presence of fast equilibrating tautomers. However, the temperature range studied is too narrow to reliably determine whether the isotope effects are temperature dependent or not. Nevertheless, in this case, the values of the isotope shifts alone indicate that both the *trans*- and *cis*-1,2-dimethylethylenebromonium ions **19a** are better represented as asymmetric, rapidly equilibrating β-bromocarbenium ions (**19a'**) in superacidic SO_2 solutions (Figure 41). An alternative interpretation is a fast equilibrium of interconverting ion-SO_2 complexes as illustrated in Scheme 14.[290]

7.2.3.2 Symmetry of the 2,3-Dimethylethylenechloronium Ion

In an attempt to ionise the diastereomeric 2,3-dichlorobutane mixture comprised of non-deuterated **47** and mono-deuterated **47-*d*** in a 1:3 ratio in SbF_5-SO_2 at -80 °C, the resulting ^{1}H NMR spectrum verified the generation of a complex mixture of ionic compounds. The peaks in the corresponding ^{1}H and ^{13}C NMR spectra at -80 °C, indicate the presence of the rearranged ions **49/49-*d*** and **50/50-*d***, characterised by Olah and co-workers,[277-278] and/or the suggested cyclic **58** with added SO_2, as the dominating products (Scheme 21). No trace of the desired 1,2-dimethylchloronium ions **19b** was seen. For further confirmation of the structures of these ions additional NMR studies, preferably on ions generated from non-deuterated **47** only to simplify the interpretations of the NMR spectra, are needed.

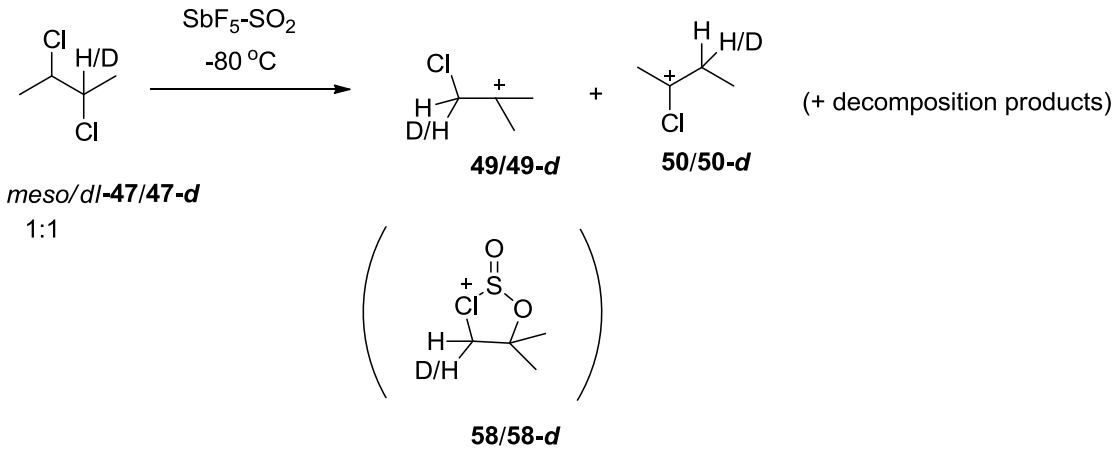

Scheme 21. Ionisation of diastereomeric 2,3-dichlorobutanes **47**/**47-*d***, and the possible cationic products formed.

For generation of the desired 1,2-dimethylethylenchloronium ions **19b**, the less nucleophilic solvent SO_2ClF instead of SO_2 is expected to be advantageous and will be attempted.[297]

7.3 ETHYLENE BROMONIUM AND CHLORONIUM IONS

7.3.1 Introduction and Aims

The preparation of the parent ethylenbromonium ion **20a** was reported by Olah and co-workers.[278, 298] 1-Bromo-2-fluoroethane (**59**) was ionised in SbF_5-SO_2 at -60 °C as shown in Scheme 22. In the resulting ^{1}H NMR spectrum at 60 MHz of the bromonium ion, a broadened singlet was observed, further broadened upon cooling to -80 °C. By raising the temperature to -30 °C, a sharpening of the singlet was observed. Olah *et al.* explained the line shape changes of the singlet signal upon temperature alteration as a result of the quadrupolar character of bromine.[278] However, this alteration of the signal line shape with temperature might perhaps be better compatible with a dynamic process.

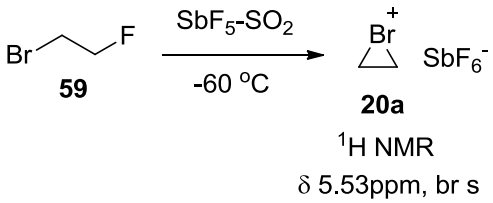

Scheme 22. Preparation of ethylenebromonium ion **20a** under stable ion conditions.[278]

When 1,2-dichloroethane **60** or 1-chloro-2-fluoroethane **61** were treated under the same reaction conditions, Olah and co-workers did not find evidence for ethylenechloronium ion (**20b**) formation. Instead, generation of donor-acceptor complex of the dihalide precursor **60** or **61** and

antimony pentafluoride (**62** and **63**) was suggested based on the observed two triplets in the ^{1}H NMR spectra of the mixture (Scheme 23).[278]

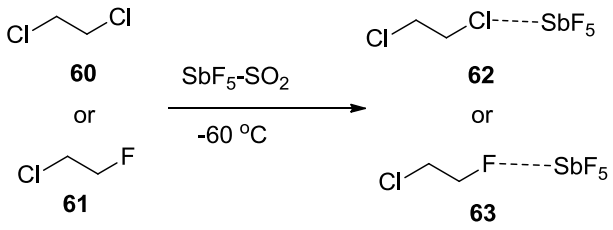

Scheme 23. Suggested formation of donor-acceptor dihalide-SbF_5 complexes, **62** and **63**, respectively.[278]

Later, however, the formation of the ethylenehloronium ion **20b** was reported.[298,299] Treating 1-chloro-2-fluoroethane **61** under superacid condition with the solvent SO_2ClF, even less nucleophilic than SO_2, at -80 °C resulted in an ion mixture, interpreted to comprise of the desired cyclic chloronium ion **20b** and the methylchlorocarbenium ion **64**, based on the observed singlet for **20b** and a doublet and quartet for **64**. The latter was suggested to be formed *via* 1,2-hydride shift from ring-opened **20b** (Scheme 24). The ratio of the ions **20b** and **64** showed to be dependent on the condition used, with the chloronium ion **20b** dominating under careful conditions with the temperature kept at -80 °C.

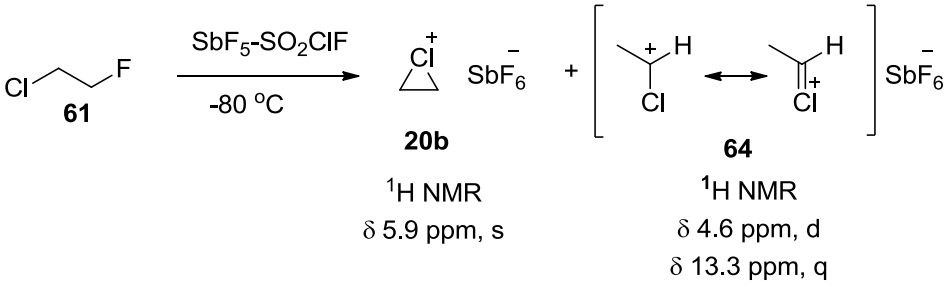

Scheme 24. Preparation of ethylenebromonium ion **20b** and α-chlorocarbenium ion **64** in SbF_5-SO_2ClF.[299]

Upon raising the temperature to -50 °C, the signals of **64** disappeared, and new, more shielded signals, a doublet and a quartet, appeared in the ^{1}H NMR spectrum. These were proposed to correspond to the methylfluorocarbenium ion **66**, formed from **65** and in equilibrium with 1,1-difluoroethane (**67**) as shown in Scheme 25.[299-300]

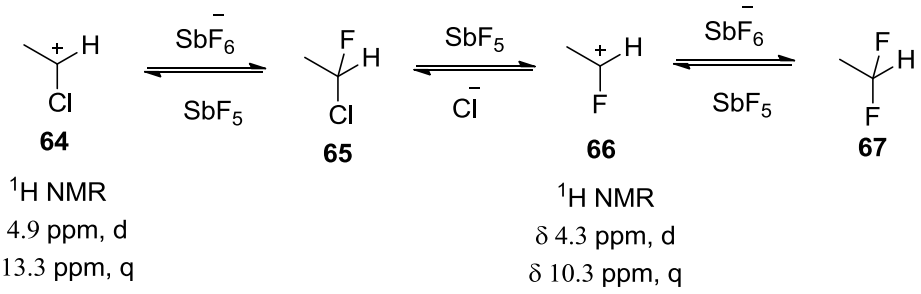

Scheme 25. Proposed equilibria, driven to the right at -50 °C, between methylfluorocarbenium ion **66** and 1,1-difluoroethane **67**.[299-300]

The goal of this part of the investigation was to elucidate the symmetry of the ethylenebromonium and -chloronium ions **20a** and **20b**, respectively, by IPE NMR spectroscopy. 1,2-dibromo- and 1,2-dichloroethane (**68** and **69**) were selected as ethylenehalonium ion precursors. For the ionisation it was decided to try similar SbF_5-SO_2 conditions as used by Olah and co-workers (Scheme 22 and 23), but at lower temperature, -80 °C instead of -60 °C.[278] For the symmetry evaluation of the ions with IPE NMR spectroscopy (Figure 47), synthesis of mono-deuterated 1,2-dihaloethane precursors (**68-*d*** and **69-*d***) was necessary.

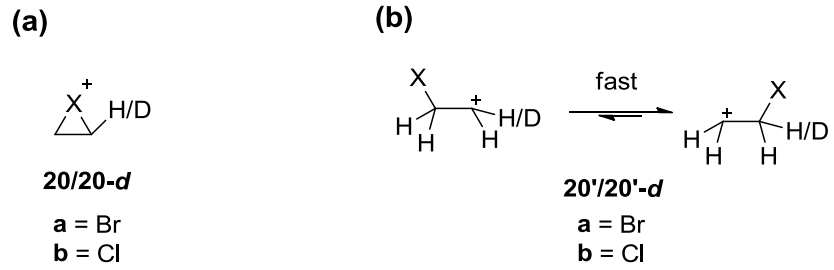

Figure 47. (a) Symmetric ethylenehalonium ions **20**/**20-*d*** and **(b)** their corresponding fast equilibrating, asymmetric β-halocarbenium ions **20'**/**20'-*d***.

7.3.2 Synthesis

The syntheses of mono-deuterated 1,2-dibromoethane **68-*d***, and the analogous 1,2-dichloroethane **69-*d*** are shown in Scheme 26. Mono-deuterated ethane (**71-*d***) was generated by careful quenching of vinylmagnesium bromide (**70**) with deuterium oxide. Subsequent trapping of gaseous **71-*d*** in a solution containing either Br_2 or ICl resulted in formation of the desired dihaloethane, **68-*d*** and **69-*d***, respectively. The 1,2-dibromoethane **68-*d*** was furnished in 19% after purification by vacuum distillation. For formation of the 1,2-dichloroethane **69-*d***, a large excess of ICl was used, and heating was required for 24 h to force the slow, second chlorine addition step forward.[295] After work-up with aqueous $Na_2S_2O_3$ solution, to remove any remaining

ICl, I_2 and/or I_3^-, and subsequent purification by distillation at atmospheric pressure, **69-*d*** was afforded in 36% yield.

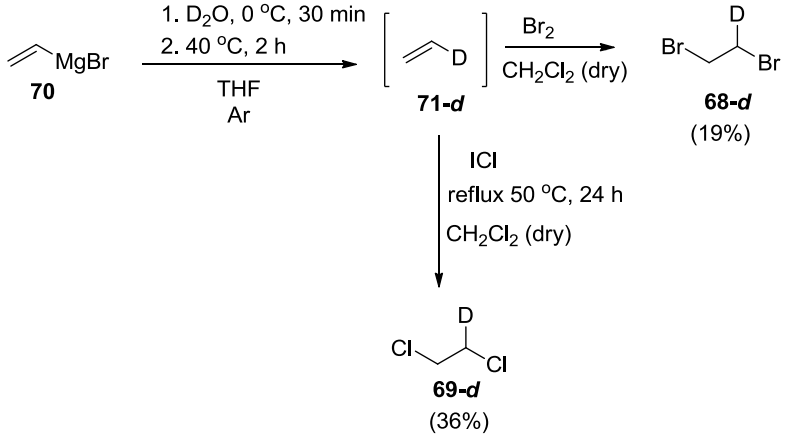

Scheme 26. Synthesis of mono-deuterated 1,2-dibromoethane **68-*d*** and 1,2-dichloroethane **69-*d***.

7.3.3 NMR Experiments

7.3.3.1 Symmetry of the Ethylenebromonium Ion

The sample concentration of the 1:1 mixture of mono-deuterated and non-deuterated 1,2-dibromoethane **68** and **68-*d*** precursors used in the IPE NMR experiments was approximately 30 mg/mL. Non-deuterated 1,2-dibromoethane **68** was obtained from Aldrich. The ionisation was carried out under superacidic SbF_5-SO_2 conditions at -80 °C as described previously in Section 7.2.3. The NMR experiments for the symmetry determination were carried out in the temperature range -90 °C to -40 °C.

Olah and co-workers observed a line-broadening of the singlet at 5.53 ppm in the ^{1}H NMR spectra of the ethylenebromonium ion **20a** at -80 °C using a 60 MHz spectrometer, which they explained as a quadrupolar effect of bromine.[278] This line-broadening may, however, be better explained by another phenomenon. Ionisation of mono-deuterated and non-deuterated 1,2-dibromoethanes, **68** and **68-*d***, resultuted in a ^{1}H NMR spectrum containing two very broad signals, at 5.46 and 4.36 ppm, respectively, at the same temperature using a 300 MHz spectrometer. Upon warming to -60 °C, the two broad signals merged and became one broad signal (5.15 ppm), which sharpened when the temperature was raised further to -40 °C (5.30 ppm). In addition, when cooling the NMR sample to -90 °C, the two broad signals separated wider apart; 5.50 and 4.30 ppm, respectively. This behaviour is indicative of a dynamic process, *i.e.*, an equilibrium slow enough to be observable on the NMR time-scale. Similar behaviour is noted in the resulting ^{13}C NMR spectra in the temperature interval -80 °C to -40 °C. At -80 °C

two broad signals are observed at 65.9 and 27.4 ppm, respectively. These two signals get closer (66.4 and 28.6 ppm) and even broader at -60 °C, and upon increasing the temperature to -40 °C, coalescence is reached. The dynamic behaviour observed in the ^{1}H and ^{13}C NMR spectra are illustrated in Figure 46.

(a) ^{1}H NMR spectra at 300 MHz at -90 °C to -40 °C; expansion 3.0 to 7.2 ppm

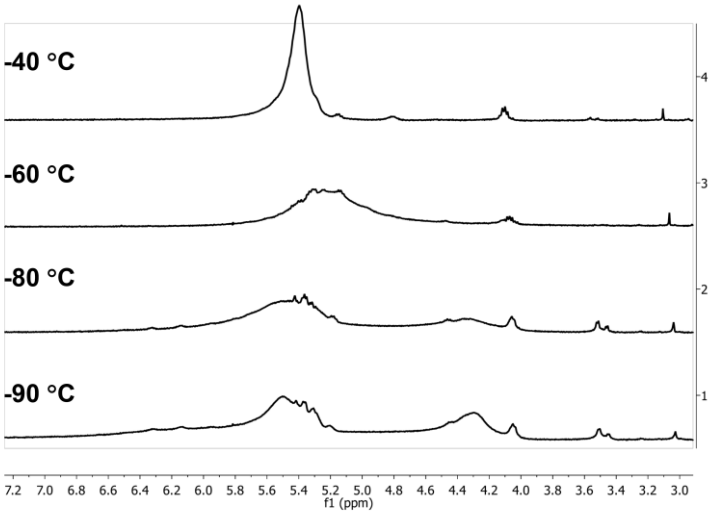

(b) ^{13}C NMR spectra at 75 MHz at -80 °C to -40 °C; expansion 0 to 110 ppm

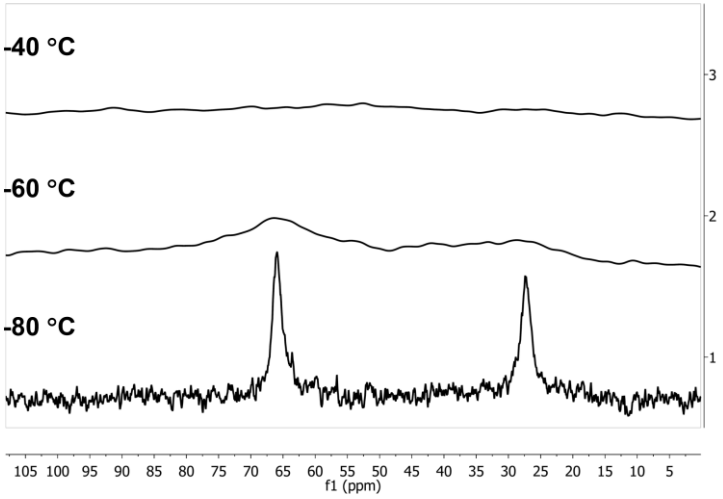

Figure 46. Dynamic NMR spectra of ions generated from **68**/**68-*d*** under SbF_5-SO_2 conditions; **(a)** ^{1}H NMR spectra, **(b)** ^{13}C NMR spectra.

Due to the line-broadening, isotope effects are impossible to detect with the required accuracy. From the ^{1}H and ^{13}C NMR spectra shown in Figure 46, it is, however, obvious that the line-broadening noted by Olah *et al.* should be reinterpreted, at least to a significant extent, as a dynamic effect resulting from a rapid equilibrium of asymmetric ions. Based on the observations, theoretical[290] and experimental,[278, 297] that SO_2 can add to the positive halocarbenium ions, it is

suggested that the asymmetric ions are better described as interconverting cations (**72**) with SO_2 covalently attached,[290] rather than primary β-bromocarbenium ions (Scheme 27).

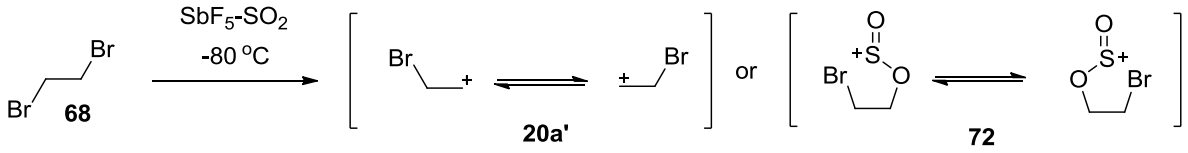

Scheme 27. Formation of fast equilibrating β-bromocarbenium ions (**20a'**) or ion-SO_2 complexes (**72**) upon ionisation of 1,2-dibromoethane (**68**).

7.3.3.2 Symmetry of the Ethylenechloronium Ion

In an attempt to generate the ethylenechloronium ion **20b** from non-deuterated 1,2-dichloroethane (**69**) in SbF_5/SO_2 at -80 °C, the same ^1H NMR spectral pattern as reported by Olah and co-workers was observed;[278] two triplets at 4.36 ppm and 6.26 ppm, respectively (Figure 47). Olah *et al.* suggested the donor-acceptor dihalide-SbF_5 complex **62** (Scheme 23) as the ionisation product. However, the two signals of the ^1H NMR spectrum are also consistent with either a static ion-SO_2 complex or rapid interconverting ion-SO_2 complexes (**73**), as illustrated in Scheme 28.

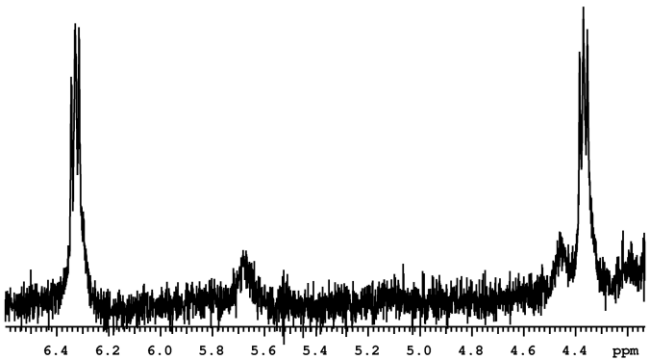

Figure 47. Expanded ^1H NMR spectrum (300 MHz) showing the two triplets of the ionisation product(s) from 1,2-dichloroethane (**69**) in SbF_5/SO_2 at -80 °C.

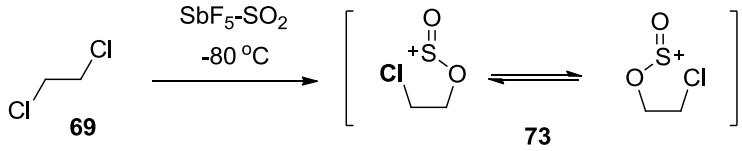

Scheme 28. Proposed formation of fast equilibrating ion-SO_2 complexes (**73**) upon ionisation of 1,2-dichloroethane (**69**) in SbF_5/SO_2 at -80 °C.

The symmetry evaluation of the ionisation products generated from a mixture of non-deuterated and mono-deuterated 1,2-dichloroethanes (**69** and **69-*d***) by IPE NMR spectroscopy is planned to be carried out in the near future.

7.4 CONCLUSIONS AND OUTLOOK

The NMR investigations provide experimental evidence that both the symmetrically substituted 1,2-dimethylethylene- and the parent ethylenebromonium ions, **19a** and **20a**, generated under superacidic conditions, are best represented as a rapid equilibrium of asymmetric cations. For the 1,2-dimethylethylenebromonium ion **19a**, the confirmation of asymmetry is obtained from IPE NMR investigations showing equilibrium isotope shifts. For the ethylenebromonium ion **20a**, the proof of equilibrating ions is given from the dynamic, temperature dependent behaviour of its ^{1}H and ^{13}C NMR signals.

Computational predictions indicate that molecular SO_2 can act as a nucleophile and add to symmetric bromonium ions, producing an asymmetric ion-solvent complex of equal stability as the symmetric ion.[290] The experimental results obtained for the 1,2-dimethylethylene- and ethylenebromonium ions (**19a** and **20a**) also suggest that SO_2 might react with the ions generated. Thus, SO_2 is not an inert solvent, but is nucleophilic and may be involved in rapid exchange processes of cations. If this is true, all ions generated under superacidic conditions with SO_2 as solvent and previously characterised as bromonium ions should neither be described as symmetric bromonium ions nor asymmetric β-bromocarbenium ions. Rather, they should be described as rapidly equilibrating sulfenium ions with the positive charge located on the sulfur atom. As, in principle, all previous characterisations of bromonium ions under superacidic conditions used SO_2 as the solvent, these new results imply that symmetric bromonium ions cannot exist under such conditions. Therefore, the ions generated under SbF_5-SO_2 conditions need to be reinvestigated. Ionisation under superacidic condition with a less nucleophilic solvent, such as SO_2ClF, might facilitate the formation of symmetric bromonium ions. To investigate whether symmetric bromonium ions can exist in solution or not, symmetry evaluation experiments should be performed with SO_2ClF as the solvent instead. Moreover, as SO_2ClF freezes at lower temperature than SO_2, a larger temperature interval is tolerated, which favours the detection of equilibrium isotope effects with IPE NMR spectroscopy.

Based on the attempt to generate the symmetric 1,2-dimethylethylenchloronium ion **19b**, and also on previous attempts of generating the ethylenechloronium ion **20b**,[278] it is evident that the precursors of the chloronium ions react more aggressively under superacidic conditions with SO_2 as solvent than the precursors of the bromonium ions. The ^1H NMR spectral pattern of the ionisation product(s) formed in the attempted preparation of the ethylenechloronium ion (**20b**) described in Section 7.3.3 supports the proposed addition of SO_2. Hence, by using a less nucleophilic solvent than SO_2, there might be a better chance of generating symmetric chloronium ions, or symmetrically substituted, rapidly interconverting β-chlorocarbenium ions with superacid SbF_5. As Olah and co-workers have reported successful generation of the ethylenechloronium ion **20b** when using SO_2ClF as solvent,[301] SO_2ClF would be the solvent of choice in future symmetry investigations of symmetric chloronium ions.

Furthermore, interesting would be to reinvestigate the characterisation of the corresponding symmetric 1,2-dimethylethylene- and ethyleneiodonium ions. As iodine is more polarisable and better at accommodating a positive charge than bromine and chlorine, it is more likely that symmetric iodonium ions are sufficiently stable and really do exist under superacidic conditions with SO_2 as the solvent.

8 SUMMARY AND CONCLUDINDG REMARKS

Within the scientific community, there has always been, and will most likely continue to be, a tremendous interest in gaining an improved understanding in molecular interactions. For medicinal chemists it is especially important to comprehend what interactions are significant to make a potential drug molecule bind to its specific enzyme or receptor protein with high selectivity and affinity. For organic chemists, however, the knowledge of molecular interactions is of great importance for understanding reaction mechanisms, and what interactions are beneficial for synthetic reagents in terms of reactivity and/or stability. As all drugs act in a solution environment within our bodies, and most organic reactions occur in solutions, it is especially advantageous to get a better understanding of molecular interactions in the solution phase.

In this thesis, two specific interaction types have been investigated in solution, the three-centre-four-electron N–X^+–N halogen bond, and the C–X^+–C interaction of a 1,2-bridged halonium ion, respectively. Common to both these interactions, is that, in solution, the positive halogen can be either centrosymmetrically arranged, with equal distances to both nitrogens/carbons, or asymmetrically arranged, always positioned closer to one of the nitrogens/carbons. The major goals of this study was to determine the solution symmetries of N–Br^+–N and N–I^+–N halogen bonds of bis(pyridine)-based $[N–X–N]^+$ halonium model structures, and of C–Br^+–C and C–Cl^+–C interactions of ethylenehalonium ions. For static, single symmetric structures, the positive halogen is centrally located, whereas for asymmetric structures it is constantly jumping between the two nitrogens/carbons in a fast equilibrium process. The symmetries of the two interaction types were evaluated with the NMR spectroscopic method IPE, which is based on measurements of isotope shifts observed for mixtures of non-deuterated and deuterated molecules with unsymmetrical deuterium substitution. The results obtained are summarised in the next two sections.

8.1 BIS(PYRIDINE)-BASED $[N–X–N]^+$ HALONIUM TRIFLATE COMPLEXES

- Non-deuterated and mono-deuterated bis(pyridine)-based $[N–X–N]^+$ halonium triflate complexes **16a,b**-**18a,b** and **16a,b**-***d***-**18a,b**-***d*** were successfully synthesised in moderate to high yields. Successful synthetic protocols for the preparation of non-deuterated and

mono-deuterated 1,2-bis(pyridine-2-ylethynyl)benzene $[N–X–N]^+$ halonium triflate complexes **17a,b-18a,b** and **17a,b-*d*-18a,b-*d*** were developed. The protocol for the mono-deuterated complexes **17a,b-*d*** and **18a,b-*d*** allowed introduction of the deuterium isotope with high regioselectivity at the α-carbon, closest to the nitrogen in one of the pyridine rings.

- The IPE NMR studies combined with VT NMR revealed that all $[N–X–N]^+$ halonium complexes (**16a,b-18a,b**) are static, single symmetric structures in dichloromethane solutions.
- The IPE NMR studies of the $[N–Br–N]^+$ complex **16a** and the $[N–I–N]^+$ complexes **16b** and **17b** for acetonitrile solutions at 25 °C implied that the symmetric $N–X^+–N$ arrangement remain despite increased polarity, which suggests that the symmetry of the halonium complexes is independent from solvent polarity. However, for confirmation of the symmetries in the more polar acetonitrile, VT NMR studies of all $[N–X–N]^+$ complexes and their corresponding static, symmetric, and equilibrating, asymmetric references are required.
- ^1H and ^{19}F NMR diffusion experiments of the $[N–X–N]^+$ halonium complexes **16a,b** and **17a,b** revealed tight binding of the triflate counter ion. Despite the close interaction of the counter ion, the structures are symmetric. This provides evidence of a high energetic gain upon formation of a symmetric three-centre-four-electron $N–X^+–N$ halogen bond.
- The ^{15}N chemical shifts, acquired from ^1H-^{15}N HMBC experiments of **16a,b** and **17a,b**, show a significantly stronger $N–X^+–N$ interaction of the $[N–I–N]^+$ complexes **16b** and **17b** than of the corresponding $[N–Br–N]^+$ complexes **16b** and **17b**, suggesting the interaction of the iodonium complexes is of covalent character, whereas the interaction of the bromonium complexes is of ionic character. The strongest $N–X^+–N$ interaction interactions were found for the bis(pyridine)halonium complexes **16a,b**, for which the N–N distance is adjustable to provide the most favourable interaction.
- From the ^{13}C chemical shifts of the pyridine rings it was evident that the shifts of the $[N–Br–N]^+$ halonium complexes **16a-18a** were comparable with the shifts of their asymmetric $[N–H–N]^+$ complex analogues **27**, **29** and **30**. This further supports that Br^+ is more loosely coordinated between the two nitrogens as compared to I^+; the $N–Br^+–N$ interaction being of ionic and the $N–I^+–N$ interaction of covalent character.
- The dichloromethane solution experiments showed that the 1,2-bis(pyridine-2-ylethynyl)benzene $[N–Br–N]^+$ complexes **17a** and **18a** are less stable as compared to their

corresponding $[N–I–N]^+$ complexes **17b** and **18b**, based on their faster decomposition. The presence of the electron donating *para*-methyl substituents in the pyridine rings proved to have a stabilising effect, as the decomposition of $[N–Br–N]^+$ complex **18a** were somewhat slower than the decomposition of analogous **17a**.

- Computational DFT geometry optimisations for dichloromethane solutions confirmed the static, symmetric structure of the $[N–X–N]^+$ halonium complexes **16a,b** and **17a,b**, respectively.

Overall, this investigation shows that both the experimental and theoretical methods used are well applicable for the symmetry evaluation of the bispyridine-based $[N–X–N]^+$ halonium model systems described. It further provides an insight in the understanding of the 3-centre-4-electron $N–X^+–N$ halogen bonds. Most likely, the same methods can be applied also for the symmetry investigations of related structures.

8.2 Ethylenehalonium Ions

- Non-deuterated and mono-deuterated diastereomeric mixtures of 2,3-dibromobutanes **44a/44a-*d*** and 2,3-dichlorobutanes **44b/44b-*d***, the precursors of the 1,2-dimethylethylenehalonium ions **19a,b**, were successfully synthesised in low to moderate yields. The mono-deuterated precursors of the parent ethylenehalonium ions **20a,b**, 1,2-dibromoethane (**47a-*d***) and 1,2-dichloroethane (**47b-*d***), respectively, were also prepared successfully and isolated in moderate yields.
- The 2,3-dimethylethylenebromonium ions **19a** were generated as a 3:1 diastereomeric mixture from its precursors **44a** in SbF_5-SO_2 at -80 °C. ^1H and ^{13}C NMR spectra revealed the presence of the 1,1-dimethylenebromonium ion **46**, formed *via* successive 1,2-methyl shifts, and two unknown ions. The proposed structures of these two ions were the ion-SO_2 complex **56**, formed *via* nucleophilic SO_2 addition to **46**, and the rearranged α-bromocarbenium ion **57**. The presence of the rearranged cations increased significantly when raising the temperature to -40 °C.
- The IPE NMR studies of the 2,3-dimethylethylenebromonium ions **19a/19a-*d*** showed that the ions are best represented as asymmetric, rapidly equilibrating structures.
- Treating the 2,3-dimethylethylenechloronium ion precursors **44b/44b-*d*** with SbF_5 in liquid SO_2 at -80 °C resulted in complex mixture of rearranged ions. No trace of the

desired chloronium ions **19b/19b-*d*** was observed, and, hence, their symmetries could not be determined.

- Ionisation of 1,2-dibromoethane **47a/47a-*d*** in SbF_5-SO_2 at -80 °C resulted in two broad peaks in the ^1H and ^{13}C NMR spectra. The peaks showed a typical dynamic behaviour upon raising or lowering the temperature. A suggested interpretation is the formation of equilibrating, asymmetric ion-SO_2 complexes (**72**), formed upon addition of nucleophilic SO_2 to either the cyclic ethylenebromonium ion **20a** or its open β-bromocarbenium ion analogue (**20a'**).
- The 1,2-dichloroethane **47b** did not provide the desired cyclic ethylenechloronium ion **47b** upon ionisation in SbF_5-SO_2 at -80 °C. Two triplets were observed in the ^1H NMR spectrum, indicating the presence of either a static ion or asymmetric, fast equilibrating ion-SO_2 complexes (**73**), generated *via* nucleophilic addition of SO_2 to the cyclic chloronium ion **20b** or its β-chlorocarbenium ion analogue (**20b'**).
- Due to the nucleophilic nature of SO_2, the 2,3-dimethylethylene- and ethylenehalonium ions **19a,b** and **20a,b** need to be generated in a less nucleophilic solvent, such as SO_2ClF, to allow proper evaluation of their symmetry, *i.e.*, static, symmetric 1,2-bridged halonium ions or asymmetric, β-halocarbenium ions in fast equilibrium.

The main conclusion obtained from this study is that SO_2 is not an inert solvent. Hence, suggesting that all previous characterisations of bromonium ions generated under SbF_5-SO_2 conditions need to be reinvestigated. Furthermore, this investigation supports the previously reported observations that cyclic chloronium ions are not generated under superacidic conditions using SO_2 as solvent.

ACKNOWLEDGEMENTS

I would like to express my sincere gratitude to the following people, who all have helped and supported me, in one way or the other, during these three years:

First of all, I would like to thank my supervisor, Associate Professor Máté Erdélyi, for taking me on as a PhD student, and making it possible for me to change direction of my studies. Thank you for introducing me to the exciting field of halogen bonding, and for helping me develop a deeper knowledge of NMR spectroscopy. Your guidance, support, commitment to research, and above all, your never-ending positive attitude, have helped me to complete this work in a considerably short time. Thanks also for giving me constructive comments on my thesis.

Professor Ann-Therese Karlberg, my examiner, for your encouragement and good advice.

Professor Göran Karlsson, my co-supervisor, for helping me out with my NMR experiments at the Swedish NMR centre, and for good advice in administration related issues.

Associate Professor Jürgen Gräfenstein, for your input to the computational studies of the $[N–X–N]^+$ halonium complex project, and for teaching me more about computational chemistry. Thank you also for helping me with my conference talk in Spain.

Professor Per-Ola Norrby, for always taking your time to discuss chemistry, and for sharing your vast knowledge about organic synthesis and computational chemistry. Your enthusiasm and jokes always lighten up the working atmosphere! Especially, thank you for giving me constructive feedback on my thesis.

Dr Ulrika Brath, for carrying out the diffusion NMR and ^{15}N shift measurements of the $[N–X–N]^+$ halonium complexes, and for your valuable input in the interpretation of the results.

Dr Roland Kleinmaier, Alavi Karim, master students Jesse Laurila and Adnan Budnjo, for your help with the syntheses of the $[N–X–N]^+$ halonium complexes. Thanks also to Ezgi Tulukcuoglu and Claudine Thevenoux, Erasmus summer students, for your contribution to the synthetic work.

Professor Charles L. Perrin, for valuable discussions about IPE NMR studies, and interpretation of NMR spectra.

All other former and present group members of the Halogen Bonding group: Dr Susanne Mecklenburg, Dr Artur Jögi, Oren Berger, Emma Danelius, Dr Sven Arenz, Dr Alberte Xose Veiga Corral, Ivan Gumula, Stefan Sannö, for help and support in the lab, interesting chemistry discussions, and for providing a good working atmosphere.

Dr Petra Rönnholm, for all your great support and encouragement during these years. Thanks for all enjoyable morning coffee breaks, lunches, and nice conversations about chemistry, and life in general.

Dr Sten Nilsson Lill, for nice lunch company, for interesting discussions about binding interactions, and, above all, for proof-reading my thesis. I very much appreciated your company at the conference in Boston.

Dr Charlotte Johansson, for your support, and for enjoyable conversations at lunches, and coffee breaks.

Former and present colleagues at Organic Chemistry, Medicinal Chemistry, Dermatochemistry, and at the Swedish NMR centre, for creating a friendly working environment.

The administrative and technical staff at the Department of Chemistry, for always being very helpful and friendly. Your help is invaluable!

Professor Brian Ohta, for making it possible for me to work in your lab at Villanova University for six months. Thank you for sharing your knowledge about halonium ion chemistry, and for teaching me new synthetic techniques. I appreciate your enormous generosity and kindness very much! Thank you so much for giving me the opportunity to celebrate Thanksgiving for the first time, and for welcoming my family so warmly.

Dr Walter Boyko, for sharing your expertise in NMR spectroscopy, and for your assistance with running the low temperature NMR experiments of the halonium ion project.

Dr Costas Agrios and Tyler Zook, for nice and interesting conversations in the lab, and for enjoyable lunches and coffee breaks.

All faculty members, administrative and technical staff, and master students at the Department of Chemistry, Villanova University, for giving me such a warm welcome, for always being very helpful, and for making my research visit to a wonderful experience.

Lotta Larsson, for all your enormous support, and for leading me in the right direction. I appreciate your help very much!

My family and friends, for your love and support, and for helping me keep a balance between work and the world outside.

Maggan and Gunnar, my "extra parents," for your generosity and for your help in all kinds of situations. I would never have managed to sort everything out without your help! I am deeply grateful for your never-ending love and support!

My parents and sister, for all your love, support and encouragement. Thank you for always believing in me, and for always being there for me. You are the best!

Last, but not least, I would like to give my gratitude to my beloved Peter and Frida, for your endless love, and enormous patience. Thank you for bringing so much joy and happiness to my life! I love you more than words can ever say!

The research leading to these results has received funding from the European Union Seventh Framework Programme (FP7/2007-2013) under grant agreement n° 259638, and The Swedish Research Council (2007:4407). The Royal Society of Arts and Sciences in Gothenburg, The Helge Ax:son Johnsons Foundation, and The Foundation BLANCEFLOR Boncompagni-Ludovisi, née Bildt are also gratefully acknowledged for making my research visit at Villanova University possible by providing support for travel and living expenses.

REFERENCES

1. Gribble, G. W., Natural Organohalogens: A New Frontier for Medicinal Agents? *J. Chem. Educ.* **2004,** *81* (10), 1441-1449.
2. Gribble, G. W., Naturally Occurring Organohalogen Compounds. *Acc. Chem. Res.* **1998,** *31* (3), 141-152.
3. Neumann, C. S.; Fujimori, D. G.; Walsh, C. T., Halogenation Strategies In Natural Product Biosynthesis. *Chem. Biol.* **2008,** *15* (2), 99-109.
4. Wermuth, C. G., *The Practice of Medicinal Chemistry*. 3rd ed.; Academic Press: London, 2008.
5. Metrangolo, P.; Resnati, G., Halogen Versus Hydrogen. *Science* **2008,** *321*, 918-919.
6. Parisini, E.; Metrangolo, P.; Pilati, T.; Resnati, G.; Terraneo, G., Halogen bonding in halocarbon-protein complexes: a structural survey. *Chem. Soc. Rev.* **2011,** *40* (5), 2267-2278.
7. Bissantz, C.; Kuhn, B.; Stahl, M., A Medicinal Chemist's Guide to Molecular Interactions. *J. Med. Chem.* **2010,** *53*, 5061-5084.
8. Lu, Y.; Shi, T.; Wang, Y.; Yang, H.; Yan, X.; Luo, X.; Jiang, H.; Zhu, W., Halogen Bondings A Novel Interaction for Rational Drug Design? *J. Med. Chem.* **2009,** *52*, 2854-2862.
9. Lu, Y.; Wang, Y.; Zhu, W., Nonbonding interactions of organic halogens in biological systems: implications for drug discovery and biomolecular design. *Phys. Chem. Chem. Phys.* **2010,** *12*, 4543-4551.
10. Barluenga, J., Transferring Iodine: More than a Simple Functional Group Exchange in Organic Synthesis. *Pure Appl. Chem.* **1999,** *71* (3), 431-436.
11. Simonot, B.; Rousseau, G., *Gem*-Dimethyl Effect in the Formation of Seven to Eleven-membered Ring Lactones by Iodolactonisation. *Tetrahedron Lett.* **1993,** *34* (28), 4527-4530.
12. Brunel, Y.; Rousseau, G., Preparation of Oxepanes, Oxepenes, and Oxocanes by Iodoetherification using Bis(*sym*-collidine)iodine(I) Hexafluorophosphate as Electrophile. *J. Org. Chem.* **1996,** *61* (17), 5793-5800.
13. Roux, M.-C.; Paugam, R.; Rousseau, G., Evaluation of *exo-endo* Ratios in the Halolactonization of ω-Unsaturated Acids. *J. Org. Chem.* **2001,** *66* (12), 4304-4310.
14. Ruasse, M.-F., Electrophilic Bromination of Carbon-Carbon Double Bonds: Structure, Solvent and Mechanism. *Adv. Phys. Org. Chem.* **1993,** *28*, 207-291.
15. Ruasse, M.-F., Stereo-, regio- and chemoselectivity of bromination of ethylenic compounds. *Industrial Chem. Lib.* **1995,** *7*, 100-112.
16. Brown, R. S., The Fates of Bromonium Ions in Solution: A Very Short Lifetime with Many Different Endings. *Industrial Chem. Lib.* **1995,** *7*, 113-127.
17. Brown, R. S., Investigation of the Early Steps in Electrophilic Bromination through the Study of the Reaction with Sterically Encumbered Olefins. *Acc. Chem. Res.* **1997,** *30* (3), 131-137.
18. Metrangolo, P.; Neukirch, H.; Pilati, T.; Resnati, G., Halogen Bonding Based Recognition Processes: A World Parallel to Hydrogen Bonding. *Acc. Chem. Res.* **2005,** *38* (5), 386-395.
19. Emsley, J., Very Strong Hydrogen Bonding. *Chem. Soc. Rev.* **1980,** *9*, 91-124.
20. Cleland, W. W.; Kreevoy, M. M., Low-Barrier Hydrogen Bonds and Enzymic Catalysis. *Science* **1994,** *264* (5167), 1887-1890.
21. Frey, P. A.; Whitt, S. A.; Tobin, J. B., A Low-Barrier Hydrogen Bond in the Catalytic Triad of Serine Proteases. *Science* **1994,** *264* (1567), 1927-1930.
22. Warshel, A.; Papazyan, A.; Kollman, P. A.; Cleland, W. W.; Kreevoy, M. M.; Frey, P. A., On Low-Barrier Hydrogen Bonds and Enzyme Catalysis. *Science* **1995,** *269* (5220), 102-106.
23. Ash, E. L.; Sudmeier, J. L.; De Fabo, E. C.; Bachovchin, W. W., A Low-Barrier Hydrogen Bond in the Catalytic Triad of Serine Proteases? Theory Versus Experiment. *Science* **1997,** *278* (5340), 1128-1132.
24. Gerlt, J. A.; Kreevoy, M. M.; Cleland, W. W.; Frey, P. A., Understanding enzymic catalysis: the importance of short, strong hydrogen bonds. *Chem. Biol.* **1997,** *4* (4), 259-267.
25. Politzer, P.; Murray, J. S.; Concha, M. C., Halogen Bonding and the Design of New Materials: Organic Bromides, Chlorides and Perhaps even Fluorides as Donors. *J. Mol. Model.* **2007,** *13* (6-7), 643-650.
26. Bellucci, G.; Bianchini, R.; Ambrosettit, R., Direct Evidence for Bromine-Olefin Charge-Transfer Complexes as Essential Intermediates of the Fast Ionic Addition of Bromine to Cyclohexene. *J. Am. Chem. Soc.* **1985,** *107* (8), 2464-2471.
27. Bellucci, G.; Chiappe, C.; Marioni, F., Evidence for a Reversible Electrophilic Step in Olefin Bromination. The Case of Stilbenes. *J. Am. Chem. Soc.* **1987,** *109* (2), 515-522.
28. Bellucci, G.; Bianchini, R.; Chiappe, C.; Marioni, F.; Ambrosettit, R.; Brown, R. S.; Slebocka-Tilk, H., The Solution Behavior of the Adamantylideneadamantane-Bromine System: Existence of Equilibrium Mixtures of Bromonium-Polybromide Salts and a Strong 1 : 1 Molecular Charge-Transfer Complex. *J. Am. Chem. Soc.* **1989,** *111* (7), 2640-2647.
29. Bellucci, G.; Bianchini, R.; Chiappe, C.; Brown, R. S.; Slebocka-Tilk, H., Different Reversibility of Bromonium vs P-Bromocarbonium Ions Formed during the Electrophilic Bromination of Substituted

Stilbenes. Evidence for Rate Determination during the Product-Forming Step. *J. Am. Chem. Soc.* **1991,** *113* (21), 8012-8016.
30. Ruasse, M.-F., Bromonium Ions or β-Bromocarbocations in Olefin Bromination. A Kinetic Approach to Product Selectivities. *Acc. Chem. Res.* **1990,** *23* (3), 87-93.
31. Clayden, J.; Greeves, N.; Warren, S.; Wothers, P., Organic Chemistry. 1st ed.; Oxford University Press Inc.: New York, 2001; pp 503-518.
32. Solomons, T. W. G., *Organic Chemistry*. 6th ed.; John Wiley & Sons, Inc.: New York, 1996.
33. McMurry, J., Organic Chemistry. 6th ed.; Thomson Learning, Inc.: Belmont, CA, 2004; pp 208-210.
34. Snyder, S. A.; Treitler, D. S.; Brucks, A. P., Halonium-Induced Cyclization Reactions. *Aldrichim. Acta* **2011,** *44* (2), 27-40.
35. Merritt, E. A.; Olofsson, B., Diaryliodonium Salts: A Journey from Obscurity to Fame. *Angew. Chem. Int. Ed.* **2009,** *48* (48), 9052-9070.
36. Brown, R. S.; Nagorski, R. W.; Bennet, A. J.; McClung, R. E. D.; Aarts, G. H. M.; Klobukowski, M.; McDonald, R.; Santarsiero, B. D., Stable Bromonium and Iodonium Ions of the Hindered Olefins Adamantylideneadamantane and Bicycle[3.3.1]nonylidenebicyclo[3.3. llnonane. X-Ray Structure, Transfer of Positive Halogens to Acceptor Olefins, and *ab Initio* Studies. *J. Am. Chem. Soc.* **1994,** *116* (6), 2448-2456.
37. Olah, G. A., *Halonium Ions*. John Wiley & Sons: New York, 1975.
38. Koser, G. F., Halonium ions. In *The Chemistry of Halides Pseudo-halides and Azides* Patai, S.; Rappoport, Z., Eds. John Wiley & Sons Ltd: Chichester, 1983; Vol. 2, pp 1265-1351.
39. Hartmann, C.; Meyer, V., *Chem. Ber.* **1894,** *27*, 426.
40. Stang, P. J.; Zhdankin, V. V., Organic Polyvalent Iodine Compounds. *Chem. Rev.* **1996,** *96* (3), 1123-1178.
41. Zhdankin, V. V.; Stang, P. J., Chemistry of Polyvalent Iodine. *Chem. Rev.* **2008,** *108* (12), 5299-5358.
42. Goldstein, E. J. C.; Citron, D. M.; Warren, Y.; Merriam, C. V.; Tyrrell, K.; Fernandez, H.; Radhakrishnan, U.; Stang, P. J.; Conrads, G., In Vitro Activities of Iodonium Salts against Oral and Dental Anaerobes. *Antimicrob. Agents Chemother.* **2004,** *48* (7), 2766-2770.
43. Shirai, A.; Kubo, H.; Takahashi, E., Novel Diaryliodonium Salts for Cationic Photopolymerization. *J. Photopolym. Sci. Technol.* **2002,** *15* (1), 29-34.
44. VanderHart, D. L.; Prabhu, V. M.; Lin, E. K., Proton NMR Determination of Miscibility in a Bulk Model Photoresist System: Poly(4-hydroxystyrene) and the Photoacid Generator, Di(*tert*-butylphenyl)Iodonium Perfluorooctanesulfonate. *Chem. Mater.* **2004,** *16* (16), 3074-3084.
45. Slegt, M.; Minne, F.; Zuilhof, H.; Overkleeft, H. S.; Lodder, G., Photochemical Generation and Reactivity of Naphthyl Cations: *cine* Substitution. *Eur. J. Org. Chem.* **2007,** (32), 5353-5363.
46. Tasdelen, M. A.; Kumbaraci, V.; Jockusch, S.; Turro, N. J.; Talinli, N.; Yagci, Y., Photoacid Generation by Stepwise Two-Photon Absorption: Photoinitiated Cationic Polymerization of Cyclohexene Oxide by Using Benzodioxinone in the Presence of Iodonium Salt. *Macromolecules* **2008,** *41* (2), 295-297.
47. Nesmeyanov, A. N.; Makarova, L. G.; Tolstaya, T. P., Heterolytic decomposition of Onium Compounds (Diphenyl Halogenonium and Triphenyloxonium Salts). *Tetrahedron* **1957,** *1* (1-2), 145-157.
48. Roberts, I.; Kimball, G. E., The Halogenation of Ethylenes. *J. Am. Chem. Soc.* **1937,** *59* (5), 947-948.
49. Olah, G. A.; Bollinger, J. M., Stable Carbonium Ions. XLVIII. Halonium Ion Formation *via* Neighboring Halogen Participation. Tetramethylethylene Halonium Ions. *J. Am. Chem. Soc.* **1967,** *89* (18), 4744-4752.
50. Olah, G. A.; Peterson, P. E., Stable Carbonium Ions. LXVII. Halonium Ion Formation *via* 1,4-Halogen Participation. Five-Membered-Ring Tetramethylenehalonium, 2-Methyltetramethylenehalonium, and 2,5-Dimethyltetramethylenehalonium Ions. *J. Am. Chem. Soc.* **1968,** *90* (17), 4675-4678.
51. Peterson, P. E.; Bonazza, B. R.; Henrichs, P. M., Cyclization of Mono- and Dimethylated Dihalides to Five- and Six-Membered Ring Halonium Ions. *J. Am. Chem. Soc.* **1973,** *95* (7), 2222-2229.
52. Olah, G. A.; DeMember, J. R., Friedel-Crafts Chemistry. IV. Dialkylhalonium Ions and Their Possible Role in Friedel-Crafts Reactions. *J. Am. Chem. Soc.* **1969,** *91* (8), 2113-2115.
53. Olah, G. A.; DeMember, J. R.; Schlosberg, R. H., Friedel-Crafts Chemistry. III. Methyl-Fluoride-Antimony Pentafluoride, a Powerful New Methylating Agent. Methylation Reactions and the Polycondensation of Methyl Fluoride. *J. Am. Chem. Soc.* **1969,** *91* (8), 2112-2113.
54. Olah, G. A.; DeMember, J. R., Friedel-Crafts Chemistry. V. Isolation and Carbon-13 Nuclear Magnetic Resonance and Laser Raman Spectroscopic Study of Dimethylhalonium Fluoroantimonates. *J. Am. Chem. Soc.* **1970,** *92* (3), 718-720.
55. Olah, G. A.; DeMember, J. R.; Mo, Y. K.; Svoboda, J. J.; Schilling, P.; Olah, J. A., Onium Ions. VII Dialkylhalonium Ions. *J. Am. Chem. Soc.* **1974,** *96* (3), 884-892.
56. Peterson, P. E.; Vidrine, D. W.; Waller, F. J.; Henrichs, P. M.; Magaha, S.; Stevens, B., Analysis of the Swain-Moseley-Bown Equation and Comparison of the Results with Nucleophilicities Derived from Halonium Ion Reactions. *J. Am. Chem. Soc.* **1977,** *99* (24), 7968-7976.
57. Olah, G. A.; Melby, E. G., Onium Ions. III. Alkylarylhalonium Ions. *J. Am. Chem. Soc.* **1972,** *94* (17), 6220-6221.

58. Olah, G. A.; DeMember, J. R., Friedel-Crafts Chemistry. VI. Alkylation of Heteroorganic Compounds with Dialkylhalonium Fluoroantimonates. A New General Preparation of Onium Ion Salts. *J. Am. Chem. Soc.* **1970,** *92* (8), 2562-2564.
59. Strating, J.; Wieringa, J. H.; Wynberg, H., The Isolation of a Stabilized Bromonium Ion. *J. Chem. Soc. D, Chem. Commun.* **1969,** (16), 907-908.
60. Wieringa, J. H.; Strating, J.; Wynberg, H., The Reaction of Chlorine with Adamantylideneadamantane. *Tetrahedron Lett.* **1970,** (52), 4579-4582.
61. Mori, T.; Rathore, R.; Lindeman, S. V.; Kochi, J. K., X-Ray Structure of Bridged 2,2′-Bi(adamant-2-ylidene) Chloronium Cation and Comparison of its Reactivity with a Singly-bonded Chloroarenium Cation *Chem. Commun.* **1998,** (8), 927-928.
62. Hassel, O., Structural Aspects of Interatomic Charge-Transfer Bonding. *Science* **1970,** *170* (3957), 497-502.
63. Metrangolo, P.; Panzeri, W.; Recupero, F.; Resnati, G., Perfluorocarbon-hydrocarbon self-assembly Part 16. ^{19}F NMR study of the halogen bonding between halo-perfluorocarbons and heteroatom containing hydrocarbons. *J. Fluorine Chem.* **2002,** *114* (1), 27-33.
64. Riley, K. E.; Hobza, P., Investigation into the Nature of Halogen Bonding Including Symmetry Adapted Perturbation Theory Analyses. *J. Chem. Theory. Comput.* **2008,** *4* (2), 232-242.
65. Clark, T.; Hennemann, M.; Murray, J. S.; Politzer, P., Halogen Bonding: The σ-Hole. *J. Mol. Model* **2007,** *13* (2), 291-296.
66. Metrangolo, P.; Resnati, G., Categorizing Halogen Bonding and Other Noncovalent Interactions Involving Halogen Atoms. *Chem. Int.* **2010,** *32* (2), 20-21.
67. Metrangolo, P.; Resnati, G., *Halogen Bonding: Fundamentals and Applications*. Springer: Berlin, 2008.
68. Desiraju, G. R.; Harlow, R. L., Cyano-Halogen Interactions and Their Role in the Crystal Structures of the 4-Halobenzonitriles. *J. Am. Chem. Soc.* **1989,** *111* (17), 6757-6764.
69. Reddy, D. S.; Craig, D. C.; Rae, A. D.; Desiraju, G. R., N-Br Mediated Diamondoid Network in the Crystalline Complex Carbon Tetrabromide: Hexamethylenetetramine. *J. Chem. Soc., Chem. Commun.* **1993**, 1737-1739.
70. Reddy, D. S.; Ovchinnikov, Y. E.; Shishkin, O. V.; Struchkov, Y. T.; Desiraju, G. R., Supramolecular Synthons in Crystal Engineering. 3. Solid State Architecture and Synthon Robustness in Some 2,3-Dicyano-5,6-dichloro-1,4-dialkoxybenzenes. *J. Am. Chem. Soc.* **1996,** *118* (17), 4085-4089.
71. Mukherjee, A.; Desiraju, G. R., Halogen Bonding and Structural Modularity in 2,3,4- and 3,4,5-Trichlorophenol. *Cryst. Growth Des.* **2011,** *11*, 3735-3739.
72. Brammer, L.; Espallargas, G. M.; Libri, S., Combining metals with halogen bonds. *CrystEngComm* **2008,** *10* (12), 1712-1727.
73. Espallargas, G. M.; Zordan, F.; Marín, L. A.; Adams, H.; Shankland, K.; van de Streek, J.; Brammer, L., Rational Modification of the Hierarchy of Intermolecular Interactions in Molecular Crystal Structures by Using Tunable Halogen Bonds. *Chem. Eur. J.* **2009,** *15*, 7554-7568.
74. Rissanen, K., Halogen bonded supramolecular complexes and networks. *CrystEngComm* **2008,** *10* (9), 1107-1113.
75. Raatikainen, K.; Huuskonen, J.; Lahtinen, M.; Metrangolo, P.; Rissanen, K., Halogen bonding drives the self-assembly of piperazine cyclophanes into tubular structures. *Chem. Commun.* **2009,** (16), 2160-2162.
76. Raatikainen, K.; Rissanen, K., Hierarchical halogen bonding induces polymorphism. *CrystEngComm* **2009,** *11* (5), 750-752.
77. Raatikainen, K.; Rissanen, K., Modulation of N···I and $^{+}$N–H···Cl^{-}···I Halogen Bonding: Folding, Inclusion, and Self-Assembly of Tri- and Tetraamino Piperazine Cyclophane. *Cryst. Growth Des.* **2010,** *10* (8), 3638-3646.
78. Metrangolo, P.; Resnati, G., Halogen bonding: a paradigm in supramolecular chemistry. *Chem. Eur. J.* **2001,** *7* (12), 2511-2519.
79. Metrangolo, P.; Meyer, F.; Pilati, T.; Resnati, G.; Terraneo, G., Halogen Bonding in Supramolecular Chemistry. *Angew. Chem., Int. Ed.* **2008,** *47* (33), 6114-6127.
80. Cavallo, G.; Metrangolo, P.; Pilati, T.; Resnati, G.; Sansotera, M.; Terraneo, G., Halogen bonding: A general route in anion recognition and coordination. *Chem. Soc. Rev.* **2010,** *39* (10), 3772-3783.
81. Sun, A.; Lauher, J. W.; Goroff, N. S., Preparation of Poly(diiododiacetylene), an Ordered Conjugated Polymer of Carbon and Iodine. *Science* **2006,** *312*, 1030-1034.
82. Metrangolo, P.; Resnati, G.; Pilati, T.; Liantonio, R.; Meyer, F., Engineering Functional Materials by Halogen Bonding. *J. Polym. Sci. Part A: Polym. Chem.* **2007,** *45*, 1-15.
83. Nguyen, H. L.; Horton, P. N.; Hursthouse, M. B.; Legon, A. C.; Bruce, D. W., Halogen Bonding: A New Interaction for Liquid Crystal Formation. *J. Am. Chem. Soc.* **2004,** *126* (1), 16-17.
84. Bruce, D. W.; Metrangolo, P.; Meyer, F.; Präsang, C.; Resnati, G.; Terraneo, G.; Whitwood, A. C., Mesogenic, trimeric, halogen-bonded complexes from alkoxystilbazoles and 1,4-diiodotetrafluorobenzene. *New. J. Chem.* **2008,** *32* (3), 477-482.

85. Präsang, C.; Whitwood, A. C.; Bruce, D. W., Halogen-Bonded Cocrystals of 4-(*N*,*N*-Dimethylamino)pyridine with Fluorinated Iodobenzenes. *Cryst. Growth Des.* **2009,** *9*, 5319-5326.
86. Roper, L. C.; Präsang, C.; Kozhevnikov, V. N.; Whitwood, A. C.; Karadakov, P. B.; Bruce, D. W., Experimental and Theoretical Study of Halogen-Bonded Complexes of DMAP with Di- and Triiodofluorobenzenes. A Complex with a Very Short N···I Halogen Bond. *Cryst. Growth Des.* **2010,** *10*, 3710-3720.
87. Bruce, D. W.; Metrangolo, P.; Meyer, F.; Pilati, T.; Präsang, C.; Resnati, G.; Terraneo, G.; Wainwright, S. G.; Whitwood, A. C., Structure–Function Relationships in Liquid-Crystalline Halogen-Bonded Complexes. *Chem. Eur. J.* **2010,** *16* (31), 9511-9524.
88. Fourmigué, M.; Batail, P., Activation of Hydrogen- and Halogen-Bonding Interactions in Tetrathiafulvalene-Based Crystalline Molecular Conductors. *Chem. Rev.* **2004,** *104* (11), 5379-5418.
89. Fourmigué, M.; Auban-Senzier, P., Anionic Layered Networks Reconstructed from $[Cd(SCN)3]_{\infty}^{-}$ Chains in Pseudo One-Dimensional Conducting Salts of Halogenated Tetrathiafulvalenes. *Inorg. Chem.* **2008,** *47* (21), 9979-9986.
90. Brezgunova, M.; Shin, K.-S.; Auban-Senzier, P.; Jeannin, O.; Fourmigué, M., Combining halogen bonding and chirality in a two-dimensional organic metal (EDT-TTF-I_2)$_2$(*D*-camphorsulfonate)·H2O. *Chem. Commun.* **2010,** *46*, 3926-3928.
91. Hardegger, L. A.; Kuhn, B.; Spinnler, B.; Anselm, L.; Ecabert, R.; Stihle, M.; Gsell, B.; Thoma, R.; Diez, J.; Benz, J.; Plancher, J.-M.; Hartmann, G.; Banner, D. W.; Haap, W.; Diederich, F., Systematic Investigation of Halogen Bonding in Protein–Ligand Interactions. *Angew. Chem. Int. Ed.* **2011,** *50* (1), 314-318.
92. Legon, A. C., Prereactive complexes of dihalogens XY with Lewis bases B in the gas phase: a systematic case for the halogen analogue B...XY of the hydrogen bond B...HX. *Angew. Chem., Int. Ed.* **1999,** *38* (18), 2687-2714.
93. Legon, A. C., The halogen bond: an interim perspective. *Phys. Chem. Chem. Phys.* **2010,** *12* (28), 7736-7747.
94. Tawarada, R.; Seio, K.; Sekine, M., Synthesis and Properties of Oligonucleotides with Iodo-Substituted Aromatic Aglycons: Investigation of Possible Halogen Bonding Base Pairs. *J. Org. Chem.* **2008,** *73* (2), 383-390.
95. Eskandari, K.; Zariny, H., Halogen bonding: A lump–hole interaction. *Chem. Phys. Lett.* **2010,** *492* (1-3), 9-13.
96. Politzer, P.; Murray, J. S.; Clark, T., Halogen Bonding: An Electrostatically-Driven Highly Directional Noncovalent Interaction. *Phys. Chem. Chem. Phys.* **2010,** *12*, 7748-7757.
97. Auffinger, P.; Hays, F. A.; Westhof, E.; Ho, P. S., Halogen bonds in biological molecules. *Proc. Natl. Acad. Sci. U. S. A.* **2004,** *101* (48), 16789-16794.
98. Hays, F. A.; Teegarden, A.; Jones, Z. J. R.; Harms, M.; Raup, D.; Watson, J.; Cavaliere, E.; Ho, P. S., How sequence defines structure: A crystallographic map of DNA structure and conformation. *Proc. Natl. Acad. Sci. U. S. A.* **2005,** *102* (20), 7157-7162.
99. Voth, A. R.; Hays, F. A.; Ho, P. S., Directing macromolecular conformation through halogen bonds. *Proc. Natl. Acad. Sci. U. S. A.* **2007,** *104* (15), 6188-6193.
100. Carter, M.; Ho, P. S., Assaying the Energies of Biological Halogen Bonds. *Cryst. Growth Des.* **2011,** *11* (11), 5087-5095.
101. Wash, P. L.; Ma, S.; Obst, U.; Rebek Jr., J., Nitrogen-Halogen Intermolecular Forces in Solution. *J. Am. Chem. Soc.* **1999,** *121* (34), 7973-7974.
102. Chudzinski, M. G.; McClary, C. A.; Taylor, M. S., Anion Receptors Composed of Hydrogen- and Halogen-Bond Donor Groups: Modulating Selectivity With Combinations of Distinct Noncovalent Interactions. *J. Am. Chem. Soc.* **2011,** *133* (27), 10559-10567.
103. Sarwar, M. G.; Dragisic, B.; Salsberg, L. J.; Gouliaras, C.; Taylor, M. S., Thermodynamics of Halogen Bonding in Solution: Substituent, Structural, and Solvent Effects. *J. Am. Chem. Soc.* **2010,** *132* (5), 1646-1653.
104. Hauchecorne, D.; Szostak, R.; Herrebout, W. A.; van der Veken, B. J., C–X···O Halogen Bonding: Interactions of Trifluoromethyl Halides with Dimethyl Ether. *ChemPhysChem* **2009,** *10*, 2105-2115.
105. Messina, M. T.; Metrangolo, P.; Panzeri, W.; Ragg, E.; Resnati, G., Perfluorocarbon-hydrocarbon self-assembly. Part 3. Liquid phase interactions between perfluoroalkyl halides and heteroatom-containing hydrocarbons. *Tetrahedron Lett.* **1998,** *39* (49), 9069-9072.
106. Glaser, R.; Chen, N.; Wu, H.; Knotts, N.; Kaupp, M., ^{13}C NMR Study of Halogen Bonding of Haloarenes: Measurements of Solvent Effects and Theoretical Analysis. *J. Am. Chem. Soc.* **2004,** *126*, 4412-4419.
107. Hauchecorne, D.; van der Veken, B. J.; Moiana, A.; Herrebout, W. A., The C–C···N halogen bond, the weaker relative of the C–I and C–Br···N halogen bonds, finally characterized in solution. *Chem. Phys.* **2010,** *374*, 30-36.
108. Hauchecorne, D.; van der Veken, B. J.; Herrebout, W. A.; Hansen, P. E., A ^{19}F NMR study of C–I···π halogen bondingp halogen bonding. *Chem. Phys.* **2011,** *381*, 5-10.

109. Tatko, C. D.; Waters, M. L., Effect of Halogenation on Edge-Face Aromatic Interactions in a β-Hairpin Peptide: Enhanced Affinity with Iodo-Substituents. *Org. Lett.* **2004,** *6* (22), 3969-3972.
110. Sarwar, M. G.; Dragisic, B.; Sagoo, S.; Taylor, M. S., A Tridentate Halogen-Bonding Receptor for Tight Binding of Halide Anions. *Angew. Chem. Int. Ed.* **2010,** *122*, 1718-1721.
111. Dimitrijević, E.; Kvak, O.; Taylor, M. S., Measurements of weak halogen bond donor abilities with tridentate anion receptors. *Chem. Commun.* **2010,** *46*, 9025-9027.
112. Guthrie, F., XXVIII. - On the Iodide of Iodoammonium. *J. Chem. Soc.* **1863,** *16*, 239-244.
113. Lachman, A., A Probable Cause of the Different Colors of Iodine Solutions. *J. Am. Chem. Soc.* **1902,** *25*, 50-55.
114. Kleinberg, J.; Davidson, A. W., The Nature of Iodine Solutions. *Chem. Rev.* **1948,** *42*, 601-609.
115. Walker, O. J., Absorption Spectra of Iodine Solutions and the Influence of the Solvent. *Trans. Faraday Soc.* **1935,** *31*, 1432-1438.
116. Benesi, H. A.; Hildebrand, J. H., A spectrophotometric investigation of the interaction of iodine with aromatic hydrocarbons. *J. Am. Chem. Soc.* **1949,** *71*, 2703-2707.
117. Keefer, R. M.; Andrews, L. J., The interaction of bromine with benzene and certain of its derivatives. *J. Am. Chem. Soc.* **1950,** *72*, 4677-4681.
118. Andrews, L. J.; Keefer, R. M., *Molecular complexes in organic chemistry*. Holden-Day: San Francisco, 1964.
119. Mulliken, R. S., Structures of Complexes Formed by Halogen Molecules with Aromatic and with Oxygenated Solvents. *J. Am. Chem. Soc.* **1950,** *72* (1), 600-608.
120. Mulliken, R. S., Molecular Compounds and their Spectra. II. *J. Am. Chem. Soc.* **1952,** *74* (3), 811-824.
121. Mulliken, R. S., Molecular Compounds and their Spectra. III. The Interaction of Electron Donors and Acceptors. *J. Phys. Chem.* **1952,** *56* (7), 801-822.
122. Hassel, O.; Hvoslef, J., The Structure of Bromine 1,4-Dioxane. *Acta Chem. Scand.* **1954,** *8* (5), 873.
123. Bondi, A., van der Waals Volumes and Radii. *J. Phys. Chem.* **1964,** *68* (3), 441-451.
124. Aylward, G.; Findlay, T., *SI Chemical Data*. 3rd ed.; John Wiley & Sons: Milton, Queensland, 1994.
125. Hassel, O.; Strømme, K. O., Halogen-Molecule Bridges in Solid Addition Compounds. *Nature* **1958,** *182*, 1155-1156.
126. Hassel, O.; Strømme, K. O., Structure of the Crystalline Compound Benzene-Bromine (1:1). *Acta Chem. Scand.* **1958,** *12*, 1146.
127. Hassel, O., Structural Aspects of Interatomic Charge-Transfer Bonding. In *Nobel Lectures, Chemistry 1963-1970*, Elsevier Publishing Company: Amsterdam, 1972; pp 314-329.
128. Bent, H. A., Structural Chemistry of Donor-Acceptor Interactions. *Chem. Rev.* **1968,** *68* (5), 587-648.
129. Foster, R., *Organic Charge-Transfer Complexes*. Academic Press: London, 1969.
130. Dumas, J.-M.; Peurichard, H.; Gomel, M., CX_4...Base Interactions as Models of Weak Charge-transfer Interactions: Comparison with Strong Charge-transfer and Hydrogen-bond Interactions. *J. Chem. Res., Synop.* **1978,** *2*, 54-57.
131. Ramasubbu, N.; Parthasarathy, R.; Murray-Rust, P., Angular Preferences of Intermolecular Forces around Halogen Centers: Preferred Directions of Approach of Electrophiles and Nucleophiles around the Carbon Halogen Bond. *J. Am. Chem. Soc.* **1986,** *108* (15), 4308-4314.
132. Lommerse, J. P. M.; Stone, A. J.; Taylor, R.; Allen, F. H., The Nature and Geometry of Intramolecular Interactions between Halogens and Oxygen or Nitrogen. *J. Am. Chem. Soc.* **1996,** *118* (13), 3108-3116.
133. Corradi, E.; Meille, S. V.; Messina, M. T.; Metrangolo, P.; Resnati, G., Halogen Bonding versus Hydrogen Bonding in Driving Self-Assembly Processes. *Angew. Chem. Int. Ed.* **2000,** *39* (10), 1782-1786.
134. Politzer, P.; Lane, P.; Concha, M. C.; Ma, Y.; Murray, J. S., An Overview of Halogen Bonding. *J. Mol. Model* **2007,** *13* (2), 305-311.
135. Metrangolo, P.; Murray, J. S.; Pilati, T.; Politzer, P.; Resnati, G.; Terraneo, G., Fluorine-Centered Halogen Bonding: A Factor in Recognition Phenomena and Reactivity. *Cryst. Growth Des.* **2011,** *11* (9), 4238-4246.
136. Metrangolo, P.; Murray, J. S.; Pilati, T.; Politzer, P.; Resnati, G.; Terraneo, G., The Fluorine Atom as a Halogen Bond Donor, *viz*. a Positive Site. *CrystEngComm* **2011,** *13* (22), 6593-6596.
137. Shields, Z. P.; Murray, J. S.; Politzer, P., Directional Tendencies of Halogen and Hydrogen Bonds. *Int. J. Quantum Chem.* **2010,** *110*, 2823-2832.
138. Larson, J. W.; McMahon, T. B., Strong Hydrogen Bonding in Gas-Phase Anions. An Ion Cyclotron Resonance Determination of Fluoride Binding Energetics to Brernsted Acids from Gas-Phase Fluoride Exchange Equilibria Measurements. *J. Am. Chem. Soc.* **1983,** *105* (10), 2944-2950.
139. Larson, J. W.; McMahon, T. B., Gas-Phase Bihalide and Pseudobihalide Ions. An Ion Cyclotron Resonance Determination of Hydrogen Bond Energies in XHY- Species (X, Y = F, C1, Br, CN). *Inorg. Chem.* **1984,** *23* (14), 2029-2033.
140. Alkorta, I.; Blanco, F.; Solimannejad, M.; Elguero, J., Computation of Hydrogen Bonds and Halogen bonds in Complexes of Hypohalous Acids. *J. Phys. Chem. A* **2008,** *112*, 10856-10863.

141. Zhou, P.-P.; Qui, W.-Y.; Liu, S.; Jin, N.-Z., Halogen as halogen-bonding donor and hydrogen-bonding acceptor simultaneously in ring-shaped $H_3N{\cdot}X(Y){\cdot}HF$ (X = Cl, Br and Y = F, Cl, Br) Complexes. *Phys. Chem. Chem. Phys.* **2011,** *13*, 7408-7418.
142. Li, Q.-Z.; Jing, B.; Li, R.; Liu, Z.-B.; Li, W.-Z.; Luan, F.; Cheng, J.-B.; Gong, B.-A.; Sun, J.-Z., Some measures for making halogen bonds stronger than hydrogen bonds in H_2CS-HOX (X = F, Cl, and Br) complexes. *Phys. Chem. Chem. Phys.* **2011,** *13*, 2266-2271.
143. Aakeröy, C. B.; Desper, J.; Helfrich, B. A.; Metrangolo, P.; Pilati, T.; Resnati, G.; Stevenazzi, A., Combining halogen bonds and hydrogen bonds in the modular assembly of heteromeric infinite 1-D chains. *Chem. Commun.* **2007,** (41), 4236-4238.
144. Aakeröy, C. B.; Fasulo, M.; Schultheiss, N.; Desper, J.; Moore, C., Structural Competition between Hydrogen Bonds and Halogen Bonds. *J. Am. Chem. Soc.* **2007,** *129* (45), 13772-13773.
145. Aakeröy, C. B.; Chopade, P. D.; Ganser, C.; Desper, J., Facile synthesis and supramolecular chemistry of hydrogen bond/halogen bond-driven multi-tasking tectons. *Chem. Commun.* **2011,** *47* (16), 4688-4690.
146. Voth, A. R.; Khuu, P.; Oishi, K.; Ho, P. S., Halogen bonds as orthogonal molecular interactions to hydrogen bonds. *Nature Chem.* **2009,** *1* (1), 74-79.
147. Keyser, S. K.; Wilcox, C. S. *Molecular Torsion Balance for Evaluation of Halogen Bonding in Polar an Nonpolar Solvents*; Poster ORGN-294, 240th ACS National Meeting, Boston, MA, United States, August 22-26, 2010.
148. Di Paolo, T.; Sandorfy, C., Fluorocarbon anaesthetics break hydrogen bonds. *Nature* **1974,** *252*, 471-472.
149. Carlsohn, H., *Habilitationsschrift: Über eine neue Klasse von Verbindungen des positive Einwertigen Jod*. Verlag von S. Hirzel: Liepzig, 1932.
150. Zingaro, R. A.; Goodrich, J. E.; Keinberg, J.; Van der Werf, C. A., Reactions of the Silver Salts of Carboxylic Acids with Iodine in the Presence of Some Tertiary Amines. *J. Am. Chem. Soc.* **1949,** *71* (2), 575-576.
151. Zingaro, R. A.; Van der Werf, C. A.; Kleinberg, J., Further Observation on the Preparation and Reactions of Positive Iodine Salts. *J. Am. Chem. Soc.* **1950,** *72* (11), 5341-5342.
152. Schmidt, H.; Meinert, H., Zur Darstellung von Salzen mit positiv einwertigen Halogen-Kationen. *Angew. Chem.* **1959,** *71* (3), 126-127.
153. Kleinberg, J., Unipositive Halogen Complexes. *Inorg. Synth.* **1963,** *7* (1), 169-176.
154. Hassel, O.; Hope, H., Structure of the Solid Compound Formed by Addition of Two Molecules of Iodine to One Molecule of Pyridine. *Acta Chem. Scand.* **1961,** *15* (2), 407-416.
155. Zingaro, R. A.; Tolberg, W. E., Infrared Spectra of Pyridine Coordinated Iodine(I) Salts. *J. Am. Chem. Soc.* **1959,** *81* (6), 1353-1357.
156. Creighton, J. A.; Haque, I.; Wood, J. L., The Iododipyridinium Ion. *Chem. Commun.* **1966,** (8), 229.
157. Haque, I.; Wood, J. L., The Vibrational Spectra and Structure of the Bis(pyridine)iodine(I), Bis(pyridine)bromine(I), Bis(γ-picoline)iodine(I) and Bis(γ-picoline)bromine(I) Cations. *J. Mol. Struct.* **1968,** *2*, 217-238.
158. Rubenacker, G. V.; Brown, T. L., Nitrogen-14 Nuclear Quadrupole Resonance Spectra of Coordinated Pyridine. An Extended Evaluation of the Coordinated Nitrogen Model. *Inorg. Chem.* **1980,** *19*, 392-398.
159. Rubenacker, G. V.; Brown, T. L., Nitrogen-14 Nuclear Quadrupole Resonance Spectra of Pyridine-Halogen Complexes. *Inorg. Chem.* **1980,** *19*, 398-401.
160. Tytko, K.-H.; Schmeisser, M., Chemische Charakterisierung des $[py_2X]^+$-Ions (X = Br, J). *Z. Naturforsch., B: Chem. Sci.* **1973,** *28*, 731-735.
161. Tassaing, T.; Besnard, M., Ionization Reaction in Iodine/Pyridine Solutions: What Can We Learn from Conductivity Measurements, Far-Infrared Spectroscopy, and Raman scattering? *J. Phys. Chem. A* **1997,** *101* (15), 2803-2808.
162. Tassaing, T.; Besnard, M., Vibrational Spectroscopic Studies of the Chemical Dynamics in Charge Transfer Complexeses of the Type Iodine-Pyridine 1. Experimental Results. *Mol. Phys.* **1997,** *92* (2), 271-280.
163. Baruah, S. K., Infrared Studies of some Sensitive Vibrational Modes of Pyridines on Complex Formation with Halogens and Interhalogens. *Asian J. Chem.* **2004,** *16* (2), 706-710.
164. Schuster, I. I.; Roberts, J. D., Halogen Complexes of Pyridines: A Proton and Carbon-13 Nuclear Magnetic Resonance Study. *J. Org. Chem.* **1979,** *44* (15), 2658-2662.
165. Baruah, S. K.; Baruah, P. K., Studies of Nuclear Magnetic Resonance spectra of Positive Halogen Salts of Pyridine and Substituted Pyridines. *Asian J. Chem.* **2004,** *16* (2), 688-694.
166. Alcock, N. W.; Robertson, B. B., Crystal and Molecular Structure of Bis(quinoline) bromine Perchlorate. *J. Chem. Soc., Dalton Trans.* **1975,** (23), 2483-2486.
167. Brayer, G. D.; James, M. N. G., A Charge-Transfer Complex: Bis(2,4,6-trimethyl-1-pyridyl)iodonium Perchlorate. *Acta Cryst.* **1982,** *B38*, 654-657.
168. Álvares-Rúa, C.; García-Granda, S.; Ballesteros, A.; González-Bobes, F.; González, J. M., Bis(pyridine)iodonium(I) tetrefluoroborate. *Acta Cryst.* **2002,** *E58*, o1381-o1383.

169. Batsanov, A. S.; Lightfoot, A. P.; Twiddle, S. J. R.; Whiting, A., Bis(2,6-dimethylpyridyl)iodonium dibromoiodate. *Acta Crystallogr., Sect. E: Struct. Rep. Online* **2006,** *62*, o901-o902.
170. Blair, L. K.; Parris, K. D.; Hii, P. S.; Brock, C. P., A Stable Br^+ Complex. A Twisted Bicycle[2.2.2]octane Derivative. Synthesis and Structure of Bis(quinuclidine)bromine(I) Tetrafluoroborate. *J. Am. Chem. Soc.* **1983,** *105* (11), 3649-3653.
171. Neverov, A. A.; Xiaomei Feng, H.; Hamilton, K.; Brown, R. S., Bis(pyridine)-Based Bromonium Ions. Molecular Structures of Bis(2,4,6-collidine)bromonium Perchlorate and Bis(pyridine)bromonium Triflate and the Mechanism of the Reactions of 1,2-Bis(2'-pyridylethynyl)benzenebrominum Triflate and Bis(pyridine)bromonium Triflate with Acceptor Olefins. *J. Org. Chem.* **2003,** *68* (10), 3802-3810.
172. Lin, G. H.-Y.; Hope, H., The Crystal Structure of Bis(thiourea)iodine(I) Iodide. *Acta Cryst.* **1972,** *B28*, 643-646.
173. Sabin, J. R., Some Calculations on the Lighter Bis(pyridine)halogen(I) Cations. *J. Mol. Struct.* **1972,** *11*, 33-51.
174. Barluenga, J.; González, J. M.; Campos, P. C.; Asensio, G., $I(py)_2BF_4$, a New Reagent in Organic Synthesis: General Method for the 1,2-Iodofunctionalization of Olefins. *Angew. Chem. Int. Ed. Engl.* **1985,** *24* (4), 319-320.
175. Barluenga, J.; Rodríguez, M. A.; Campos, P. J., Electrophilic Additions of Positive Iodine to Alkynes through an Iodonium Mechanism. *J. Org. Chem.* **1990,** *55*, 3104-3106.
176. Barluenga, J.; González, J. M.; García-Martín, M. A.; Campos, P. J., Polyiodination on Benzene at Room Temperature A Regioselective Synthesis of Derivatives. *Tetrahedron Lett.* **1993,** *34* (24), 3893-3896.
177. Barluenga, J.; González-Bobes, F.; Murguía, M. C.; Ananthoju, S. R.; González, J. M., Bis(pyridine)iodonium Tetrafluoroborate (IPy_2BF_4): A Versatile Oxidizing Reagent. *Chem. Eur. J.* **2004,** *10* (4206-4213).
178. Huang, K.-T.; Winssinger, N., IPy_2BF_4-Mediated Glycosylation and Glycosyl Fluoride Formation. *Eur. J. Org. Chem.* **2007**, 1887-1890.
179. López, J. C.; Bernal-Albert, P.; Uriel, C.; Valverde, S.; Gómez, A. M., IPy_2BF_4/HF-Pyridine: A New Combination of Reagents for the Transformation of Partially Unprotected Thioglycosides and *n*-Pentenyl Glycosides to Glycosyl Fluorides. *J. Org. Chem.* **2007,** *72*, 10268-10271.
180. Lemieux, R. U.; Morgan, A. R., The Synthesis of β-D-Glucopyranosyl 2-deoxy-α-D-*arabino*-hexapyranoside. *Can. J. Chem.* **1965,** *43*, 2190-2198.
181. Kano, S.; Yokomatsu, T.; Iwasawa, H.; Shibuya, S., A Regio and Diastereoselective Bromolactamization of δ,γ-Unsaturaterd Thioimidates. *Heterocycles* **1987,** *26* (2), 359-362.
182. Simonot, B.; Rousseau, G., Preparation of Seven-Membered and Medium-Ring Lactones by Iodo Lactonization. *J. Org. Chem.* **1993,** *58* (1), 4-5.
183. Simonot, B.; Rousseau, G., Oxygen Effect in the Iodo Lactonization of Unsaturated Carboxylic Acids Leading to 7- to 12-Membered Ring Lactones. *J. Org. Chem.* **1994,** *59* (20), 5912-5919.
184. Homsi, F.; Rousseau, G., Preparation of Medium-Ring Lactones and Lactams by Electrophilic Cyclizations. *J. Org. Chem.* **1998,** *63* (15), 5255-5258.
185. Homsi, F.; Rousseau, G., 4-*Endo-Trig* Cyclization Processes Using Bis(collidine)bromine(I) Hexafluorophosphate as Reagent: Preparation of 2-Oxetanones, 2-Azetidinones, and Oxetanes. *J. Org. Chem.* **1999,** *64* (1), 81-85.
186. Homsi, F.; Rousseau, G., Halodecarboxylation of α,β-acetylenic and α,β-ethylenic acids. *Tetrahedron Lett.* **1999,** *40*, 1495-1498.
187. Lahrache, H.; Robin, S.; Rousseau, G., Halodephosphorylation of α,β-unsaturated phosphonic acid monoesters. *Tetrahedron Lett.* **2005,** *46* (10), 1635-1637.
188. Rousseau, G.; Robin, S., Bis(*sym*-collidine)bromine(I) hexafluorophosphate as oxidant. *Tetrahedron Lett.* **2000,** *41* (46), 8881-8885.
189. Günther, H., *NMR Spectroscopy*. 2nd ed.; John Wiley & Sons: New York, 1995.
190. Saunders, M.; Jaffe, M. H.; Vogel, P., A New Method for Measuring Equilibrium Deuterium Isotope Effects. Isomerization of 3-Deuterio-2,3-dimethylbutyl-2-ium Ion. *J. Am. Chem. Soc.* **1971,** *93* (10), 2558-2559.
191. Siehl, H.-U., Isotope Effects on NMR Spectra of Equilibrating Systems. *Adv. Phys. Org. Chem.* **1987,** *23*, 63-163.
192. Saunders, M.; Telkowski, L.; Kates, M. R., Isotopic Perturbation of Degeneracy. Carbon-13 Nuclear Magnetic Resonance Spectra of Dimethylcyclopentyl and Dimethylnorbornyl Cations. *J. Am. Chem. Soc.* **1977,** *99* (24), 8070-8071.
193. Perrin, C. L., Symmetry of hydrogen bonds in solution. *Pure Appl. Chem.* **2009,** *81* (4), 571-583.
194. Perrin, C. L., Symmetries of Hydrogen Bonds in Solution. *Science* **1994,** *266* (5191), 1665-1668.
195. Perrin, C. L.; Lau, J. S., Hydrogen-bond symmetry in zwitterionic phthalate anions: symmetry breaking by solvation. *J. Am. Chem. Soc.* **2006,** *128* (36), 11820-11824.
196. Perrin, C. L.; Ohta, B. K., Symmetry of N-H-N Hydrogen Bonds in 1,8-Bis(dimethylamino)naphthalene·H^+ and 2,7-Dimethoxy-1,8-bis(dimethylamino)naphthalene·H^+. *J. Am. Chem. Soc.* **2001,** *123* (27), 6520-6526.

197. Perrin, C. L.; Ohta, B. K., Symmetry of O-H-O and N-H-N Hydrogen Bonds in 6-Hydroxy-2-formylfulvene and 6-Aminofulvene-2-aldimines. *Bioorg. Chem.* **2002,** *30* (1), 3-15.
198. Saunders, M.; Kates, M. R., Deuterium Isotope Effect on the Carbon-13 NMR Spectrum of the Bicyclo[2.2.1]heptyl Cation. Nonclassical Norbornyl Cation. *J. Am. Chem. Soc.* **1980,** *102* (22), 6867-6868.
199. Saunders, M.; Siehl, H. U., Deuterium Isotope Effects on the Cyclobutyl-Cyclopropylcarbinyl Cation. *J. Am. Chem. Soc.* **1980,** *102* (22), 6868-6869.
200. Saunders, M.; Kates, M. R., Isotopic Perturbation Effects on a Single Averaged NMR Peak: Norbornyl Cation. *J. Am. Chem. Soc.* **1983,** *105* (11), 3571-3573.
201. Ahlberg, P.; Engdahl, C.; Jonsäll, G., The 9-Barbaralyl Cation, Isotopic Perturbation by Eight Deuteriums of a Totally Degenerate ^{13}C-Labeled $C_9H_9^+$ Carbonium Ion. *J. Am. Chem. Soc.* **1981,** *103* (6), 1583-1584.
202. Engdahl, C.; Jonsäll, G.; Ahlberg, P., The Totally Degenerate $(CH)_9^+$ Ion 9-Barbaralyl Cation Studied by ^{13}C Labeling and Isotopic Perturbation by Eight Deuteriums. *J. Am. Chem. Soc.* **1983,** *105* (4), 891-897.
203. Ohta, B. K.; Hough, R. E.; Schubert, J. W., Evidence for β-Chlorocarbenium and β-Bromocarbenium Ions. *Org. Lett.* **2007,** *9* (12), 2317-2320.
204. Servis, K. L.; Domenick, R. L., NMR Isotope Shifts as a Probe of Electronic Structure. *J. Am. Chem. Soc.* **1985,** *107* (24), 7186-7187.
205. Perrin, C. L.; Kim, Y.-J., Symmetry of Metal Chelates. *Inorg. Chem.* **2000,** *39* (17), 3902-3910.
206. Saunders, M.; Kates, M. R.; Wiberg, K. B.; Pratt, W., Isotopic Perturbation of Resonance. Carbon-13 Nuclear Magnetic Resonance of 2-Deuterio-2-bicyclo[2.1.1]hexyl Cation. *J. Am. Chem. Soc.* **1977,** *99* (24), 8072-8073.
207. Davies, J. E.; Nunn, E. K., The Crystal Structure of CsIBr. *J. Chem. Soc. D, Chem. Commun.* **1969,** (23), 1374.
208. Slater, R. C. L. M., The Triiodide Ion in Tetraphenyl Arsonium Triiodide. *Acta Cryst.* **1959,** *12* (3), 187-196.
209. Tasman, H. A.; Boswijk, K. H., Re-investigation of the crystal structure of CsI_3. *Acta Cryst.* **1955,** *8* (1), 59-60.
210. Gonschorek, W.; Küppers, H., The Crystal structure of Lithium Hydrogen Phthalate Dihydrate, Containing a Very Short Hydrogen Bond *Acta Cryst.* **1975,** *B31*, 1068-1072.
211. Adiwidjaja, G.; Küppers, H., Lithium Hydrogen Phthalate-Methanol. *Acta Cryst.* **1978,** *B34*, 2003-2005.
212. Wilson, C. C.; Thomas, L. H.; Morrison, C. A., A symmetric hydrogen bond revisited: potassium hydrogen maleate by variable temperature, variable pressure neutron diffraction and plane-wave DFT methods. *Chem. Phys. Lett.* **2003,** *381*, 102-108.
213. Forsyth, D. A., Isotope Effects on ^{13}C NMR Shifts and Coupling Constants. *Isot. Org. Chem.* **1984,** *6*, 1-66.
214. Jameson, C., J.; Osten, H. J., Theoretical Aspects of Isotope Effects on Nuclear Shielding. *Annu. Rep. NMR Spectrosc.* **1986,** *17*, 1-78.
215. Hansen, P. E., Isotope Effects in Nuclear Shielding. *Prog. Nucl. Magn. Reson. Spectrosc.* **1988,** *20*, 207-255.
216. Friebolin, H., *Basic One- and Two-Dimensional NMR Spectroscopy*. 3rd ed.; Wiley- VCH: Weinheim, 1998.
217. Weston, R. E., Jr. , The Magnitude of Electronic Isotope Effects. *Tetrahedron* **1959,** *6* (1), 31-35.
218. Laurie, V. W.; Herschbach, D. R., Influence of Vibrations on Molecular Structure Determinations. II. Average Structures Derived from Spectroscopic Data. *J. Chem. Phys.* **1962,** *37* (8), 1687-1693.
219. Jameson, C., J.; Osten, H. J., The additivity of NMR isotope shifts. *J. Phys. Chem.* **1984,** *8* (10), 4293-4299.
220. Dziembowska, T.; Hansen, P. E.; Rozwadowski, Z., Studies based on deuterium isotope effect on ^{13}C chemical shifts. *Prog. Nucl. Magn. Reson. Spectrosc.* **2004,** *45*, 1-29.
221. Vujanić, P.; Gacs-Baitz, E.; Meić, Z.; Šuste, T.; Smrečki, V., Prinary and Secondary Deuterium-Induced Isootope Effects for ^{13}C NMR Parameters of Benzaldehyde. *Magn. Reson. Chem.* **1995,** *333*, 426-430.
222. Novak, P.; Meić, Z.; Vikić-Topić, D.; Smrečki, V.; Plavec, J., Structural dependence of isotope effects in ^{1}H and ^{13}C nuclear magnetic resonance spectra of the *trans*-N-benzylideneaniline imino group. *Spectrochim. Acta, Part A* **1998,** *54* (2), 327-333.
223. Vikić-Topić, D.; Novak, P.; Smrečki, V.; Meić, Z., Deuterium isotope effects in ^{13}C NMR spectra of trans-azobenzene. *J. Mol. Struct.* **1997,** *410-411*, 5-7.
224. Smirnov, S. N.; Golubev, N. S.; Denisov, G. S.; Benedict, H.; Schah-Mohammedi, P.; Limbach, H.-H., Hydrogen/Deuterium Isotope Effects on the NMR Chemical Shifts and Geometries of Intermolecular Low-Barrier Hydrogen-Bonded Complexes. *J. Am. Chem. Soc.* **1996,** *118* (17), 4094-4101.
225. Mazzini, S.; Merlini, L.; Mondelli, R.; Nasini, G.; Ragg, E.; Scaglioni, L., Deuterium isotope effect on ^{1}H and ^{13}C chemical shifts of intramolecularly hydrogen bonded perylenequinones. *J. Chem. Soc., Perkin Trans. 2* **1997**, 2013-2021.
226. Dunitz, J. D.; Ibberson, R. M., Is Deuterium Always Smaller than Protium? *Angew. Chem. Int. Ed.* **2008,** *47*, 4208-4210.
227. Lambert, J. B.; Vagenas, A. R.; Somani, S., Concerning the Generality of the Temperature Dependence of Carbon-13 Shieldings as a Probe for Conformational or Structural Equilibria. *J. Am. Chem. Soc.* **1981,** *103* (21), 6398-6402.

228. Kronja, O.; Köhli, T.-P.; Mayr, H.; Saunders, M., The Structure of the Nonamethylcyclopentyl Cation. *J. Am. Chem. Soc.* **2000,** *122* (33), 8067-8070.
229. Hartshorn, S. R.; Shiner, V. J., Jr., Calculation of H/D, $^{12}C/^{13}C$, and $^{12}C/^{14}C$ Fractionation Factors from Valence Force Fields Derived for a Series of Simple Organic Molecules. *J. Am. Chem. Soc.* **1972,** *94* (26), 9002-9012.
230. Perrin, C. L.; Ohta, B. K.; Kuperman, J.; Liberman, J.; Erdélyi, M., Stereochemistry of β-Deuterium Isotope Effects on Amine Basicity. *J. Am. Chem. Soc.* **2005,** *127* (26), 9641-9647.
231. Muñoz-Caro, C.; Niño, A.; Dávalos, J. Z.; Quintanilla, E.; Abboud, J. L., Experimental and Theoretical Study of the Secondary Equilibrium Isotope Effect (SEIE) in the Proton Transfer between the Pyridinium-d_5 Cation and Pyridine. *J. Phys. Chem. A* **2003,** *107*, 6160-6167.
232. Saunders, M.; Kates, M. R., Isotopic Perturbation of Resonance. Carbon-13 Nuclear Magnetic Resonance Spectra of Deuterated Cyclohexenyl and Cyclopentenyl Cations. *J. Am. Chem. Soc.* **1977,** *99* (24), 8071-8072.
233. Prakash, G. K. S.; Arvanaghi, M.; Olah, G. A., Deuterium Isotope Effects on the ^{13}C NMR Spectra of 1-Methylcyclobutyl and Trishomocyclopropenyl Cations. *J. Am. Chem. Soc.* **1985,** *107* (21), 6017-6019.
234. Anet, F. A. L.; Basus, V. J.; Hewett, A. P. W.; Saunders, M., Isotopic Perturbation of Degenerate Conformational Equilibriums. *J. Am. Chem. Soc.* **1980,** *102* (11), 3945-3946.
235. Anet, F. A. L.; O'Leary, D. J.; Williams, P. G., Tritium NMR in Conformational Analysis: Isotopic Perturbation of the Ring Inversion Equilibrium in [^{3}H]cyclohexane. *J. Chem. Soc., Chem. Commun.* **1990,** (20), 1427-1429.
236. Perrin, C. L.; Ohta, B. K., Symmetry of NHN hydrogen bonds in solution. *J. Mol. Struct.* **2003,** *644* (1-3), 1-12.
237. Perrin, C. L.; Thoburn, J. D., Symmetries of hydrogen bonds in monoanions of dicarboxylic acids. *J. Am. Chem. Soc.* **1992,** *114* (22), 8559-65.
238. Perrin, C. L.; Lau, J. S.; Kim, Y.-J.; Karri, P.; Moore, C.; Rheingold, A. L., Asymmetry of the "Strongest" OHO Hydrogen Bond, in the Monoanion of (±)-α,α'-Di-*tert*-butylsuccinate. *J. Am. Chem. Soc.* **2009,** *131* (37), 13548-13554.
239. Calvert, B. R.; Shapley, J. R., $HOs_3(CO)_{10}CH_3$: NMR Evidence for C¨H¨Os Interaction. *J. Am. Chem. Soc.* **1978,** *100*, 7726-7727.
240. Perrin, C. L.; Kim, Y.-J.; Kuperman, J., Structures of 1,6-Dioxa-6aλ^4-thiapentalene and of 1,6,6aλ^4-Trithiapentalene: C_s or C_{2v} Symmetry? *J. Phys. Chem. A* **2001,** *105* (50), 11383-11387.
241. Zingaro, R. A.; VanderWerf, C. A.; Kleinberg, J., Evidence for the Existence of Unipositive Iodine Ion in Solutions of Iodine in Pyridine. *J. Am. Chem. Soc.* **1951,** *73* (1), 88-90.
242. Kleinberg, J.; Colton, E.; Sattizahn, J.; VanderWerf, C. A., The Bahavior of Iodine Species in Pyridine and Quinoline. *J. Am. Chem. Soc.* **1953,** *75* (2), 442-445.
243. Kortüm, G.; Wilski, H., Über die elektrische Leitfähigkeit von Jod-Pyridin-Lösungen. *Z. Phys. Chem.* **1953,** *202*, 35-55.
244. Popov, A. I.; Pflaum, R. T., Studies on the Chemistry of Halogens and of Polyhalides. X. The Reactions of Iodine Monochloride with Pyridine and with 2,2 '-Bipyridine. *J. Am. Chem. Soc.* **1957,** *79* (3), 570-572.
245. Sabin, J. R., A Theoretical Study of the Bis(pyridine)iodine(I) Cation. *J. Mol. Struct.* **1971,** *7*, 407-419.
246. Barluenga, J.; Álvarez-Pérez, M.; Fañanás, F. J.; González, J. M., A Smooth and Practicable Azido-Iodination reaction of Alkenes Based on IPy_2BF_4 and Me_3SiN_3. *Adv. Synth. Catal.* **2001,** *343* (4), 335-337.
247. Koser, G. F., Hypervalent halogen compounds. *Chem. Halides, Pseudo-Halides Azides* **1983,** *1*, 721-811.
248. Bosch, E.; Barnes, C. L., 1,2-Bis(2-pyridylethynyl)benzene, a Novel Trans-Chelating Bipyridyl Ligand. Structural Characterization of the Complexes with Silver(I) Triflate and Palladium(II) Chloride. *Inorg. Chem.* **2001,** *40*, 3097-3100.
249. Kawano, T.; Shinomaru, T.; Ueda, I., Highly Active Pd(II) Catalysts with trans-Bidentate Pyridine Ligands for the Heck Reaction. *Org. Lett.* **2002,** *4* (15), 2545-2547.
250. Hu, Y.-Z.; Chamchoumis, C.; Grebowics, J. S.; Thummel, R. P., Unique 2:1 Complex with a trans-Chelating Bis-Pyridine Ligand. *Inorg. Chem.* **2002,** *41* (8), 2296-2300.
251. Kawano, T.; Kuwana, J.; Shinomaru, T.; Du, C.-X.; Ueda, I., Copper(I) Chelate Complexes with Novel π-Conjugated 1,2-Bis(2-pyridinylethynyl)benzene Ligands: Synthesis, Structure, and Reactivity. *Chem. Lett.* **2001**, 1230-1231.
252. Shotwell, S.; Ricks, H. L.; Morton, J. G. M.; Laskoski, M.; Fiscus, J.; Smith, M. D.; Shimizu, K. D.; zur Loye, H.-C.; Bunz, U., H. F., Trans-spanning acetylenic bispyridine ligands: synthesis and structural characterization of novel organic and organometallic pseudodehydroannulenes. *J. Organomet. Chem.* **2003,** *671*, 43-51.
253. Chen, J.; McAllister, M. A.; Lee, J. K.; Houk, K. N., Short, Strong Hydrogen Bonds in the Gas Phase and in Solution: Theoretical Exploration of pKa Matching and Environmental Effects on the Strengths of Hydrogen Bonds and Their Potential Roles in Enzymatic Catalysis. *J. Org. Chem.* **1998,** *63* (16), 4611-4619.

254. Metrangolo, P.; Neukirch, H.; Pilati, T.; Resnati, G., Halogen Bonding Based Recognition Processes: A World Parallell to Hydrogen Bonding. *Acc. Chem. Res.* **2005,** *38* (5), 386-395.
255. Perrin, C. L.; Ohta, B. K.; Kuperman, J., β-Deuterium Isotope Effects on Amine Basicity, "Inductive" and Stereochemical. *J. Am. Chem. Soc.* **2003,** *125* (49), 15008-15009.
256. Perrin, C. L.; Karri, P., Position-Specific Secondary Deuterium Isotope Effects on Basicity of Pyridine. *J. Am. Chem. Soc.* **2010,** *132* (34), 12145-12149.
257. Harwood, L. M.; Moody, C. J.; Percy, J. M., *Experimental Organic Chemistry*. 2nd ed.; Blackwell Science Ltd: Oxford, 1999.
258. Huber, S.; Grassi, G.; Bauder, A., Structure and Symmetry of Azulene as Determined from Microwave Spectra of Isotopomers. *Mol. Phys.* **2005,** *103* (10), 1395-1409.
259. Takahashi, S.; Kuroyama, Y.; Sonogashira, K.; Hagihara, N., A Convenient Synthesis of Ethynylarenes and Diethynylarenes. *Synthesis* **1980,** (8), 627-630.
260. Sonogashira, K.; Tohda, Y.; Hagihara, N., A Convenient Synthesis of Acetylenes: Catalytic Substitution of Acetylenic Hydrogen with Bromoalkenes, Iodoarenes, and Bromopyridines. *Tetrahedron Lett.* **1975,** *16* (50), 4467-4470.
261. Erdélyi, M.; Gogoll, A., Rapid Homogeneous-Phase Sonogashira Coupling Reactions Using Controlled Microwave Heating. *J. Org. Chem.* **2001,** *66* (12), 4165-4169.
262. Erdélyi, M.; Langer, V.; Karlém, A.; Gogoll, A., Insight into β-hairpin stability: a structural and thermodynamic study of diastereomeric β-hairpin mimetics. *New J. Chem.* **2002,** *26* (7), 834-843.
263. Gros, P.; Choppin, S.; Mathieu, J.; Fort, Y., Lithiation of 2-Heterosubstituted Pyridines with BuLi-LiDMAE: Evidence for Regiospecificity at C-6. *J. Org. Chem.* **2002,** *67*, 234-237.
264. Gros, P.; Choppin, S.; Fort, Y., Lithiation of 2-Chloro- and 2-Methoxypyridine with Lithium Dialkylamides: Initial Ortho-Direction or Subsequent Lithium Ortho-Stabilization? *J. Org. Chem.* **2003,** *68*, 2243-2247.
265. Bublitz, G. U.; Boxer, S. G., Effective Polarity of Frozen Solvent Glasses in the Vicinity of Dipolar Solutes. *J. Am. Chem. Soc.* **1998,** *120* (16), 3988-3992.
266. Reichardt, C., *Solvents and Solvent Effects in Organic Chemistry*. 2nd ed.; VCH: Weinreb, 1988.
267. Butler, B. J.; Hool, J. M.; Harper, J. B., Recent Advances in the NMR Spectroscopy of Chlorine, Bromine, and Iodine. *Annu. Rep. NMR Spectrosc.* **2011,** *73*, 63-82.
268. Claridge, T. D. W., *High-Resolution NMR Techniques in Organic Chemistry*. 2nd ed.; Elsevier Ltd.: Oxford, 2009.
269. Pregosin, P. S., Ion pairing using PGSE diffusion methods. *Prog. Nucl. Magn. Reson. Spectrosc.* **2006,** *49*, 261-288.
270. Pregosin, P. S., NMR spectroscopy and ion pairing: Measuring and understanding how ions interact. *Pure Appl. Chem.* **2009,** *81* (4), 615-633.
271. Duthaler, R. O.; Roberts, J. D., Effects of Solvent, Protonation, and N-Alkylation on the ^{15}N Chemical Shifts of Pyridine and Related Compounds. *J. Am. Chem. Soc.* **1978,** *100* (16), 4969-4973.
272. Pugmire, R. J.; Grant, D. M., Carbon-13 Magnetic Resonance. X. The Six-Membered Nitrogen Heterocycles and Their Cations. *J. Am. Chem. Soc.* **1968,** *90* (3), 697-706.
273. Dewar, M. J. S.; Worley, S. D., Photoelectron Spectra of Molecules. I. Ionization Potentials of Some Organic Molecules and Their Interpretation. *J. Chem. Phys.* **1969,** *50* (2), 654-667.
274. Bartoszak, E.; Jaskolski, M.; Grech, E.; Gustafsson, T.; Olovsson, I., Structure of Thiocyanate Salt of 1,8-Bis(dimethylamino)naphthalene ($dmanH^+.SCN^-$) at 188 and 290 K. *Acta Crystallogr., Sect. B: Struct. Sci.* **1994,** *50* (3), 358-363.
275. Grech, E.; Malarski, Z.; Sawka-Dobrowolska, W.; Sobczyk, L., The structure and IR spectra of the 1:1 and 1:2 adducts of 1,8-bis(dimethylamino)naphthalene (DMAN) with 4,5-dicyanoimidazole (DCI). *J. Mol. Struct.* **1997,** *406* (1-2), 107-117.
276. Growiak, T.; Majerz, I.; Malarski, Z.; Sobczyk, L.; Pozharskii, A. F.; Ozeryanskii, V. A.; Grech, E., Structure and IR spectroscopic behaviour of 2,7-dichloro-1,8-bis(dimethylamino)naphthalene and its protonated form. *J. Phys. Org. Chem.* **1999,** *12* (12), 895-900.
277. Olah, G. A.; Bollinger, J. M., Stable Carbonium Ions. LVII. Halonium Ion Formation *via* Neighboring Halogen Participation. Trimethyl- and 1,1-Dimethylethylenehalonium Ions. *J. Am. Chem. Soc.* **1968,** *90* (4), 947-953.
278. Olah, G. A.; Bollinger, J. M.; Brinich, J., Stable Carbonium Ions. LXII. Halonium Ion Formation *via* Neighboring Halogen Participation: Ethylenehalonium, Propylenehalonium, and 1,2-Dimethylethylenehalonium Ions. *J. Am. Chem. Soc.* **1968,** *90* (10), 2587-2594.
279. Olah, G. A.; Westerman, P. W.; Melby, E. G.; Mo, Y. K., Onium Ions. X. Structural Study of Acyclic and Cyclic Halonium Ions by Carbon-13 Nuclear Magnetic Resonance Spectroscopy. The Question of Intra- and Intermolecular Equilibration of Halonium Ions with Haloalkylcarbenium Ions. *J. Am. Chem. Soc.* **1974,** *96* (11), 3565-3573.

280. Olah, G. A.; White, A. M., Stable Carbonium Ions. XCI. Carbon-13 Nuclear Magnetic Resonance Spectroscopic Study of Carbonium Ions. *J. Am. Chem. Soc.* **1969,** *91* (21), 5801-5810.
281. Olah, G. A.; Prakash, G. K. S.; Krishnamurthy, V. V., The 2,3-Dimethyl-3-fluoro-2-butyl Cation Revisited: Exclusive Methyl Exchange Ruling Out Fluorine Shift through Bridged Fluoronium Ion. *J. Am. Chem. Soc.* **1983,** *48* (25), 5116-5117.
282. Bonazza, B. R.; Peterson, P. E., Carbon-13 Nuclear Magnetic Resonance Spectroscopy of Tetramethylenehalonium Ions. *J. Org. Chem.* **1973,** *38* (5), 1010-1015.
283. Slebocka-Tilk, H.; Ball, R. G.; Brown, R. S., The Question of Reversible Formation of Bromonium Ions during the Course of Electrophilic Bromination of Olefins. 2. The Crystal and Molecular Structure of the Bromonium Ion of Adamantylideneadamantane. *J. Am. Chem. Soc.* **1985,** *107* (15), 4504-4508.
284. Hehre, W. J.; Hiberty, P. C., Theoretical Approaches to Rearrangements in Carbocations. I. The Haloethyl System. *J. Am. Chem. Soc.* **1974,** *96* (9), 2665-2677.
285. Hamilton, T. P.; Schaefer, H. F., Structure and Energetics of $C_2H_4Br^+$: Ethylenebromonium Ion vs Bromoethyl Cations. *J. Am. Chem. Soc.* **1990,** *112* (23), 8260-8265.
286. Reynolds, C. H., Structure and Relative Stability of Halogenated Carbocations: The $C_2H_4X^+$ and $C_4H_8X^+$ (X = F, Cl, Br) Cations. *J. Am. Chem. Soc.* **1992,** *114* (22), 8676-8682.
287. Damrauer, R.; Leavell, M. D.; Hadad, C. M., Computational Studies of Halonium Ions of Cyclohexene and Cyclopentene. *J. Org. Chem.* **1998,** *63* (25), 9476-9485.
288. Teberekidis, V. I.; Sigalas, M. P., Density functional study of potential energy surfaces and relative stabilities of halonium cations of ethylene and cyclopentenes. *Tetrahedron* **2002,** *58* (31), 6171-6178.
289. Cossi, M.; Persico, M.; Tomasi, J., Aspects of Electrophilic Bromination of Alkenes in Solution. Theoretical Calculation of Atomic Charges in Bromonium Ions. *J. Am. Chem. Soc.* **1994,** *116* (12), 5373-5378.
290. Ohta, B. K.; Scupp, T. M.; Dudley, T. J., Theoretical Evidence for the Nucleophilic Addition of Sulfur Dioxide to 1,2-Bridged Chloronium and Bromonium Ions. *J. Org. Chem.* **2008,** *73* (18), 7052-7059.
291. DeFrees, D. J.; Taagepera, M.; Levi, B. A.; Pollack, S. K.; Summerhays, K. D.; Taft, R. W.; Wolfsberg, M.; Hehre, W. J., Role of Hyperconjugation in Secondary β–Deuterium Isotope Effects. *J. Am. Chem. Soc.* **1979,** *101* (19), 5532-5536.
292. Olah, G. A., In *Halonium Ions*, John Wiley & Sons: New York, 1975; pp 103-106.
293. Barluenga, J.; Yus, M.; Concellón, J. M.; Bernad, P., Direct and Regioselective Transformation of α-Chloro Carbonyl Compounds into Alkenes and Deuterioalkenes. *J. Org. Chem.* **1981,** *46* (13), 2721-2726.
294. Nystrom, R. F., Reduction of Organic Compounds by Mixed Hydrides. III. 3-Bromopropionic Acid, 3-Bromopropionyl Chloride, Methyl 3-Bromopropionate and Halides. *J. Am. Chem. Soc.* **1959,** *81* (3), 610-612.
295. Schmid, G. H.; Gordon, J. W., Involvement of Neighboring Chlorine in the Exchange Reactions of Iodine Monochloride and Vicinal Organic Iodochlorides. *J. Org. Chem.* **1983,** *48* (22), 4010-4013.
296. Olah, G. A., In *Halonium Ions*, John Wiley & Sons: New York, 1975; pp 113-118.
297. Olah, G. A.; Donovan, D. J., Effect of Solvents of Decreasing Nucleophilicity (Sulfur Dioxide, Sulfuryl Chloride Fluoride, Sulfuryl Fluoride, and Methylene Fluoride) on the Complex Formation and Ionization of Alkyl Fluorides (Chlorides) with Antimony and Arsenic Pentafluoride. *J. Am. Chem. Soc.* **1978,** *100* (16), 5163-5169.
298. Olah, G. A., In *Halonium Ions*, John Wiley & Sons: New York 1975; pp 98-101.
299. Olah, G. A.; Beal, D. A.; Westerman, P. W., Stable Carbocations. CLV. The Ethylenechloronium and Methylchlorocarbenium Ions. *J. Am. Chem. Soc.* **1973,** *95* (10), 3387-3389.
300. Olah, G. A.; Mo, Y. K.; Halpern, Y., Stable Carbocations. CXXXI. Intermolecular Fluorine Exchange of the Methylfluorocarbenium and Dimethylfluorocarbenium Ions in $HF\text{-}SbF_5\text{-}SO_2ClF$ Solution. *J. Org. Chem.* **1972,** *37* (8), 1169-1174.
301. Olah, G. A.; Beal, D. A.; Westerman, P. W., Stable Carbocations. CLV. Ethylenechloronium and Methylchlorocarbenium Ions. *J. Am. Chem. Soc.* **1973,** *95* (10), 3387-3389.

APPENDIX

Synthesis of $[N–X–N]^+$ Halonium Complexes (**18a**, **18b**, **18a-*d*** and **18b-*d***)

General Experimental

Unless otherwise stated, all reagents and solvents were obtained from commercial suppliers and used without further purification. CH_2Cl_2 was freshly distilled from CaH_2, and *n*-hexane was distilled from sodium metal/benzophenone ketyl prior to use. Anhydrous Et_2NH and dry DMF were provided from Sigma-Aldrich. Microwave-assisted reactions were carried out with fixed hold-time in capped vials using a Biotage Initiator instrument. Analytical thin layer chromatography (TLC) was performed on aluminum sheets coated with Merck silica gel, grade F_{254}. Spots were visualized by UV (254 nm) or by treatment with a dip solution of aqueous $KMnO_4$ (1.0 g $KMnO_4$, 6.7 g K_2CO_3, and 1.7 mL 5 % aqueous NaOH in 100 mL H_2O) followed by heating. Flash chromatography was performed on Merck Silica gel 60 (0.040-0.063 mm). All glassware used in the syntheses of **[**$N\cdots X\cdots N]^+$ complexes **18a,b** was dried in an oven at 150 °C for several hours prior to use. The halogenations reactions were all performed under dry conditions in dry solvents, and in a nitrogen atmosphere. Centrifugations were carried out with a Heraeus Christ Labofuge A centrifuge. Melting points were recorded on a Büchi B-545 apparatus and are uncorrected. ^{1}H NMR and ^{13}C NMR spectra were recorded on a Varian VNMR-S 500 spectrometer or on a JEOL Eclipse 400-spectrometer at 25 °C in $CDCl_3$ or CD_2Cl_2, at 500 or 400 MHz and 126 or 100 MHz, respectively. ^{19}F NMR (376 MHz) spectra were recorded on a Varian 400-MR spectrometer in CD_2Cl_2 at 25 °C. Chemical shifts are reported on the δ scale in ppm using residual solvent signal as internal standard; $CDCl_3$ (δ_H 7.26, δ_C 77.00), CD_2Cl_2 (δ_H 5.32, δ_C 54.00). For the ^{19}F NMR spectra, a sealed capillary filled with hexafluorobenzene (δ_F -164.4) was used as an internal standard. ^{1}H-^{1}H COSY, ^{1}H-^{13}C HMQC, and ^{1}H-^{13}C HMBC NMR spectroscopy were used for assignment of ^{1}H and ^{13}C signals. For ^{1}H-NMR, each resonance was assigned according to the following conventions: chemical shift (δ) measured in ppm, observed multiplicity, number of hydrogens, observed coupling constant (*J* Hz), and assignment. Multiplicities are denoted as: s (singlet), d (doublet), t (triplet), q (quartet), quint (quintet), sex (sextet), sep (septet), m (multiplet) and br (broad). The numbering of the structures refers to those used for NMR assignment. GC-MS analyses were performed on a Varian 3400 GC/Varian Saturn 2000 MS, with a DB-5 equivalent capillary column (length 30 m, i.d. 25 μm) using helium as carrier gas (injector temperature 300 °C; temperature program 40 – 300 °C, 12 °C/min and 4 min hold-time). The MS detector consisted of an ion trap with70 eV ionization. High resolution mass spectroscopy (HRMS) data were obtained on an Agilent LC/MSD TOF instrument (Uppsala University, Department of Physical and Analytical Chemistry) or on a Q-TOF-MS at Stenhagen Analyslab AB, Gothenburg, Sweden, with detection in the positive ion mode. Agilent TOF software and Agilent QS software were used to record and analyze mass spectra, respectively. Standard autotune of masses was performed in the TOF-MS instruments before the experimental runs, and typical mass errors of 1-3 ppm were achieved in the calibration.

4-Methyl-2-((trimethylsilyl)ethynyl)pyridine (74)

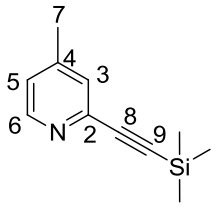

2-Chloro-4-methylpyridine (1.76 mL, 15.76 mmol), ethynyltrimethylsilane (2.6 mL, 18.76 mmol), $Pd(PPh_3)_2Cl_2$ (0.880 g, 1.26 mmol), CuI (0.380 g, 2.00 mmol), triphenylphosphine (0.848 g, 3.22 mmol), Et_2NH (24.0 mL, 232 mmol), and DMF (8.0 mL) were added equally to two 20-mL microwave vials, which were then sealed with septa. Nitrogen was bubbled through both yellow reaction mixtures for 30 s before they were stirred at 120 °C for 27 min each under microwave irradiation. The resulting black mixtures were combined, and filtered through a plug of celite, which was subsequently washed with CH_2Cl_2 (300 mL). To the filtrate H_2O (150 mL) was added, and the two phases were separated. The aqueous phase was extracted with CH_2Cl_2 (3 x 50 mL). The combined organic phases were washed with brine (150 mL), dried with anhydrous $MgSO_4$, filtered, and concentrated *in vacuo*. The crude black residue was purified by column chromatography eluting with Et_2O/hexanes (3:7) to furnish **74** (2.32 g, 78%) as dark brown, low melting, crystalline solid (solidifies upon storage in the freezer). TLC (Et_2O/hexanes; 1:1) R_f = 0.39; ^{1}H NMR (400 MHz, $CDCl_3$) δ 8.35 (dd, 1H, *J* = 5.1 and 0.7 Hz, H6), 7.23 (app. sep, 1H, *J* = 0.7 Hz, H3), 6.97 (app. dsex, 1H, *J* = 5.1, 0.7 Hz , H5), 2.25 (app. t, 3H, *J* = 0.7 Hz, CH_3), 0.21 (s, 9H, $Si(CH_3)_3$); ^{13}C NMR (126 MHz, $CDCl_3$) δ 149.66 (C6), 147.23 (C4), 142.82 (C2), 128.10 (C3), 124.05 (C5), 103.85 (C8), 94.18 (C9), 20.75 (CH_3), -0.28 ($Si(\underline{C}H_3)_3$); GC-MS *m/z* (relative intensity): 189 (M^+, 40), 175 (19), 174 (100), 146 (15); HRMS calcd for $(C_{11}H_{16}NSi)^+$ *m/z* 190.1047, found 190.0983.

2-Ethynyl-4-methylpyridine (35)

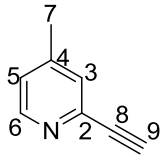

A mixture of TMS-protected **74** (2.22 g, 11.74 mmol) and KF (2.08 g, 35.80 mmol) in MeOH (60 mL) was stirred for 18 h at room temperature. After evaporation of the solvent under reduced pressure, the dark brown residue was partitioned between CH_2Cl_2 (150 mL) and H_2O (150 mL). The aqueous phase was extracted with CH_2Cl_2 (3 x 50 mL). The combined organic extracts were washed with brine (100 mL), dried with anhydrous $MgSO_4$, filtered, and concentrated *in vacuo* to afford **35** (1.36 g, 99%) as a dark brown thin oil, which turned into a crystalline solid when kept in the freezer. TLC (Et_2O/hexanes; 1:1) R_f = 0.22; ^{1}H NMR (400 MHz, $CDCl_3$) δ 8.39 (dd, 1H, *J* = 5.1, 0.7 Hz, H6), 7.27 (app. sep 1H, *J* = 0.7 Hz, H3), 7.04 (app. dsex, 1H, *J* = 5.1 and 0.7 Hz, H5), 3.08 (s, 1H, C≡CH), 2.30 (app. t, *J* = 0.7 Hz, CH_3); ^{13}C NMR (126 MHz, $CDCl_3$) δ 149.68 (C6), 147.34 (C4), 142.03 (C2), 128.22 (C3), 124.38 (C5), 82.82 ($\underline{C}$≡CH). 76.56 (C≡$\underline{C}$H), 20.70 (CH_3); GC-MS *m/z* (relative intensity): 118 (10), 117 (M^+, 100), 116 (18), 90 (18), 89 (32), 63 (11), 50 (14); HRMS calcd for $(C_8H_8N)^+$ *m/z* 118.0651, found 118.0595.

1,2-Bis((4-methylpyridine-2-yl)ethynyl)benzene (22)

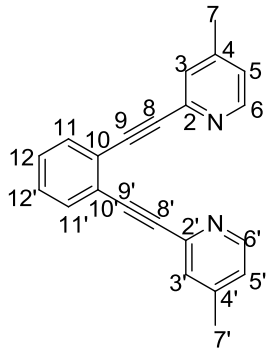

1,2-Diiodobenzene (250 μL, 1.91 mmol), 2-ethynyl-4-methylpyridine (**35**)(0.588 g, 5.02 mmol), $Pd(PPh_3)_2Cl_2$ (0.139 g, 0.20 mmol), CuI (0.047 g, 0.25 mmol), Et_2NH (3.0 mL, 28.9 mmol), and DMF (0.5 mL) were added to a 5-mL microwave vial, which was then sealed with a septum. Nitrogen was bubbled through the dark brown reaction mixture for 30 s before it was stirred at 120 °C for 10 min under microwave irradiation. Thereafter, the resulting brown/black mixture was filtered through a plug of celite, which was subsequently washed with CH_2Cl_2 (150 mL). To the filtrate H_2O (100 mL) was added, and the two phases were separated. The aqueous phase was extracted with CH_2Cl_2 (3 x 30 mL). The combined organic phases were dried with anhydrous $MgSO_4$, filtered and concentrated *in vacuo*. Purification of the brown/black residue by column chromatography two consecutive times using CH_2Cl_2/EtOAc/Et_3N (90:10:0.5) followed by CH_2Cl_2/EtOAc/Et_3N (90:10:0.5 → 80:20:0.5) as eluents furnished **22** (0.489 g, 83%) as a yellow, crystalline solid. TLC (EtOAc/CH_2Cl_2; 1:4) R_f = 0.28; ^{1}H NMR (500 MHz, CD_2Cl_2) δ 8.48 (d, 2H, *J* = 4.7 Hz, H6 and H6'), 7.63-7.67 (m, 2H, AA' part of AA'BB', H11 and H11'), 7.60-7.62 (br m, 2H, H3 and H3'), 7.38-7.43 (m, 2H, BB' part of AA'BB', H12 and H12'), 7.11 (d, 2H, *J* = 4.7 Hz, H5 and H5'), 2.35 (s, 6H, 2 x CH_3); ^{13}C NMR (126 MHz, CD_2Cl_2) δ (150.36 (C6 and C6'), 148.03 (C4 and C4'), 143.58 (C2 and C2'), 132.62 (C11 and C11'), 129.35 (C12 and C12'), 129.28 (C3 and C3'), 126.07 (C10 and C10'), 124.70 (C5 and C5'), 93.20 (C8 and C8'), 87.43 (C9 and C9'), 21.14 (2 x CH_3); HRMS calcd for $(C_{22}H_{17}N_2)^+$ *m/z* 309.1386, found 309.1280; mp 143.6-147.7 °C.

1,2-Bis((4-methylpyridine-2-yl)ethynyl)benzenebromonium triflate (18a)

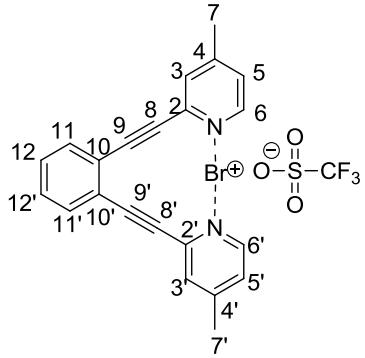

A mixture of **22** (49 mg, 0.16 mmol) and AgOTf (47 mg, 0.18 mmol) was dissolved in CH_2Cl_2 (11.0 mL) under stirring at room temperature in nitrogen atmosphere. To the clear, light yellow solution was added a solution of Br_2 (0.58 M, 330 μL, 0.19 mmol) in CH_2Cl_2 dropwise by syringe. Immediately upon the addition, a light yellow precipitate (AgBr) was formed. The

reaction mixture was stirred vigorously for 30 min. Thereafter, the mixture was centrifuged at 2000 rpm for 10 min. The clear, orange supernatant was carefully removed and transferred by syringe to a 50-mL pear-shaped flask sealed with a rubber septum. After concentration of the supernatant by keeping it under a stream of nitrogen for 1 h, precipitation was carried out by addition of *n*-hexane (20 mL). The formation of the light yellow/beige precipitate was continued at 0 °C in an ice-bath for 45 min. The clear, light yellow solution was removed carefully by syringe, and the remaining solid was washed twice with dry *n*-hexane (2 x 10 mL). After solvent removal by syringe, and drying under vacuum, the bromonium complex **18a** was furnished as a yellow solid (42 mg, 49%). ^{1}H NMR (500 MHz, CD_2Cl_2) δ 8.66 (d, 2H, *J* = 5.9 Hz, H6 and H6'), 7.74-7.79 (m, 2H, AA' part of AA'BB', H11 and H11'), 7.70-7.73 (br s/m, 2H, H3 and H3'), 7.56-7.61 (m, 2H, BB' part of AA'BB', H12 and H12'), 7.42 (d, 2H, *J* = 5.9 Hz, H5 and H5'), 2.54 (s, 6H, 2 x CH_3); ^{13}C NMR (126 MHz, CD_2Cl_2) δ 155.62 (C4 and C4'), 147.48 (C6 and C6'), 139.87 (C2 and C2'), 134.13 (C11 and C11'), 131.74 (C12 and C12'), 131.41 (C3 and C3'), 127.64 (C5 and C5'), 125.01 (C10 and C10'), 121.32 (q, *J* = 321.0 Hz, $\underline{C}F_3$), 97.55 (C9 and C9'), 88.97 (C8 and C8'), 21.90 (2 x CH_3); ^{19}F NMR (376 MHz, CD_2Cl_2) δ -76.91 (s, CF_3); HRMS calcd for $(C_{23}H_{17}BrF_3N_2O_3S)^+$ *m/z* 537.0090, found 536.9939; mp 130.3 – 143.2 °C (decomposition), 114.5 °C (discoloured).

1,2-Bis((4-methylpyridine-2-yl)ethynyl)benzeneoiodonium triflate (18b)

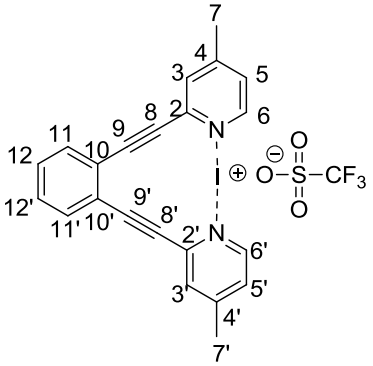

A mixture of **22** (92 mg, 0.30 mmol) and AgOTf (79 mg, 0.31 mmol) was dissolved in CH_2Cl_2 (25.0 mL) under stirring at room temperature in nitrogen atmosphere. To the clear, light yellow solution was added I_2 (90 mg, 0.35 mmol), and immediately upon the addition a yellow precipitate (AgI) was formed. The reaction mixture was stirred vigorously for 30 min. Thereafter, the mixture was centrifuged at 2000 rpm for 10 min. The clear, dark red supernatant was carefully removed and transferred by syringe to a 50-mL pear-shaped flask sealed with a rubber septum. After concentration of the supernatant by keeping it under a stream of nitrogen for 1.5 h, precipitation was carried out by addition of *n*-hexane (25 mL). The formation of the light yellow/beige precipitate was continued at 0 °C in an ice-bath for 30 min. The clear, dark red solution was removed carefully by syringe, and the remaining solid was washed twice with dry *n*-hexane (2 x 20 mL). After solvent removal by syringe, and drying under vacuum, the iodonium complex **18b** was furnished as a beige/yellow solid (0.119 g, 68%). ^{1}H NMR (500 MHz, CD_2Cl_2) δ 8.67 (dd, 2H, *J* = 5.9 and 0.5 Hz, H6 and H6'), 7.76-7.80 (m, 2H, AA' part of AA'BB', H11 and H11'), 7.71 (app. dt, 2H, *J* = 1.9 and 0.7 Hz, H3 and H3'), 7.57-7.61 (m, 2H, BB' part of AA'BB', H12 and H12'), 7.29 (ddd, 2H, *J* = 5.9, 1.9 and 0.7 Hz, H5 and H5'), 2.53 (app. t, 6H, *J*

= 0.7 Hz, 2 x CH_3); ^{13}C NMR (126 MHz, CD_2Cl_2) δ 155.86 (C4 and C4'), 150.38 (C6 and C6'), 142.60 (C2 and C2'), 134.79 (C11 and C11'), 131.41 (C12 and C12'), 131.38 (C3 and C3'), 127.90 (C5 and C5'), 124.75 (C10 and C10'), 98.28 (C9 and C9'), 91.00 (C8 and C8'), 21.94 (2 x CH_3); ^{19}F NMR (376 MHz, CD_2Cl_2) δ -76.77 (s, CF_3); HRMS calcd for $(C_{22}H_{16}IN_2)^+$ *m/z* 435.0358, found 435.0413.

2-((2-Iodophenyl)ethynyl)-4-methylpyridine (38)

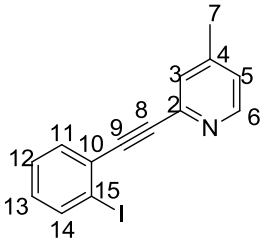

1,2-Diiodobenzene (900 μL, 6.69 mmol), 2-ethynyl-4-methylpyridine (**35**) (0.53 g, 4.52 mmol), $Pd(PPh_3)_2Cl_2$ (0.254 g, 0.36 mmol), CuI (0.106 g, 0.56 mmol), Et_2NH (12.0 mL, 115.5 mmol), and DMF (4.0 mL) were added to a 20-mL microwave vial, which was then sealed with a septum. Nitrogen was bubbled through the dark brown reaction mixture for 30 s before it was stirred at 120 °C for 4 min under microwave irradiation. Thereafter, the resulting brown/black mixture was filtered through a plug of celite, which was subsequently washed with CH_2Cl_2 (150 mL). To the filtrate H_2O (100 mL) was added, and the two phases were separated. The aqueous phase was extracted with CH_2Cl_2 (3 x 30 mL). The combined organic phases were dried with anhydrous $MgSO_4$, filtered and concentrated *in vacuo*. Purification of the brown/black residue by column chromatography two consecutive times using EtOAc/hexanes (2:3 → 3:2) and CH_2Cl_2/MeOH (100:0 → 98:2) as eluting agents furnished **38** as a light yellow solid (0.671 g, 46%). The corresponding di-coupled compound **22** was isolated as a yellowish solid (0.190 g, 27%). TLC (EtOAc/hexanes; 1:1) R_f = 0.43; ^1H NMR (500 MHz, CD_2Cl_2) δ 8.46 (d, 1H, *J* = 5.1 Hz, H6), 7.91 (ddd, 1H, *J* = 8.0, 1,2, 0.4 Hz, H14), 7.61 (ddd, 1H, *J* = 7.7, 1.7, 0.4 Hz, H11), 7.46 (app. sep, 1H, *J* = 0.7 Hz, H3), 7.38 (app. td, 1H, *J* = 7.6, 1.2 Hz, H12), 7.11 (app. dsex,1H, *J* = 5.1 and 0.7 Hz, H5), 7.09 (ddd, 1H, *J* = 8.0, 7.5, 1.7 Hz, H13), 2.37 (app. t, 3H, *J* = 0.7 Hz, CH_3); ^{13}C NMR (126 MHz, CD_2Cl_2) δ 150.48 (C6), 148.12 (C4), 143.32 (C2), 139.43 (C14), 133.62 (C11), 130.66 (C13), 129.51 (C10), 128.85 (C3), 128.58 (C12), 124.82 (C5), 101.40 (C15), 92.80 (C8), 90.66 (C9), 21.14 (CH_3); GC-MS *m/z* (relative intensity): 320 (18), 319 (M^+, 100), 192 (22); HRMS calcd for $(C_{14}H_{11}IN)^+$ *m/z* 319.9931, found 319.9923; mp 98.4 -100.5 °C.

2-Chloro-6-deutero-4-methylpyridine (36-*d*)

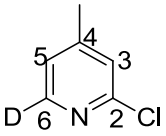

A solution of DMAE (4.5 mL, 44.8 mmol) in dry *n*-hexane (25 mL) was cooled to -78 °C under stirring in a nitrogen atmosphere. *n*-BuLi (2.5 M in hexanes, 36 mL, 90.0 mmol) was added dropwise by syringe over 30 min. The resulting colourless solution was stirred at -78 °C for 1 h. Then, a solution of 2-chloro-4-methylpyridine (1.5 mL, 13.4 mmol) in dry *n*-hexane (25 mL) was

added over 40 min by syringe. Upon the addition, the mixture turned light yellow. After stirring at -78 °C for 35 min, a large excess of CH_3OD (10.0 mL, 246 mmol) was added to the light orange mixture by syringe over 10 min. The resulting brown mixture was stirred for additional 15 min at -78 °C, then at 15 min at room temperature. Subsequently, H_2O (140 mL) was added, and the two phases were separated. The aqueous phase was extracted with Et_2O (3 x 50 mL). The combined organic phases were washed with brine (150 mL), dried with anhydrous $MgSO_4$, filtered, and concentrated under reduced pressure to furnish a clear, orange oil. Purification by column chromatography using Et_2O/hexanes (2:3) as eluent yielded **36-*d*** (1.28 g, 75%, > 95% D) as a clear, light yellow oil, which turned crystalline in the freezer. TLC (Et_2O/hexanes; 2:3) R_f = 0.34; ^{1}H NMR (500 MHz, $CDCl_3$) δ 7.14 (app. sex, *J* = 0.7 Hz, 1H, H3), 7.02 (br s, 1H, H5), 2.34 (app. t, 3H, *J* = 0.7 Hz, CH_3); ^{13}C NMR (126 MHz, $CDCl_3$) δ 151.49 (t, *J* = 1.8 Hz, C2), 150.38 (t, *J* = 0.9 Hz, C4), 148.92 (t, *J* = 27.7 Hz, C6), 124.82 (C3), 123.25 (t, *J* = 1.1 Hz, C5), 20.73 (CH_3); GC-MS *m/z* (relative intensity): 130 (36), 129 (45), 128 ($M^{+,}$ 100), 127 (22), 94 (28), 93 (79), 66 (56), 65 (25); HRMS calcd for $(C_6H_6DClN)^+$ *m/z* 129.0324, found 129.0307.

6-Deutero-4-methyl-2-((trimethylsilyl)ethynyl)pyridine (74-*d*)

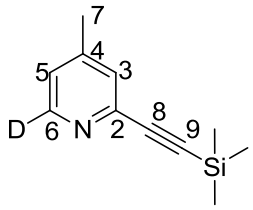

2-Chloro-6-deutero-4-methylpyridine (1.008 g, 7.84 mmol), ethynyltrimethylsilane(1.4 mL, 10.01 mmol), $Pd(PPh_3)_2Cl_2$ (0.483g, 0.69 mmol), CuI (0.205 g, 1.08 mmol), triphenylphosphine (0.427 g,1 .63 mmol), Et_2NH (12.0 mL, 116 mmol), and DMF (4.0 mL) were added to a 20-mL microwave vial, which was then sealed with a septum. Nitrogen was bubbled through the yellow reaction mixture for 30 s before it was stirred at 120 °C under microwave irradiation for 27 min. The resulting brown/black mixture was filtered through a plug of celite, which was subsequently washed with CH_2Cl_2 (250 mL). The black solution was washed with H_2O (150 mL), and the aqueous phase was extracted with CH_2Cl_2 (3 x 40 mL). The combined organic phases were washed with brine (150 mL), dried with anhydrous $MgSO_4$, filtered, and concentrated *in vacuo*. Purification of the crude black residue two consecutive times by column chromatography first eluting with CH_2Cl_2, and then with Et_2O/hexanes (3:7) furnished **74-*d*** (1.112 g, 75%) as a clear, yellow oil. TLC (CH_2Cl_2) R_f = 0.19; (Et_2O/hexanes; 1:1) R_f = 0.34; ^{1}H NMR (400 MHz, $CDCl_3$) δ 7.30 (app. sex, 1H, *J* = 0.7 Hz, H3), 7.02-7.04 (br. m, 1H, H5), 2.32 (app. t, 3H, *J* = 0.7 Hz, CH_3), 0.25 (s, 9H, $Si(\underline{C}H_3)_3$); ^{13}C NMR (126 MHz, $CDCl_3$) δ 149.31 (t, *J* = 27.1 Hz, C6), 147.25 (t, *J* = 0.7 Hz, C4), 142.80 (t, *J* = 1.5 Hz, C2), 128.12 (C3), 123.93 (C5), 103.86 (C8), 94.18 (C9), 20.76 (CH_3), -0.28, ($Si(CH_3)_3$); GC-MS *m/z* (relative intensity): 191 (12), 190 (M^+, 42), 176 (32), 175 (100), 147 (19), 121 (14); HRMS calcd for $(C_{11}H_{15}DNSi)^+$ *m/z* 191.1109, found 191.1104

6-Deutero-2-ethynyl-4-methylpyridine (35-*d*)

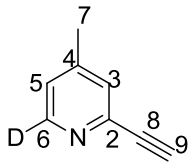

A mixture of TMS-protected **74-*d*** (1.102 g, 5.79 mmol) and KF (1.011 g, 17.40 mmol) in MeOH (30 mL) was stirred at room temperature for 16 h. The solvent was removed by concentration under reduced pressure, and the brownish residue was partitioned between CH_2Cl_2 (100 mL) and H_20 (100 mL). The aqueous phase was extracted with CH_2Cl_2 (3 x 30 mL). The combined organic phases were washed with brine (100 mL), dried with anhydrous $MgSO_4$; filtered, and concentrated *in vacuo* to afford **35-*d*** (0.641 g, 94%) as a brown, thin oil. TLC (EtOAc/hexanes; 2:3) R_f = 0.31; ^{1}H NMR (500 MHz, $CDCl_3$) δ 7.31 (app. sex, *J* = 0.7 Hz, C3), 7.07-7.09 (br. m., 1H, Hz, C5), 3.10 (s, 1H, C≡CH), 2.34 (app. t, 3H, *J* = 0.7 Hz, CH_3); ^{13}C NMR (100 MHz, $CDCl_3$) δ 149.42 (t, *J* = 27.2 Hz, C6), 147.40 (t, *J* = 1.0 Hz, C4), 142.09 (t, *J* = 1.5 Hz, C2), 128.29 (C3), 124.30 (t, *J* = 1.1 Hz, C5), 82.88 (*C*≡CH), 76.58 (C≡*C*H), 20.77 (CH_3); GC-MS *m/z* (relative intensity): 118 (M^+, 100), 117 (19), 90 (33), 63 (12), 51 (10); HRMS calcd for $(C_8H_7DN)^+$ *m/z* 119.0714, found 119.0788.

1,2-Bis((4-methylpyridine-2-yl)ethynyl)benzene-*d* (22-*d*)

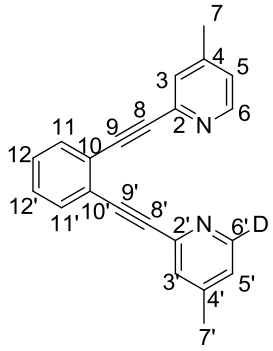

2-((2-Iodophenyl)ethynyl)-4-methylpyridine (**38**)(0.589 g, 1.85 mmol), **35-*d*** (0.267 g, 2.26 mmol), $Pd(PPh_3)_2Cl_2$ (0.141 g, 0.20 mmol), CuI (0.048 g, 0.25 mmol), Et_2NH (3.5 mL, 33.7 mmol), and DMF (0.5 mL) were added to a 5-mL microwave vial, which was then sealed with a septum. Nitrogen was bubbled through the mixture for 30 s before it was stirred at 120 °C for 13 min under microwave irradiation. Thereafter, the resulting brown/black mixture was filtered through a plug of celite, which was subsequently washed with CH_2Cl_2 (150 mL). To the filtrate H_2O (100 mL) was added, and the two phases were separated. The aqueous phase was extracted with CH_2Cl_2 (3 x 30 mL). The combined organic phases were dried with anhydrous $MgSO_4$, filtered and concentrated *in vacuo*. Purification of the brown/black residue by column chromatography two consecutive times using EtOAc/hexanes (1:1) followed by CH_2Cl_2/MeOH (99:1) as eluting agents furnished **22-*d*** as a yellow solid (0.338 g, 59%). TLC (EtOAc/hexanes; 1:1) R_f = 0.20; ^{1}H NMR (500 MHz, CD_2Cl_2) δ 8.48 (d, 1H, *J* = 5.1 Hz, H6), 7.63-7.67 (m, 2H, AA' of AA'BB', H11 and H11'), 7.61-7.62 (br m, 2H, H3 and H3'), 7.38-7.42 (m, 2H, BB' of AA'BB', H12 and H12'), 7.09-7.12 (br m, 2H, H5 and H5'), 2.35 (br s, 6H, 2 x CH_3); ^{13}C NMR (126 MHz, CD_2Cl_2) δ 150.35 (C6), 150.02 (t, *J* = 27.1 Hz, C6'), 148.02 (C4'), 148.01 (C4),

143.58 (C2), 143.56 (C2'), 132.60, (C11 and C11'), 129.34 (C12 and C12'), 129.27 (C3'), 129.26 (C3), 126.07 (C10 and C10'), 124.67 (C5), 124.54 (C5'), 93.93 (C9 and C9'), 87.41 (C8 and C8'), 21.13 (2 x CH_3); HRMS calcd for $(C_{22}H_{16}DN_2)^+$ *m/z* 310.1443 found 310.1412; mp 141.2 – 144.9 °C.

1,2-Bis((4-methylpyridine-2-yl)ethynyl)benzenebromonium triflate-*d* (18a-*d*)

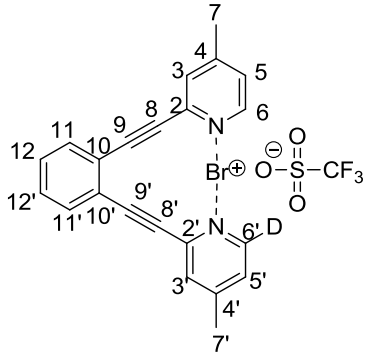

A mixture of mono-deuterated **22-*d*** (47 mg, 0.15 mmol) and AgOTf (39 mg, 0.15 mmol) was dissolved in CH_2Cl_2 (15.0 mL) under stirring at room temperature in nitrogen atmosphere. To the clear, light yellow solution was added a solution of Br_2 (0.58 M, 270 µL, 0.16 mmol) in CH_2Cl_2 dropwise by syringe. Immediately, a light yellow precipitate (AgBr) was formed. The reaction mixture was stirred vigorously for 30 min. Thereafter, the mixture was centrifuged at 2000 rpm for 10 min. The clear, light orange supernatant was carefully removed and transferred by syringe to a 50-mL pear-shaped flask sealed with a rubber septum. Precipitation was carried out by addition of *n*-hexane (20 mL). The formation of the light yellow/beige precipitate was continued at 0 °C in an ice-bath for 30 min. The clear, light yellow solution was removed carefully by syringe, and the remaining solid was washed twice with dry *n*-hexane (2 x 10 mL). After solvent removal by syringe, and drying under vacuum, the bromonium complex **18a-*d*** was furnished as a light yellow solid (61 mg, 76%). ^{1}H NMR (500 MHz, CD_2Cl_2) δ 8.65 (d, 1H, *J* = 5.9 Hz, H6), 7.74-7.79 (m, 2H, AA' of AA'BB', H11 and H11'), 7.70-7.72 (br m, 2H, H3 and H3'), 7.56-7.61 (m, 2H, BB' of AA'BB', H12 and H12'), 7.40-7.43 (m, 2H, H5 and H5'), 2.54 (s, 6H, 2 x CH_3); ^{13}C NMR (126 MHz, CD_2Cl_2) δ 155.65 (C4') 155.62 (C4), 147.52 (C6), 147.21 (t, *J* = 27 Hz, C6'), 139.89 (C2), 139.86 (C2'), 134.14 (C11 and C11'), 131.74 (C12 and C12'), 131.41 (C3 and C3'), 127.65 (C5), 127.52 (C5'), 125.02 (C10 and C10'), 97.55 (C9 and C9'), 88.99 (C8 and C8'), 21.90 (2 x CH_3); ^{19}F NMR (376 MHz, CD_2Cl_2) δ -76.82 (s, CF_3); HRMS calcd for $(C_{22}H_{15}DBrN_2)^+$ *m/z* 388.0560, found 388.0619; mp 129.0 - 137.3 °C (decomposition), discoloured 115.5 °C.

1,2-Bis((4-methylpyridine-2-yl)ethynyl)benzeneiodonium triflate-*d* (18b-*d*)

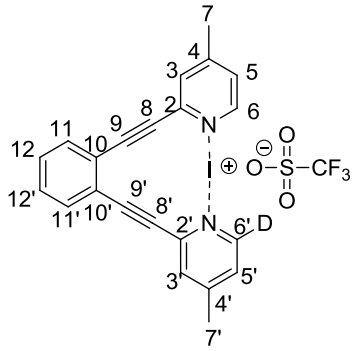

A mixture of mono-deuterated **22-*d*** (42 mg, 0.14 mmol) and AgOTf (36 mg, 0.14 mmol) was dissolved in CH_2Cl_2 (15.0 mL) under stirring at room temperature in nitrogen atmosphere. To the clear, light yellow solution was added I_2 (40 mg, 0.16 mmol), and immediately upon the addition a yellow precipitate (AgI) was formed. The reaction mixture was stirred vigorously for 30 min. Thereafter, the mixture was centrifuged at 2000 rpm for 10 min. The clear, light orange supernatant was carefully removed and transferred by syringe to a 50-mL pear-shaped flask sealed with a rubber septum. Precipitation was carried out by addition of *n*-hexane (20 mL). The formation of the light yellow/beige precipitate was continued at 0 °C in an ice-bath for 30 min. The clear, dark red solution was removed carefully by syringe, and the remaining solid was washed twice with dry *n*-hexane (2 x 10 mL). After solvent removal by syringe, and drying under vacuum, the iodonium complex **18b-*d*** was furnished as a light yellow solid (48 mg, 59 %). ^{1}H NMR (500 MHz, CD_2Cl_2) δ 8.67 (d, 2H, *J* = 5.9 Hz, H6 and H6'), 7.75-7.80 (m, 2H, AA' of AA'BB', H11 and H11'), 7.70-7.72 (m, 2H, H3 and H3'), 7.57-7.62 (m, 2H, BB' of AA'BB', H12 and H12'), 7.28-7.30 (m, 2H, H5 and H5'), 2.53 (app. t, 6H, *J* = 0.7 Hz, 2 x CH_3); ^{13}C NMR (126 MHz, CD_2Cl_2) δ 155.87 (C4'), 155.85 (C4) 150.39 (C6), 150.06 (t, *J* = 27.6 Hz, C6'), 142.59 (C2), 142.46 (C2'), 134.79 (C11 and C11'), 131.41 (C12 and C12'), 131.37 (C3 and C3'), 127.91 (C5), 127.77 (C5'), 124.75 (C10 and C10'), 98.27 (C9 and C9'), 121.61 (q, *J* = 321.7 Hz, $\underline{C}F_3$), 91.00 (C8 and C8'), 21.94 (2 x CH_3); ^{19}F NMR (376 MHz, CD_2Cl_2) δ -76.79 (s, CF_3); HRMS calcd for $(C_{22}H_{15}DIN_2)^+$ *m/z* 436.0421, found 436.0475.